Metal Separation by Using Various Biomass Wastes

September 2019

Department of Energy and Material Science,

Graduate School of Science and Engineering,

Saga University, Japan

Yu Dan

ACKNOWLEDGEMENTS

This dissertation is the comprehensive including all the research works in almost three years at Saga university. It could not be finished without the thoughtful guidance and a lot of helps from my professors, all previous and present lab members and my friends.

Mostly, I would like to express my deepest gratitude to my supervisor Professor Keisuke Ohto for all the supports. He generously supported the chance to study at Saga University, all the chemicals for experiment and always kindly discussed with me about the experimental problems. I always got the valuable suggestions and constructive criticism from him. The most worth spirts I learned from him is the strict attitude to all the links of works.

Secondly, I would like to be grateful to the members of examination committee, Prof. Hidetaka Kawakita, Prof. Shintaro Morisada and Prof. Takayuki Narita. I truly appreciate the helpful comment to the revising thesis from them. In additional, I would sincerely express my thanks to Prof. Kawakita and Prof. Morisada, in the past three years, they provided a lot of advices to my improvement of experiments. And they always kindly forgave my mistakes and patiently explained the detail to me.

Next, I would like to express my thanks to all my previous and present lab members. They are my first Japanese friends. I firstly learned about the Japanese culture from them with the patient and selfless help. I learned a lot of measured operations learned from them as well.

At last, I would like to express my deeply thankful and love to my family and my friends. Without their supports, I could not make my dream come true and go so much further. My all foreign friends totally changed my opinion of life. I learned various culture background from them.

Yu Dan

September, 2019, Saga University, Japan.

ABSTRACT

Research of metal adsorption on biomass adsorbents has played the important role of metal recovery and radioactive metal removal, because of low cost and less pollution to environment. For the commercial technological recovery of precious metals from electronic waste, the preferable selectivity of adsorbents is certainly required, because the leaching solutions contain various metals. Biomass adsorbents produced from abundant resource not only possess various functional groups but also have high selectivity and capacity to various metal adsorption, which is comparable to other designed and synthesized organic adsorbents. Based on the advantaged priorities of biomass adsorbents, to find the simple and commercial method for recovery of precious and cesium removal on various biomass wastes were investigated in this research work. Depending on that objective purpose, the thesis consists of three parts.

The first chapter introduces the properties of precious metals and alkali metals, the supply and demand of precious metals, as well as advantages of biomass adsorbents for metal adsorption. From main component in biomass wastes, they are simply divided into three classes, polysaccharides-, polyphenols-, proteins-rich adsorbents. Hence, four representative substances, chitin powder, kiwi peels, tea leave and human hair were selected for investigation of metal adsorption and separately described at chapter 2, chapter 3 and chapter 4.

In second chapter, typical and natural polysaccharides adsorbents: chitin, cellulose and chitosan powder, were employed for gold, platinum and palladium adsorption. Two types of chitins from different resources had better performance on palladium and platinum adsorption than that of cellulose. Because of the solubility of chitosan into acidic solution, chitosan was not employed. The adsorption capacities of natural chitins for palladium and platinum were remarkable, capacities have potential to be improved by simple modification. To further study whether the modification of natural polysaccharides can improve the ability of precious metal adsorption, kiwi peel wastes with high content of cellulose were investigated for precious metal adsorption after crosslinking. The high adsorption ability and selectivity for Au(III) over Pd(II) or Pt(IV)

were demonstrated by the simple modification. In addition, the result of XRD proved to the reduction of Au(III) during adsorption processes. It also led to long time to reach adsorption equilibrium.

The third chapter described cesium metal removal on the polyphenol adsorbents. Fresh and used tea leaves were used for cesium removal. Considered the real situation of polluted water and soil with cesium which contain large amount of sodium and some amount of potassium, adsorption of three kinds of alkali metals, sodium, potassium and cesium, was independently investigated. After modification with concentrated sulfuric acid, the crosslinked fresh and used tea leaves showed high adsorption capacity of cesium, compared with reported other materials. The proton exchange mechanism of alkali adsorption on crosslinked tea leaves was elucidated and the adsorption reaction was also supported by coordination between oxygen atoms from ether groups and alkali metal ions to dehydrate water molecules of them. Therefore, both crosslinked tea leaves had preferable selectivity of cesium because of its low hydration energy. Moreover, cesium from the mixed solution with excess amount of sodium was removed by chromatographic column. The completely separation revealed the practical value of tea leaves for cesium removal in industrial application.

At fourth chapter, investigation of protein rich biomass adsorbents, human hair, for precious metal recovery was described. Without any modification, either the white or black hair exhibited higher adsorption ability for gold than those for platinum or palladium. Gold adsorption capacity of human hair is much higher than those of other reported biomass adsorbents. After adsorption, the shape of human hair was not changed by any damages and it was found that gold particles were aggregated on its surface rather than inner layer. Through the contacting of gold with various amino acids as a monomer of protein, it was observed that cystine was the main compound for gold adsorption on human hair as well as less effect of gold adsorption on amino acids with hydroxyl groups. The speculation of cystine appeared oxidation S-S bonds of protein in outmost and middle layers of human hair was confirmed by result of EDS analysis. The most of Pd(II) could be eluted from human hair within 5 minutes after competitive adsorption. Finally, the successful purification of three precious metals using human

hair is proposed by three steps: adsorption of Au(III) and Pd(II) over Pt(IV) on human hair from mixed solution, elution of Pd(II) from gold loading human hair, incineration of gold loading human hair.

The fifth chapter summarizes the results and discussion described in each chapter. Three types of biomass adsorbents had good performance on metal recovery and purification. Even some natural biomass adsorbents having weak adsorption performance, by simple modification, the adsorption of efficiency was improved. One of the most meaningful adsorbents are the protein rich adsorbents, human hair, without any modification. Purification of three precious metals, especially pure gold recovery was accomplished by combined processes as adsorption, elution and incineration with simple and effective routes.

As a result of research works concluded that biomass wastes have high potential for precious metals recovery and hazardous metal removal.

CONTENTS OF TABLES

ACKNOWLEDGEMENTS I
ABSTRACT II
Chapter 1 1
Introduction and research background 1
1.1 Precious metals 1
1.1.1 Platinum group metals 1
1.1.2 The chemical properties of gold and gold compound 7
1.2 Alkali metals 9
1.2.1 Applications of alkali metals 9
1.2.2 Properties of alkali metals 10
1.3 Recovery of precious metals 11
1.3.1 Worldwide supply and demand of precious metals 11
1.3.2 Metallurgical recovery of precious metals from electronic wastes 14
1.4 Hydrometallurgical recovery of precious metals from electronic waste 14
1.4.1 Leaching of precious metal 15
1.4.2 Recovery of precious metals from leaching solution 16
1.5 Cesium removal from polluted water 20
1.5.1 Ion exchange 20
1.5.2 Solvent extraction and solid adsorption 20
1.6 Factors to precious and alkali metals recovery 21
1.6.1 Free energy of ionic hydration 21
1.6.2 Hard and soft acids and bases (HSAB) theory 23
1.7 Biosorption of precious metals and alkaline metals 25
1.7.1 Polysaccharides adsorbents 25
1.7.2 Polyphenol adsorbents 26
1.7.3 Protein rich adsorbents 28
1.8 Objectives and motivation of present research works 28
1.9 References 29
Chapter 2 37
Precious metal ions adsorption on natural polysaccharides and modified kiwi peel adsorbents 37
2.1 Introduction 38
2.2 Experimental 40
2.2.1 Materials and chemicals 40
2.2.2 Preparation of adsorbents 41
2.2.3 Preparation of test solutions 41
2.2.4 Adsorption tests 41
2.2.5 Evaluation of adsorption measurements 42
2.3 Results and discussion 43
2.3.1 Precious metal adsorption on polysaccharides and kiwi peels adsorbents 43

2.3.2 Effect of shaking time of precious metals adsorption on polysaccharides and crosslinked kiwi peels adsorbents 45
2.3.3 Effect of pH on Pt(IV) and Pd(II) adsorption 47
2.3.4 Adsorption isotherms of Pt(IV) and Pd(II) 48
2.3.5 IR spectra of polysaccharides and crosslinked kiwi peel adsorbents ... 49
2.4 Conclusions 52
2.5 References 54
Chapter 3 57
Selective cesium adsorptive removal using crosslinked tea leaves 57
3.1 Introduction 58
3.2 Materials and methods 60
3.2.1 Reagents 60
3.2.2 Preparation method for adsorbents 60
3.2.3 Batch adsorption experiments 60
3.2.4 Column adsorption experiment 61
3.2.5 Evaluation of adsorption measurements 62
3.3 Results and discussion 62
3.3.1 Adsorption of cesium ions on crude and crosslinked tea leaves 62
3.3.2 Effect of shaking time on adsorption of alkali metal ions 65
3.3.3 Effect of pH on adsorption of alkali metal ions 66
3.3.4 Adsorption isotherms of Na^+ and Cs^+ ions on crosslinked fresh and used tea leaves adsorbents 69
3.3.5 Chromatographical separation of Cs^+ over Na^+ ions using crosslinked tea leaves 72
3.3.6 Fourier-transfer infrared analysis 74
3.4 Conclusions 76
3.5 References 76
Chapter 4 80
Effective and selective adsorption of gold from precious metals on unmodified biomass adsorbents-human hair 80
4.1 Introduction 80
4.2 Materials and Methods 83
4.2.1 Reagents 83
4.2.2 Preparation method for adsorbents 83
4.2.3 Experiments of precious metal adsorption in acidic media 84
4.2.4 Au (III) loading experiment with amino acidic solution 84
4.2.5 Au (III) loading with cystine 85
4.2.6 Gold refining from human hair 85
4.2.7 Evaluation of adsorption measurements 85
4.3 Results and discussion 86
4.3.1 Time course dependency of precious metals adsorption on human hair 86
4.3.2 Adsorption of precious metals in individual and competitive systems. 87
4.3.3 Adsorption Langmuir isotherms of precious metals on human hair and

white human hair....89
4.3.4 The oxidation states of Au on human hair after adsorption....92
4.3.5 Characterization of human hair and loading Au (III) human hair....92
4.3.6 Mechanism of gold adsorption on human hair....95
4.3.7 Changed content of element on human hair before and after Au(III) adsorption....98
4.3.8 FT-IR analysis of original and gold loading human hair....101
4.3.9 ^{1}H NMR spectra of the cystine and cystine-coated gold nanoparticles....102
4.3.10 The proposed adsorption model....103
4.3.11 Elution of Pd (II) from human hair after competitive adsorption....104
4.4 Conclusion....105
4.5 References....106
Chapter 5....111
Overall conclusions and future direction....111
5.1 Overall conclusions....111
5.2 Future direction....113

LIST of FIGURES, TABLES, and SCHEMES

List of figures

Fig. 1-1 (a) Synthesis of metal–boryl complexes *via* oxidative addition and (b) oxidative addition and insertion of diborons. 2
Fig. 1-2 Globally marketed platinum-containing drugs. 3
Fig. 1-3 The structures of Pd(II) complexes. 5
Fig. 1-4 Schematic representation of the hydration shell architectures: (a) cubic arrangement of first shell around $[MCl_6]^{n-}$, (b) tetragonal prism arrangement of first shell around $[MCl_4]^{2-}$ (c) cub-octahedral arrangement of second shell around $[MnCl_6]^{n-}$ and (d) combined first and second shell around $[MCl_6]^{n-}$ . . 6
Fig. 1-5 PGMs chloride speciation diagrams, (a) palladium(II), K_1=5.012×10^4, K_2=1.000×10^3, K_3=3.981×10^2, K_3=3.981×10, (b) platinum(IV), K_5=1.037×10^2, K_6=1.023×10^2, (c) rhodium(III), K_1=2.818×10^2, K_2=1.230×10^2, K_3=2.399×10, K_4=1.445×10, K_5=3.981×10, K_6=4.786×10^{-1}, (d) ruthenium(III), K_1=2.512×10^3, K_2=6.310×10^2, K_3=3.326×10^2, K_4=2.570×10^2, K_5=1.413×10^2. 6
Fig. 1-6 Gold(III) chloride speciation diagram, K_1 = 3.236×10^8, K_2 = 1.148×10^8, K_3 = 1.000×10^7, K_4 = 1.175×10^6. 7
Fig. 1-7 The scheme for the stability of gold complexes among properties of elements. 7
Fig. 1-8 The geometric configuration of Au(I) and Au(III) complexes. 8
Fig. 1-9 a World supply of Pt by region (Unit: tons). 11
Fig. 1-10 (a) World supply of Pd by region (Unit: tons). 12
Fig. 1-11 Proposed flowsheet for the recovery of precious metals from electronic scrap by Quinet *et* al. 17
Fig. 1-12 Proposed Pd(II) extraction mechanism for extractant of calix[4]arene derivative by M. Yamada *et* al. 18
Fig. 1- 13 Structures of polysaccharides, R: NH_2 (chitosan), R: OH (cellulose), R: $NHCOCH_3$ (chitin) 25
Fig. 1-14 Chemical structures of the complexane types of chemically modified chitosan. 26
Fig. 1-15 Chemical structures of persimmon tannin and its characteristic units. . 27

Fig. 2-1 Chemical structures of compounds (1)-(7) 39
Fig. 2-2 Operational processes of precious metals adsorption. 42
Fig. 2-3 % adsorption of Au(III), Pd(II) and Pt(IV) on polysaccharides tested in 0.10 M HCl at 30.0°C. 44
Fig. 2-4 Individual adsorption of 1.0 mM Au(III), Pd(II) and Pt(IV) on crude and crosslinked kiwi peels in 0.1 M HCl for 24 h at 30°C. 44
Fig. 2-5 Effect of shaking time on adsorption of (a) Pd(II) and (b) Pt(IV) on chitin adsorbents in 0.10 M HCl at 30.0°C. 45

Fig. 2-6 Effect of shaking time on adsorption of 1.1 mM Au(III), Pd(II) and Pt(IV) on CKP adsorbents in 0.10 M HCl at 30.0°C. 46
Fig. 2-7 XRD spectra of CKP adsorbents in different contacting period with Au(III) ions. 47
Fig. 2-8 Effect of pH on adsorption of (a) Pd(II) and (b) Pt(IV) at 30.0°C for 24 h. 48
Fig. 2-9 Langmuir analysis of adsorption isotherms of (a) Pt(IV) on chitin-EX and (b) Pd(II) on chitin-S in 0.1M HCl media at 30.0°C for 24 h. 49
Fig. 2-10 (a) FT-IR spectra of adsorbed amount of Pd(II) on chitin-EX. 50
Fig. 2-11 FT-IR spectra of (a) KP and (b) CKP. 52

Fig. 3-1 SEM images of tea leaves before and after the crosslinking, (a) FT, (b) CFT, (c) UT and (d) CUT. 63
Fig. 3-2 X-ray diffraction patterns of (a) fresh and (b) used tea leaves before and after the crosslinking. 64
Fig. 3-3 Adsorption of Cs^+ ions on crude and crosslinked tea leaves as a function of equilibrium pH, adsorbent weight=0.05 g, solution volume=10.0 cm^3, $[Cs^+]_i$ =1.0 mM, shaking time=24 h. 64
Fig. 3-4 Effect of time for alkali metal ion adsorption on (a) CFT adsorbents and (b) CUT adsorbents, adsorbent weight=0.05 g, solution volume=10.0 cm^3, $[M^+]_i$ =1.0 mM, pH_e=2.5, shaking time= several hours. 66
Fig. 3-5 Effect of pH dependency on adsorption of alkali metal ions on (a) CFT adsorbents and (b) CUT adsorbents at 303K, adsorbent weight=0.05 g, solution volume=10.0 cm^3, $[M^+]_i$ =1.0 mM each, shaking time=24 h. 68
Fig. 3-6 Effect of pH_e value on distribution ratio of alkali metal ion at 303K, (a) CFT adsorbents and (b) CUT adsorbents, adsorbent weight=0.05 g, solution volume=10.0 cm^3, $[M^+]_i$ =1.0 mM each, shaking time=24 h. 69
Fig. 3-7 Adsorption isotherms: (a) Cs^+ ion on CFT and CUT adsorbents, (b) Na^+ ion on CFT and CUT adsorbents, adsorbent weight=0.05 g, solution volume=10.0 cm^3, pHe=7.0 ± 1.0 (Cs^+) and 7.5 ± 0.5 (Na^+), shaking time=24 h. 70
Fig. 3-8 The Langmuir isotherm kinetic models: (a) Cs^+ ion adsorption on CFT and CUT adsorbents, (b) Na^+ ion on CFT and CUT adsorbents, adsorbent weight=0.05 g, solution volume=10.0 cm^3, pHe=7.0 ± 1.0 (Cs^+) and 7.5 ± 0.5 (Na^+), shaking time=24 h. 71
Fig. 3-9 Breakthrough profiles of Cs^+ and Na^+ ions upon passing the column packed with (a) CFT adsorbents and (b) CUT adsorbents, pH_e= 7.7 (CFT) and 7.4 (CUT), weight of adsorbents= 0.15 g (0.515 cm^3), $[Cs^+]_i$ = 1.84 mM (CFT), 1.80 mM (CUT), $[Na^+]_i$ = 2.68 mM (CFT), 2.39 mM (CUT), flow rate= 5.52 $cm^3\ h^{-1}$ (CFT) and 5.85 $cm^3\ h^{-1}$ (CUT) 73
Fig. 3-10 Elution profiles of the adsorption Cs^+ and Na^+ ion on (a) CFT adsorbents and (b) CUT adsorbents with HCl solution, pH= 1.9, flow rate= 4.68 $cm^3\ h^{-1}$ (CFT), 4.62 $cm^3\ h^{-1}$ (CUT). 74
Fig. 3-11 FT-IR spectra of adsorbents, (a) 1 FT, 2 CFT, 3 CFT- adsorbed Cs^+ and

(b) 1 UT, 2 CUT, 3 CUT- adsorbed Cs^{+}. 75

Fig. 4-1 Effect of shaking time on Au(III), Pd(II) and Pt(IV) adsorption on HH in competitive system of 0.10 M HNO_3 media at 303K, $[Precious\ metal]_i$ = 0.1 mM. 86
Fig. 4-2 Effect of nitric acid concentration on percentage adsorption of precious metals on HH in individual system at 303K, $[Precious\ metal]_i$ = 0.1 mM. ... 87
Fig. 4-3 Effect of hydrochloric acid concentration on percentage adsorption of precious metals on HH at 303K, $[Precious\ metal]_i$ = 0.1 mM. 88
Fig. 4-4 Effect of nitric acid concentration on percentage adsorption of precious metals on HH in competitive system at 303K, $[Precious\ metal]_i$ = 0.1 mM. 89
Fig. 4-5 (a) Adsorption isotherms of precious metals on HH and Au (III) on WHH in 0.1 M nitric acid media at 303K. 90
Fig. 4-6 XRD spectra of (a) Original HH and (b) Au(III)-loading (1.07 mmol g^{-1}) HH. 92
Fig. 4-7 SEM and microscope images of HH before and after Au (III) adsorption: (a) original HH; (b) Au(III)-loading HH(0.493 mmol g^{-1}); (c) the cut section of Au(III)-loading-HH; (d) Au(III)-loading HH (2.881 mmol g^{-1}); (e) the burned Au(III)-loading HH (f) Au(III) loading WHH (0.532 mmol g^{-1}). 94
Fig. 4-8 Individual adsorption of 1.0 mM Au (III) on various amino acid in 0.10 M nitric acid media. 95
Fig. 4-9 Chemical structures of amino acids contained in HH. 97
Fig. 4-10 Digital image of surface of filter membrane after filtration of cystine with Au(III) mixed solution. 98
Fig. 4-11 Analysis of EDS before and after gold loading on the surface of HH (a) original HH, (b) Au loaded HH in HCl, (c) and (d) same sample with different detected area of Au loaded HH in HNO_3. 100
Fig. 4-12 Images of reported source of detected point on the surface of HH (a) corresponded to report in 4.11 (c) and (b) corresponded to reported in 4.11(d). 101
Fig. 4-13 FTIR spectra of original HH and Au(III)-loading HH (0.42 mmol g^{-1}). 102
Fig. 4-14 ^{1}H NMR spectrum of (a) cystine in D_2O-DCl, (b) Au(III) mixture (0 h), (c) Au(III) mixture (1h later), (d) Au (III) mixture (14.5 h later). 103
Fig. 4-15 Elution of loaded precious metals from HH with 0.05 M thiourea containing 0.01 M hydrochloric acid at 303K. 105

List of tables

Table 1-1 Catalytic performance of carbon-supported Pd catalysts in the FA dehydrogenation reaction 3
Table 1-2 PGM species found in aqueous chloride media 4
Table 1-3 Imported of silver and precious metal scrap (unit: kg) 13
Table 1-4 Experimental and calculated hydration enthalpies for cations in kJ $mole^{-1}$ 22
Table 1-5 Classification of acids according to HSAB theory 24
Table 1-6 Classification of bases according to HSAB theory 24

Table 2-1 Amounts of compounds found in pulp and peel of kiwi fruits[a] 39

Table 3-1 Calculated slope value of alkali metal ions based on the Equation (3.5) 68
Table 3-2 Langmuir isotherm constants for adsorption of Na^+ and Cs^+ on adsorbents 71
Table 3-3 Comparisons of adsorption capacities of present adsorbents with various kinds of other adsorbents for Cs^+ ion reported in the literature 72
Table 3-4 Separation and removal Cs^+ from the mixture of Na^+ ions 74

Table 4-1 Amount amino acids present in normal human hair in order their quantity. 82
Table 4-2 Langmuir isotherm constants for adsorption of Au (III) on HH and WHH. 91
Table 4-3 Comparison of adsorption capacities of Au (III) on the present adsorbent with various bio-adsorbents. 91
Table 4-4 Adsorption percentage of Au with different amount percentage amino acids in HH. 96

List of schemes

Scheme 2-1 Possible reactional adsorptions of Pd(II) and Pt(IV) on chitins. 51

Scheme 3-1 Modification of tea leaves and Cs adsorption process in aqueous phase. 65

Scheme 4-1 Proposed adsorption of Au(III) on HH model. 104

Chapter 1
Introduction and research background

The limited resource of precious metals hardly arrives at the demand of their utilizations. Meanwhile, the accidently leakage of cesium dust from nuclear plant also caused serious pollution. Such as these metal problems have been obtained attention and developed the technique of metal recovery at last decades. Biomass-adsorbents as the cheaper, less pollution, and high efficiency materials has become important process of metal separation in hydrometallurgy technique.

1.1 Precious metals

Precious metals are rare and naturally occurring metallic chemical elements with high economic value. Some of precious metals are widely known as the coinage metals, such as silver and gold, and applied in the art and jewelry as well. Besides that, other precious metals included platinum group metals (PGMs): ruthenium, rhodium, palladium, osmium, iridium, and platinum are also widely employed [1].

1.1.1 Platinum group metals

1.1.1.1 Application of PGMs

Platinum-group metals are extremely rare resource by comparison to the other precious metals but are required for the various application. Due to the high temperature stability, melting points and corrosion resistance, platinum, rhodium, iridium and their alloys have been used to make industrial crucibles, which are involved to virtually every industrial process.

Besides that, platinum, palladium and rhodium are also employed to form the intermediate as organic complexes to catalyze the organic reaction [2-3]. Such as the metal-

catalyzed borylation of alkenes, alkynes, and organic electrophiles with B-B compounds was developed to synthesize organoboronic esters from simple organic substrates [4], as shown in Fig. 1-1.

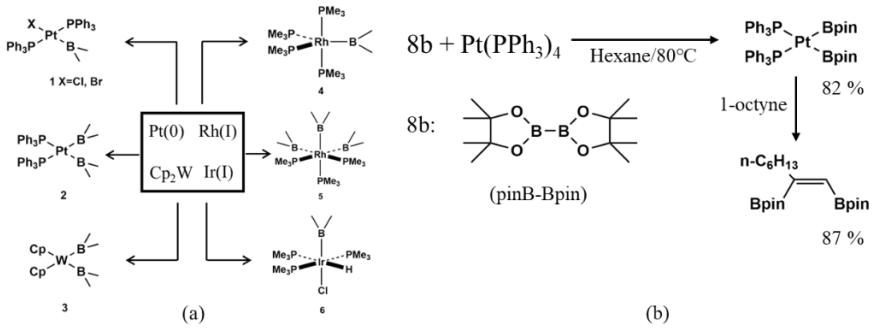

Fig. 1-1 (a) Synthesis of metal–boryl complexes *via* oxidative addition and (b) oxidative addition and insertion of diborons [4].

Moreover, platinum and palladium, as the essential members of PGMs, not only have the high value for commercial utilization such as jewelry, electronics, currency, but also have been employed to apply for hydrogen generator system. The transition metal hydrides have been applied to molecular complexes of transition metals which contain hydrogen in their structures [5]. As the hydrogen carrier, lot of research works have been focused on the performance of formic acid (FA) on Pd based catalytic system and shown the optimizing performance of stability and selectivity as listed in Table 1-1 [6].

Table 1-1 Catalytic performance of carbon-supported Pd catalysts in the FA dehydrogenation reaction

Catalyst	Additive	T (°C)	TOF (h^{-1})	Reference
Monometallic				
Pd/C	HCOONa	25	64[a]	7
Pd/C	HCOONa	25	304[b]	8
$Pd/CN_{0.25}$	None	25	752[b]	9
Pd/C	HCOONa	25	835[b]	10
Pd-B/C	HCOONa	25	1884[b]	8
Pd/C	HCOONa	30	228.3[a]	11
Pd/carbon black	HCOONa	30	1815[b]	12
Pd/N-C	HCOONa	45	645	13
Pd/MSC-30	HCOONa	50	2623[b]	14
Pd/C	$HCOONH_4$	50	7959[b]	15
Pd/C nanospheres	HCOONa	60	7256	16
Pd/N-MSC-30	HCOONa	60	8414[b]	17

Note, "TOF": turnover value
"a": TOF calculated according to the volume of released H_2 in overall testing time
"b": initial TOF number

In addition, certain chemical compounds derived from platinum are antineoplastic, can cause living cells to stop division. As a result of the cells continue to grow, but they never divide or reproduce. Chemotherapy drugs made from platinum, such as cisplatin, have saved thousands of patients. The structures of drugs contain Pt shows in Fig. 1-2.

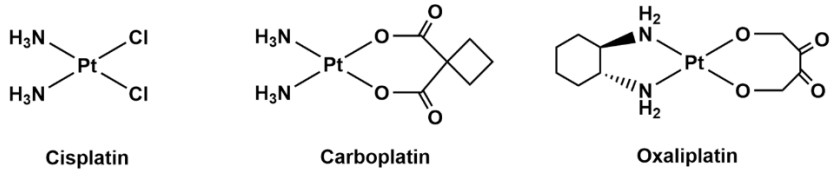

Fig. 1-2 Globally marketed platinum-containing drugs [18].

1.1.1.2 The chemical properties of PGMs

Some of PGMs such as, Ir, Ru, Rh, and Os are referred as the insoluble PGMs into aqueous solution which dissolve more slowly than Pt and Pd. Such difference provides the possibility to partly sperate between these groups under appropriate conditions.

All PGMs can be leached into solution and concentrated as the PGM-chloro complexes in aqueous chloride solution. The major PGM species existed in chloride media are shown in Table 1-2 [19].

Table 1-2 PGM species found in aqueous chloride media

Ruthenium		Rhodium		Palladium	
Ru(III)	$[RuCl_6]^{3-}$ $[RuCl_5(H_2O)]^{2-}$ $[RuCl_4(H_2O)_2]^{-}$ $[RuCl_3(H_2O)_3]$	Rh(III)	$[RhCl_6]^{3-}$ $[RhCl_5(H_2O)]^{2-}$ $[RhCl_4(H_2O)_2]^{-}$	Pd(II)	$[PdCl_4]^{-}$
Ru(IV)	$[RuCl_6]^{2-}$ $[Ru_2OCl_{10}]^{4-}$ $[Ru_2OCl_8(H_2O)_2]^{2-}$	Rh(IV)	$[RhCl_6]^{2-}$	Pd(IV)	$[PdCl_6]^{2-}$
Osmium		Iridium		Platinum	
Os(IV)	$[OsCl_6]^{2-}$	Ir(III)	$[IrCl_6]^{3-}$ $[IrCl_5(H_2O)]^{2-}$ $[IrCl_4(H_2O)_2]^{-}$	Pt(II)	$[PtCl_4]^{2-}$
		Ir(IV)	$[IrCl_6]^{2-}$	Pt(IV)	$[PtCl_6]^{2-}$

The reactivity of PGM depends on the oxidation state of the metal and the property of the reactant ligands. Metals in their divalent oxidation state are easy to toward substitution with soft donor ligands and rates of substitution can be faster than in those for metals in several orders of magnitude their high oxidation states. Pd(II) complexes have high affinity for sulfur and nitrogen donor ligands, the substitution can easily take place with the high reaction rates[20]. Figure 1-3 shows the bi-functional and mono-functional complexes of Pd(II). The mono-complexes have only one coordination site for substitution which are usually used as model molecules in different kinetic studies.

Mono-functional complexes:

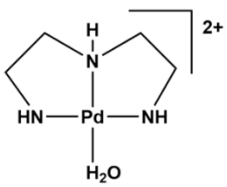

$[Pd(dien)H_2O]^{2+}$

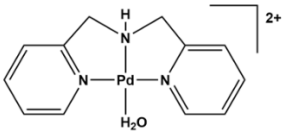

$[Pd(bpma)(H_2O)]^{2+}$

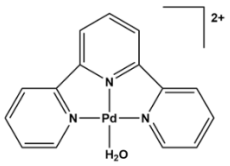

$[Pd(terpy)(H_2O)]^{2+}$

Bio-functional complexes:

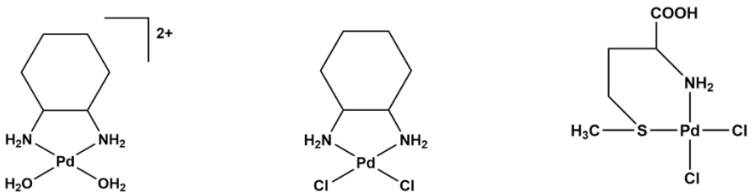

Fig. 1-3 The structures of Pd(II) complexes [20].

All of the PGMs in their tetravalent oxidation state form hexachloro complex anions predominantly in strong chloride media. Anionic complexes of PGMs can be anion-exchanged with other anions of organic bases:

$$nB^{+}Cl^{-} + [MCl_6]^{n-} \rightleftharpoons [B]_n [MCl_6] + nCl^{-} \quad ,$$

where B is cationic species of organic base.

The tendency for metal-chloro complexes to form ion pairs with anion-exchangers is: $[MCl_6]^{2-} > [MCl_4]^{-} >> [MCl_6]^{3-}$> aquo species [21]. That is determined by the charge to size ratio or charge density of the species. The densely charged complexes having larger hydration shells than those of low charge density. And oulombic interactions with their counter ions are consequently became low.

Hence, the solvation shells surrounding complexes of PGMs anions are important in their dissolution, precipitation and reaction. Oxygen atom of water molecule can align with chloro anion by hydrogen bond to form hydration shell. As shown in Fig. 1-4, the octahedral complexes, $[PtCl_6]^{2-}$ and $[RhCl_6]^{2-}$, have two hydration shells. In the first hydration shell, eight water molecules located at eight vertexes of a tetragonal prism. The second geometric arrangement is occupied by 14 water molecules with the formation of O--O bond at the vertexes of a regular 14-sided cuboctahedron (with 8 triangular faces and 6 square faces). Besides, $[RhCl_6]^{-3}$ has a more strongly bound second hydration shell, while second shell of $[PtCl_6]^{2-}$ is more diffuse. The square planar complexes, $[PtCl_4]^{2-}$ and $[PdCl_4]^{2-}$, have only one hydration shell. The 8 water oxygen atoms are each equidistant from two adjacent chlorine atoms to form a less symmetric tetragonal prism [22].

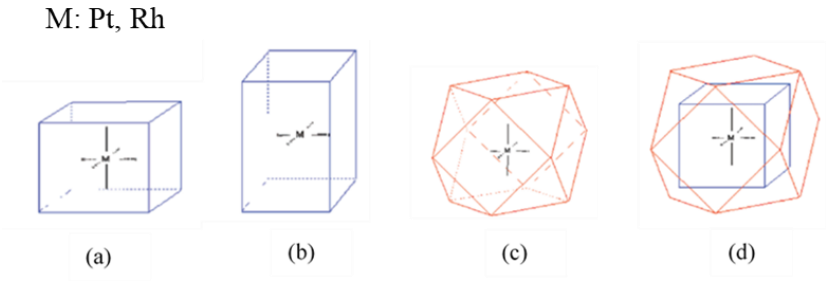

Fig. 1-4 Schematic representation of the hydration shell architectures: (a) cubic arrangement of first shell around $[MCl_6]^{n-}$, (b) tetragonal prism arrangement of first shell around $[MCl_4]^{2-}$ (c) cub-octahedral arrangement of second shell around $[MnCl_6]^{n-}$ and (d) combined first and second shell around $[MCl_6]^{n-}$ [22].

In addition, the protonation of strong base is much easier than weak base. That means behavior of ion-exchangers has relation to acid concentration. Strong organic base can be easily protonated with low hydrochloric acid concentration. On contrary, weak organic base prefers to be protonated at high hydrochloric acid concentration. While the increasing of chloride concentration makes $[Cl]^-$ and metal-complex anion become competitive.

The species of chloride complexes anions can be transferred to each other with the adjustment of $[Cl]^-$ concentration as shown in Fig. 1-5 [23-26].

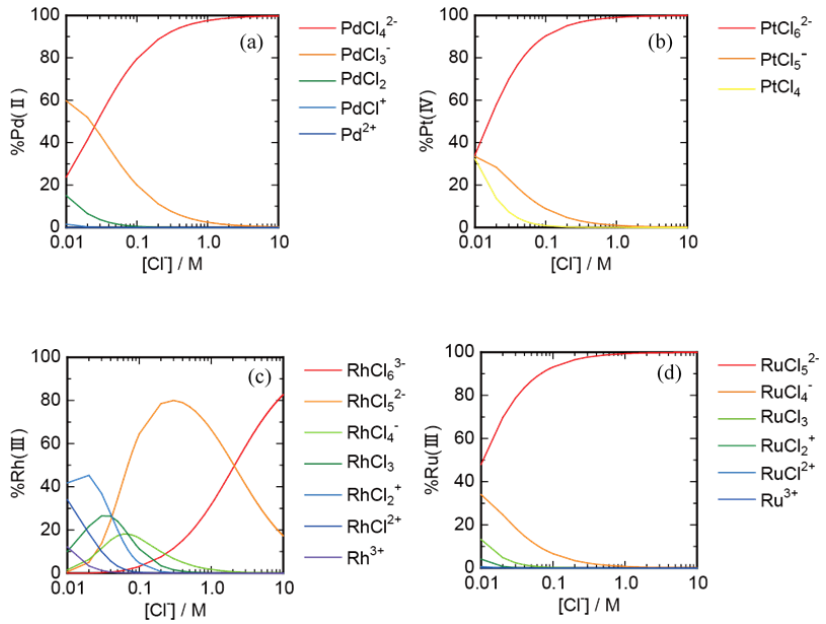

Fig. 1-5 PGMs chloride speciation diagrams, (a) palladium(II), K_1=5.012×10^4, K_2=1.000×10^3, K_3=3.981×10^2, K_3=3.981×10, (b) platinum(IV), K_5=1.037×10^2, K_6=1.023×10^2, (c) rhodium(III), K_1=2.818×10^2, K_2=1.230×10^2, K_3=2.399×10, K_4=1.445×10, K_5=3.981×10, K_6=4.786×10^{-1}, (d) ruthenium(III), K_1=2.512×10^3, K_2=6.310×10^2, K_3=3.326×10^2, K_4=2.570×10^2, K_5=1.413×10^2 [23-26].

1.1.2 The chemical properties of gold and gold compound

Gold is the only metal which can not be affected by the air or water by either oxygen or sulfur atoms and has durability under the most corrosive conditions. Hence, it has high value as jewelry and coinage. Although, gold has oxidation states of -1, +2, +4 and +5, it in nature states are the $AuTe_2$ and $AuSb_2$ species. Gold complexes in aqueous solution exist two oxidation states: the aurous(+1) and auric(+3) which are widely applied in the gold complexes of hydrometallurgy. The chloro-complexes of Au at high concentration of Cl^- media exist as auric (+3) as shown in Fig. 1-6 [26].

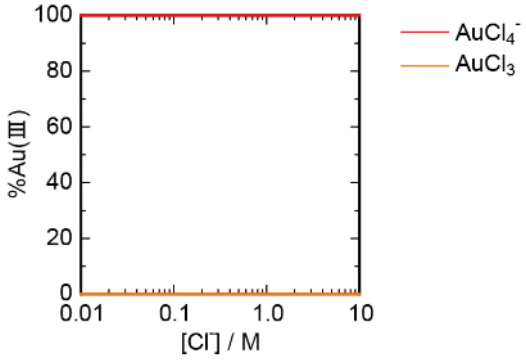

Fig. 1-6 Gold(III) chloride speciation diagram, K_1 = 3.236×10^8, K_2 = 1.148×10^8, K_3 = 1.000×10^7, K_4 = 1.175×10^6 [26].

Au(I) and Au(III) are unstable in aqueous solution and easy to be reduced by oxygen molecules in water to metallic gold. The stability of complexes of Au(I) and Au(III) tends to decrease as the increase of electronegativity from ligand donor atom. For example, according to the order of electronegativity among halogen, $F^->Cl^->Br^->I^-$, the stability of complexes is decreased as that order. The possible formation of gold complexes is followed the scheme, as shown in Fig. 1-7 [27].

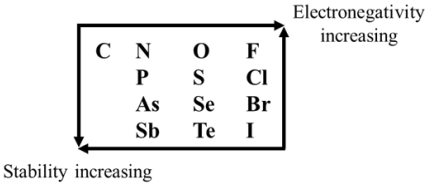

Fig. 1-7 The scheme for the stability of gold complexes among properties of elements [27].

According to the scheme accounts for the stability orders, such orders as $SeCN^-$> SCN> OCN> or CN>NH_3> H_2O. The weak electronegativities of Te and Sb make the states of $AuTe_2$ and $AuSb_2$ enough stable to be found in nature.

Generally, oxidation of gold complexes, AuL_2^+ or AuL_4^{3+} depends on the strength of the oxidizing reagents and on the relative standard reduction potential for the reduction. The less electronegative or "soft" donor atoms prefers metal ions with low valency. On the contrary, the "hard" donor atoms are suitable for metal ions with high valency [28]. Therefore, Au(I) forms more stable complexes with ligands containing less electronegative "soft" donor atoms, such as, S, C, Se and P. While, Au(III) has more stable complexes with more electronegative or "hard" donor atoms such as, N, O, F, Cl. It indicates that for the transfer between Au(I) and Au (III), the complexes of Au(III) with soft ligands are easy to be reduced to gold(I) complexes. It also means the formation of gold chloro-complexes in chloride anion exists as $[AuCl_4]^-$ rather than $AuCl_3$.

In additional, the general coordination number of Au(I) is 2 and 4 for Au(III). They were determined from the different geometric configuration of the complexes, Au(I) tends to form linear complexes, while Au(III) tends to form square planar complexes, such as $AuCN^{2-}$ and $AuCl_4^-$ as shown in Fig. 1-8. Neither Au(I) nor Au(III) exists as a metal ion itself in solution, but in a hydrated states as complexes, the number of water molecules to the coordination is different. At hydrated states, the atom bound to gold is oxygen, these complexes are not stable.

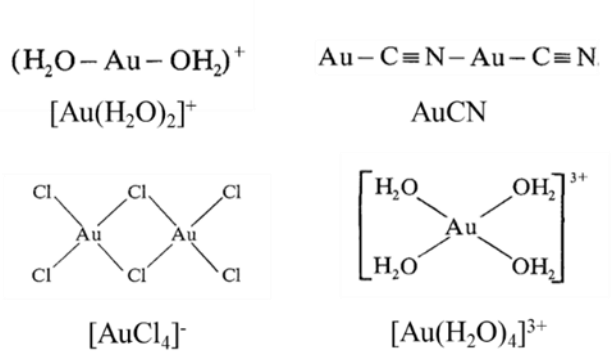

Fig. 1-8 The geometric configuration of Au(I) and Au(III) complexes.

1.2 Alkali metals

Alkali metals locate at the first group in periodic table and contain lithium (Li), sodium (Na), potassium (K), rubidium (Rb), cesium (Cs) and francium (Fr). Due to superbly strong activity of metallic alkali metals, such as reaction with water or air, there is no alkali metals themselves in the nature.

1.2.1 Applications of alkali metals

Lithium has been always used in lithium-batteries as the anode and mixed in alloys with magnesium and aluminum to improve metallic strength and luster. The lithium oxide is introduced into silica to prevent from corrosion [29]. Lithium carbonate is used as a mood stabilizer in psychiatry [30].

Sodium and potassium as the essential elements have been in all known biological system functioning as electrolytes inside and outside cells [31-32]. Their salts have various applications in wide fields, such as sodium salts of fatty acids in soap, sodium-vapour lamps, potassium nitrate in plant nutrient solution, potassium hydroxide solution in pH adjuster, potassium superoxide breathing masks.

Rubidium and cesium are usually used in atomic clocks to improve accuracy. Cesium is the most active metal in the alkali metals. Its radioisotope, ^{137}Cs, is applied for nuclear fuel but gives damage for human body. In addition, potassium alloys with sodium can be used in faster breeder nuclear reactors. Francium has been used in spectroscopy experiments to study the energy levels and coupling constants between subatomic particles [33].

1.2.2 Properties of alkali metals

Due to the ns^1 valence electron configuration (n=1,2,3,4,5,6) which determined weak metallic bonding, all alkali metals mechanically are soft and have low densities, melting and boiling points [34]. Alkali metals have high thermal and electrical conductivity as well. Furthermore, electronegative, melting point and boiling point decrease as the increase of atomic radii, reactivity oppositely increases as the increase.

All the alkali metals are never found in elemental forms in nature. The alkali metal halides have white ionic crystalline compounds and are soluble in water except lithium fluoride. The solubility of alkali metal salts in water is high, it is caused by large entropies of solution and endotherm when it was dissolved [35]. Therefore, it implies low hydration energy of alkali metals which are weakly hydrated with water molecules in aqueous phase [36]. Unlike high charge metals ordering their vicinity of water molecules around by strong hydration, alkali metals have a tendency to disrupt the aqueous bulk structure.

Hydration energy of alkali metals is dependent by the size of ionic radii. As the increase of cation radius, decrease of charge density leads to low hydration energy. Sufficiently high hydration energy of Li^+ makes the it reduce as being most electropositive alkali metal. On the contrary, Cs^+ with lowest charge density has the less effect to water matrix than other alkali ions. At the same time, its large size increased the geometrical possibility of higher coordination number than eight. Hydrated alkali metals lithium ion is four-coordinate in water. Sodium(I) is with five and six-coordinate, potassium(I) is with six and seven-coordinate, rubidium(I) and cesium(I) are with eight-coordinate. Sodium, potassium, rubidium and cesium ions are only weakly hydrated with a single shell of water molecules. Furthermore, smaller lithium is more strongly hydrated most probably with a second hydration shell [37].

1.3 Recovery of precious metals

1.3.1 Worldwide supply and demand of precious metals

As the world population and global economies continuously grow with fast pace, special advancement in technology and the demand of precious metals has been rapidly risen.

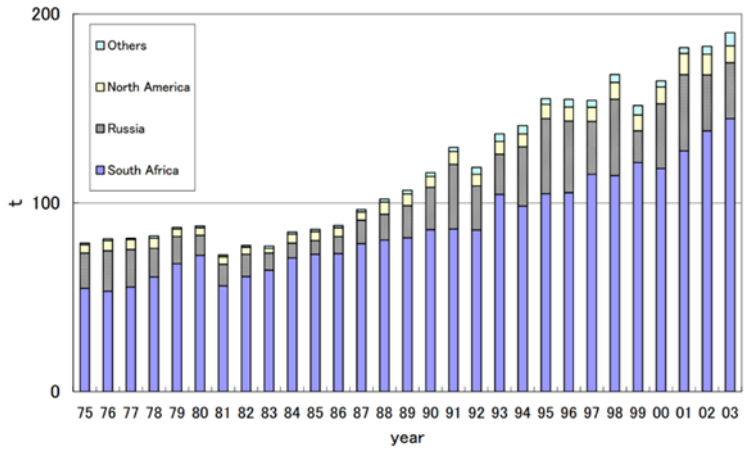

Fig. 1-9a World supply of Pt by region (Unit: tons).

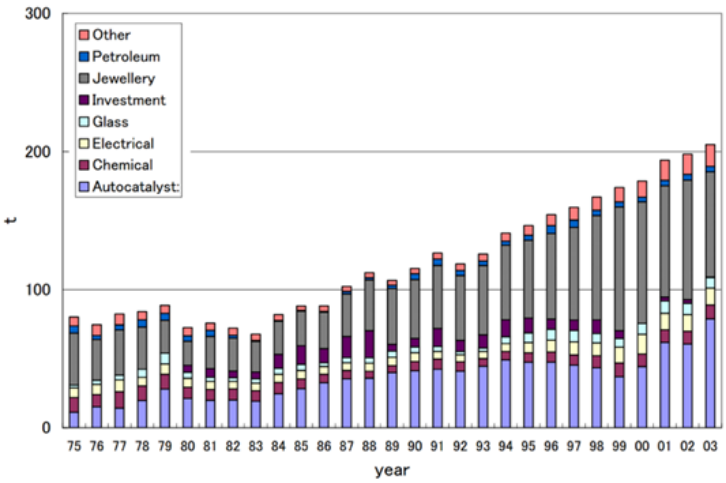

Fig. 1-9b World demand of Pt by market sector (Unit: tons).

Due to high value to store, in PGMs, Pt shows largest supply and demand [38]. Figures 1-9 (a) and (b) exhibit the world supply and demand of Pt from 1975 to 2003 [38]. In the past decades, largest of demand of Pt as jewelry has dramatically grown up. Meanwhile,

the increased number of diesel-powered vehicles led to surge demand of Pt in autocatalyst as well. While, the ongoing consumption of the limited resource will eventually lead to a rapid depletion of metal ores. It was found that demand of Pt was furtherly over the its supply from 2001 to 2003. The apparent difference illustrates that recovery of precious metals from waste has been gradually aware and partially worked out.

The world supply and demand of Pd are shown in Figs. 1-10 (a) and (b) [38]. The efficient application of Pd in mobile phones accelerated its demand for electronics. On contrary, tremendous amounts of electronic waste are generated from electronic productions in the constantly innovated technology.

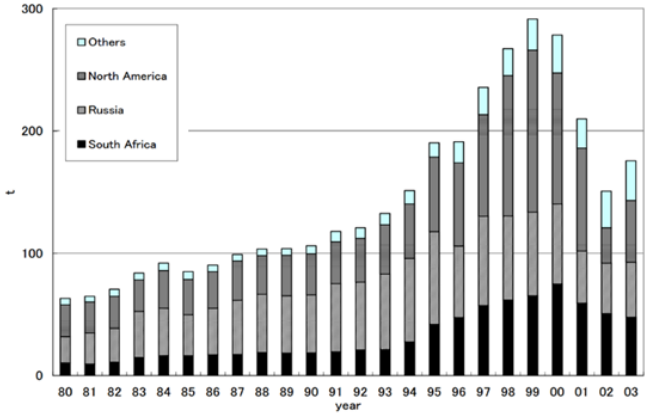

Fig. 1-10 (a) World supply of Pd by region (Unit: tons).

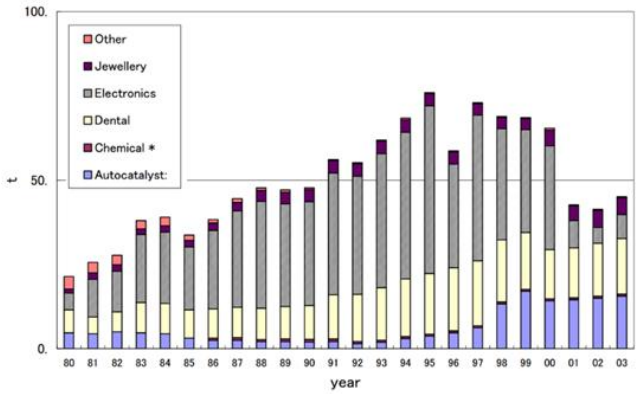

Fig. 1-10 (b) World demand of Pd by market sector (Unit: tons).

Decades ago, amounts of metal scrap have been imported in Japan to recycle metal resource. Table 1-3 lists the amount of precious metal scrap that has been imported by Japan since 1994 [38]. Since 2002, the scrap was reclassified into gold, silver and platinum.

Table 1-3 Imported of silver and precious metal scrap (unit: kg)

Year	HS number				Korea	Hong Kong	Singapore	United States	Total imports
1994	7112-90-000	Silver scrap			-	87539	216019	242817	685257
1995	7112-90-000	Silver scrap			1469	126415	207982	258455	764498
1996	7112-90-000	Silver / precious metal scrap			275435	1256187	2618874	53577294	15125733
1997	7112-90-000	Silver / precious metal scrap			3609047	1112175	2967760	5937871	18296905
1998	7112-90-000	Silver / precious metal scrap			3826064	999363	3174250	5996768	17679525
1999	7112-90-000	Silver / precious metal scrap			2841844	1621476	2103179	2646708	11692212
2000	7112-90-000	Silver / precious metal scrap			975530	783510	2086540	3530482	10977147
2001	7112-90-000	Silver / precious metal scrap			841615	223351	2498637	3619785	11012030
2002	7112-9	Silver / precious metal scrap	(1)	(2)+(3)+(4)	659866	142099	2832088	3585037	11999739
	7112-90-000	Gold scrap (*1)	(2)		3490	64	62390	-	355692
	7112-90-000	Platinum scrap (*2)	(3)		97989	78	11108	1453171	1859398
	7112-90-000	Silver scrap (*3)	(4)		558387	141957	2758590	2131866	9784649

*1) 7112-90-000: Gold scrap (including scrap metal with gold attached, excluding other precious metals)

*2) 7112-90-000: Platinum scrap (including scrap metal with platinum attached, excluding other precious metals)

*3) 7112-90-000: Sliver scrap (including scrap metal with sliver attached) other types of scrap used in the recovery of precious metals and scrap containing precious metals or their alloys)

1.3.2 Metallurgical recovery of precious metals from electronic wastes

Newly, the proposed treatment of electronic wastes includes reduce, reuse, recycling and replacement. Reuse is the priority and cheaper operation to electronic waste. When some electronic equipments are far behind the technological footsteps, they are treated as waste as incineration or recycling for other purposes.

As Cui *et* al. reported, precious metals make up more than 60% of value to cell phones, calculators and printed circuit board scraps [39]. There generally has main three steps of recycling electronic waste [40]. First process is disassembly, selectively disassembly, targeting on singling out hazardous or valuable components. Secondly, use mechanical process and metallurgical processes to up-grade desirable materials content for preparation of refining process. Final step is purification of the recovered materials by chemical processes.

Generally, metallurgical techniques have two methods for melting or dissolving the recovered metals at the third step to remove the impurity, pyrometallurgical and hydrometallurgical processes. In addition, bio-metallurgical processes involving biosorption of precious metals are also focused on.

Pyrometallurgical process has been a remarkably traditional method to recover precious metals in the past decades, it includes incineration, smelting in furnace or blast furnace, drossing, sintering and melting and reaction at high temperature [41-42]. Although, pyrometallurgical techniques are massively employed into the factories, the limited separated ability and serious pollution are not avoidable.

1.4 Hydrometallurgical recovery of precious metals from electronic waste

Compared with pyrometallurgical processes, hydrometallurgical method is more predictable to easily control. By hydrometallurgical method, the recovered materials are firstly leached into solution. After the first treatment, the solution is separated on the purpose of purification procedures such as precipitation of impurities, solvent extraction, adsorption and ion-exchange to individually concentrate metal. Furthermore, some of the

treated solution possibly get through the electrorefining processes which involves reduction or crystallization to recover metal [43-44].

1.4.1 Leaching of precious metal

The most common leaching agents for precious metal recovery are cyanide, halide, thiourea and thiosulfate [45-47].

1. Halide leaching

Sometimes, halide system is used for gold dissolution pre-dates cyanidation [48]. Among all halides, only chlorine/chloride has been applied industrially on large scale. The PGMs concentrated materials are generally leached in high concentration of hydrochloric acid solution together with chlorine gas as an oxidant [49]. It is also well known that aqua regia, a mixture of concentrated hydrochloride and nitric acids (3:1), has been an effective leachant for PGMs and gold.

Leaching platinum by hydrochloride acid and regia solution is expressed in equations (1.1) and (1.2):

$$Pt + 2HCl + 2Cl_2 \rightleftharpoons H_2PtCl_6 \quad (1.1)$$

$$3Pt + 18HCl + 4HNO_3 \rightleftharpoons 3H_2PtCl_6 + 4NO + 8H_2O \quad (1.2)$$

Palladium is partially soluble in HCl without any oxidizing reagents and totally soluble in aqua regia. Only PGMs are soluble in nitric acid. The reactions are expressed in equations (1.3), (1.4) and (1.5).

$$Pd + 2HCl + 2Cl_2 \rightarrow H_2PdCl_6 \quad (1.3)$$

$$3Pd + 18HCl + 4HNO_3 \rightarrow 3H_2PdCl_6 + 4NO + 8H_2O \quad (1.4)$$

$$Pd + Cl_2 \rightarrow PdCl_2 \quad (1.5)$$

While, the valent stable state of Pt is tetravalent and divalent state for Pd at the above reactions [49].

2. Cyanide leaching

Dissolution of gold in aerated cyanide solution is frequently used in electrochemistry. The dissolution reactions are shown in equations (1.6) and (1.7) [50]:

$$4Au + 8CN^- \rightarrow 4Au(CN)_2^- + 4e^- \quad (1.6),$$

$$O_2 + 2H_2O + 4e^- \rightarrow 4OH^- \quad (1.7).$$

Dorin groups investigated the maximum dissolution of precious metals in cyanide solution at pH 10-10.5. The order of activity of noble metals is Au > Ag > Pd> Pt [50].

3. Thiourea leaching

Gold(I) forms strong cationic complex $Au[SC(NH_2)_2]_2^+$ with thiourea, the reaction as equation (1.8):

$$Au + 2CS(NH_2)_2 \rightarrow Au(CS(NH_2)_2)_2^+ + e^- \quad (1.8).$$

Thiourea as gold leaching reagent with higher effectiveness still has defect for commercial application, such as, higher consumption and cost compared with cyanide leaching [51].

4. Thiosulfate leaching

Gold dissolution in ammoniacal thiosulfate is an electrochemical reaction catalyzed by the presence of cupric ions, as expressed in equations (1.9) and (1.10). Conversion of $Cu(NH_3)_4^{2+}$ to $Cu(S_2O_3)_3^{5-}$ ions is dependent on the concentration of $S_2O_3^{2-}$ [52].

$$Au + 5S_2O_3^{2-} + Cu(NH_3)_4^{2+} \rightarrow Au(S_2O_3)_2^{3-} + 4NH_3 + Cu(S_2O_3)_3^{5-} \quad (1.9)$$

$$2Cu(S_2O_3)_3^{5-} + 8NH_3 + 1/2O_2 + H_2O \rightarrow 2Cu(NH_3)_4^{2+} + 2OH^- + 6S_2O_3^{2-} \quad (1.10)$$

Zipperian et al. reported that a loss of up to 50% of thiosulfate in ammoniacal thiosulfate solutions which contain copper [53].

1.4.2 Recovery of precious metals from leaching solution

To recover the precious metals, leaching solution is usually treated together with several methods of precipitation, solvent extraction, liquid-solid adsorption and ion exchange. Quinet *et* al. investigated their bench-scale extraction study on the applicability of feasible hydrometallurgical processing routes to recover precious metals from mobile phones [46]. The summarized proposed flowsheet is shown in Fig 1-11.

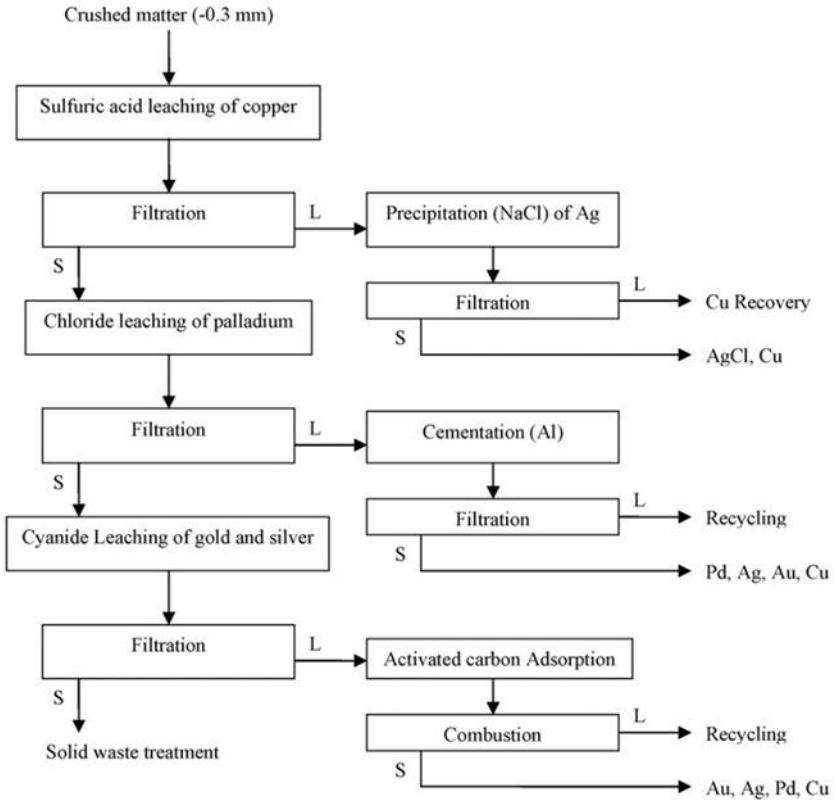

Fig. 1-11 Proposed flowsheet for the recovery of precious metals from electronic scrap by Quinet *et* al [46].

The beginning crude material contained 27.37% copper, 0.52% silver, 0.06% gold and 0.04 palladium. After crushing and size separation, the smallest size portion was studied by a series of hydrometallurgical processes, such as, sulfuric acid leaching, chloride leaching, thiourea leaching, cyanide leaching, cementation, precipitation, ion exchange, and activated carbon adsorption. The permitted recoveries are 93% silver, 95% gold, 99% palladium.

1. Cementation

Zinc cementation has been used for gold recovery from cyanide solution on a commercial scale. The reactions [54] are expressed in equations (1.11) and (1.12):

$$2Au(CN)_2^- + 2e^- \rightarrow 2Au + 4CN^- \quad (1.11),$$

$$Zn + 4CN^- \rightarrow Zn(CN)_4^{2-} + 2e^- \quad (1.12).$$

Awadalla and Ritcey reported that sodium borohydride (SBH) could be recovered gold from thiourea, thiosulfate or thiocyanate solution and stably formed reduction-

precipitation [55]. The result also indicates that thiourea is not only an effective leachant for gold material but also a stripping reagent of gold from loading solvents or resins.

2. Solvent extraction

The designable functional groups of extractant tremendously promote the selectivity to target metal, hence, solvents extraction has been popularly investigated in many years. From the perspective of extractant, effective factors of extraction include: polarity of extractant, main function groups, molecular size of extractant *etc*.

For precious metal extraction, extractants includes, organophosphorus derivatives, guanidine derivatives and small polymer such as calixarene derivatives [56-59]. Yamada *et* al. reported that calix[4]arene type extractant with sulfur atoms had selectivity to Pd(II) in among of precious metals and other heavy metals [59]. The proposed mechanism of Pd(II) extraction is shown in Fig. 1-12. Furthermore, most of Pd(II) was stripped from 0.1 M (M= mol dm^{-3}) thiourea in 1.0 M HCl solution as eluents. The effective recycled recovery is feasible.

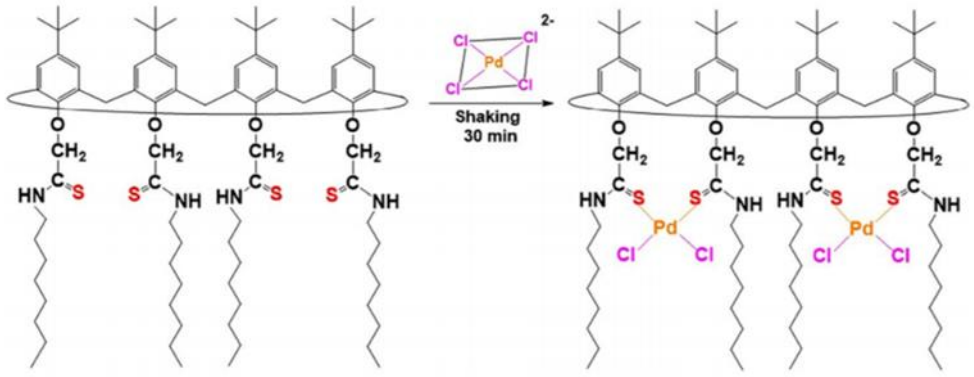

Fig. 1-12 Proposed Pd(II) extraction mechanism for extractant of calix[4]arene derivative by M. Yamada *et* al [59].

Additionally, synergistic extractant that contains more than two coinciding extractants is occasionally employed into extraction to increase thermodynamic effect [60]. While, large scaled consumption of organic solvent could cause the environmental pollution and the high cost for synthesis also challenges the development of extractant in factory application.

3. Liquid-solid adsorption

Adsorption on solid with priority to solvent extraction is distinct by the reactive phases. Adsorption not only takes place the surface of solid phase or at the interface between solid and liquid, but also takes place inside adsorbent layers. It depends on physical structure of adsorbents, such as crystallinity, size of pore or degree of polymerization for some polymers *etc*.

According to material source, there exists two kinds adsorbents: synthesized and biomass adsorbents. Synthesized adsorbents for precious metal adsorption include, polymer gels, silica gel, crown ether functionalized composite and activated carbon *etc*. [61-65]. Biomass adsorbents will be introduced at next section. Although, metal adsorption consumes less solvent, the complicated synthesized or modified processes of adsorbents are inevitable.

4. Ion exchange

Ion-exchange resins have functional groups which could concentrate salt ions. Commercial ion-exchange resins with small quaternary ammonium moieties have high yield of recovered gold [66]. According to basicity of resins, the resins are simply classified into weak base resins and strong base resins. Weak base resins contain primary, secondary or tertiary amine functional groups and the ion-exchange is affected by the proton concentration. The protonated resins could form complexes with gold by anionic exchange in thiosulfate solution, as expressed in equations (1.13) and (1.14) [67].

$$|\text{—}NR_2 + HX \rightleftharpoons | \text{—}NR_2H^+X^- \quad (1.13)$$

$$3|\text{—}NR_2H^+X^- + [Au(S_2O_3)_2]^{3-} \rightleftharpoons (|\text{—}NR_2H)_3^+[Au(S_2O_3)_2]^{3-} + 3X^- \quad (1.14)$$

Strong base resins contain quaternary ammonium functional groups and have no limitation of proton concentration. They can directly form the complex with gold by anionic exchange without protonation, as expressed in equation (1.15) [67].

$$|\text{—}NR_3^+X^- + [Au(S_2O_3)_2]^{3-} \rightleftharpoons (|\text{—}NR_3)_3^+ [Au(S_2O_3)_2]^{3-} + 3X^- \quad (1.15)$$

As Dong *et* al. reported that when other competitive anions coexisted strong base resins exhibited poor selectivity for gold. However, they have higher gold loading capacities than those of weak base resins [67].

In addition, ion exchange resins have been broadly applied for base metals exchange to improve the hardness of water. It would be introduced at next section.

1.5 Cesium removal from polluted water

Cesium is the byproduct of fuel fission nuclear, leakage of it is crucial. Accident leakage nuclear dust which contains hazardous radioactive metals will be eventually adsorbed onto soil and contaminated into the groundwater and nearby seawaters *etc*. Water contaminating cesium and other radioactive elements reached into human body through the food chain causing several ill health effects including cancers for longer terms. Recovery of radioactive metals from polluted water is much different from recovery of precious metals, due to high water solubility and competitive ions. In other words, much amount of natural metal ions in water such as, sodium, potassium, calcium, have similar properties and make competition complicated.

1.5.1 Ion exchange

Ion exchange is preferable and cheap method on large scale of water quality treatment, such as water softening. As stated chemical component in ion exchangers, they are classfied into organic and inorganic types. Classic inorganic materials include synthetic or natural zeolites, titanates, zirconium phosphates, ammonium oxides, hydrous oxides and pillarfed clay *etc*. [68-70]. The organic resins such as resorcinol and formaldehyde polymers with attaching chelating groups are favorable to cesium removal as well [71].

1.5.2 Solvent extraction and solid adsorption

Selection of optimal functional groups and extractants with optimal cavity size can enhance the selectivity to cesium extraction. Calix[4]arene derivatives, dicarbollides and crown ethers are generally proposed for cesium recovery.

Butyl or pentyl calixarenes has selectivity for cesium over other alkali cations. In addition, increasement of molecular size decreased the selectivity: calix[8]arene < calix[6]arene < calix[4]arene [72].

In acidic medium, poorly hydrated dicarbollide anions associate with cations to neutral compounds which is insoluble in water as expressed in equation (1.16),

$$M^{n+}_{aq} + nH^{+}_{org} + nCoB^{-}_{2org} \Leftrightarrow nH^{+}_{aq} + M^{n+}_{org} + nCoB^{-}_{2org} \quad (1.16).$$

Due to lipophilicity of anion, it has trouble in protonation and discrimination to cations according to their Gibbs energies of transfer. Cesium is consequently and effectively extracted by dicarbollide anion, because of its lowest energy of transfer to polar organic solvents among other cations [73].

Introduction of alkyl or aryl group onto 15-crown-5 and 18-crown-6 can increase their lipophilicity as well. Benzocrown ethers are preferable for monovalent cations extraction, while, divalent cations are privileged to cyclohexano crowns [74].

Adsorbents of cesium adsorption are largely made from biomass resource. Those materials have low cost and high efficiency for cesium removal, they would be introduced at next section.

1.6 Factors to precious and alkali metals recovery

Either precious metal or alkali metals, when they were adsorbed or extracted from aqueous phase to the other phase, the processes always involve release of metal ions from aqueous phase, attaching with adsorbents or extractants.

1.6.1 Free energy of ionic hydration

Generally, metal ion exists in aqueous solution as a hydration ion by coordination with oxygen atom from water molecule. Thus, for transfer the metal ion from aqueous phase to organic liquid or solid phase, the higher hydration energy brings difficulty to convert. Ionic hydration plays an important role in many chemical processes. In general, ionic hydration of enthalpy is related to the ionic radius and polarizing power of the ion. Derek *et*. al. studied ionic hydration enthalpies of various metal ions, parts of which are listed in Tables 1-4 [75].

From the comparison in tables, each alkali metal ion has same valency but different energy, due to the different ionic radius. On the other hand, potassium has similar ionic

radius with calcium but less energy than it because of the different charge. Hence, charge density has effect on movement of metal ions from aqueous phase to the organic or solid phase and contacting with extractants or adsorbents. In addition, hydration energies of alkali metal ions are much less than those of precious metal ions. It means that most of alkali ions can totally be separated from water molecular by attaching on adsorbents or with extractant. For precious metals, some of its hydration water can be replaced by other molecules or ions. Besides, they are directly complexed with stronger electronegativity anion, such Cl^- in HCl solution, the complexed anion has interaction with water molecule, as mentioned in section 1.1. Complexation of a metal ion can be viewed as the process in which the hydrated water molecules are replaced with other molecules or ligands [76].

Table 1-4 Experimental and calculated hydration enthalpies for cations in kJ $mole^{-1}$

Ion	$-\Delta H^o_{hyd}$ (expt)	$-\Delta H^o_{hyd}$ (calc) (2)	$-\Delta H^o_{hyd}$ (calc) (1)
H^+	1091	1190	820
Li^+	519 (3)	540	480
Na^+	409 (3)	410	390
K^+	322 (3)	320	330
Rb^+	293 (3)	300	300
Cs^+	264 (3)	270	280
Ag^+	473 (3)	490	330
NH_4^+	307 (10)	300	300
Mg^{2+}	1921 (6)	1920	1870
Ca^{2+}	1577 (6)	1560	1520
Pd^{2+}	1989 (20)	1970	1640
Pt^{2+}	2100 (20)	2050	1640
Ag^{2+}	1931 (20)	1960	1600
Au^{3+}	4735 (100)	4830	3990

The probable error existed in kJ $mole^{-1}$, without regard for the inherent systematic error of ± 10 kJ $mole^{-1}$. The calculated values ΔH^o_{hyd} (calc) (2) and ΔH^o_{hyd} (calc) (1) refer, respectively, to values obtained from eqs.: $\Delta H^o_{hyd}=\frac{700z^2}{r+0.85}$ kJ $mole^{-1}$(1) and $\Delta H^o_{hyd}=-\frac{930(z-0.2)^2}{r+1-(1/2z)}$ kJ $mole^{-1}$ (2).

1.6.2 Hard and soft acids and bases (HSAB) theory

There has selective relation between metal ions and functional groups from compounds. The principle of hard and soft acids and bases (HSAB) states that hard bases prefer to coordinate to hard acids and soft acids prefer to be coordinated with soft bases.

According to definition by R. G. Pearson, soft base as donor atom with high polarizability and low electronegativity can be easily oxidized and associated with empty or low-lying orbitals. While hard base as donor atom with low polarizability and high electronegativity are hard to oxidize or associated with empty orbitals of high energy and hence inaccessible. Outer electrons of soft acid as an acceptor atom with of low positive charge and large size are easily excited. Outer electrons of hard acid as an acceptor with high positive charge and small size are not easily excited [77].

N (base) + S-X (acid-base complex) ⇌ N-S (acid-base complex) + X (base) (1.17)

As expressed in equation (1.17), X may simply exist in the solution as solvent, such as water molecule, while, when N-S is more stable, the complex of S-X would be converted. N-S could be that of a stable organic or inorganic molecule, a complex ion, or a charge transfer complex. The classification of acids and bases is listed in Tables 1-5 and 1-6.

Table 1-5 Classification of acids according to HSAB theory [78]

Hard	Border line	Soft
H^+, Li^+, Na^+, K^+ Be^{2+}, Mg^{2+}, Ca^{2+}, Sr^{2+}, Sn^{2+} Al^{3+}, Sc^{3+}, Ga^{3+}, In^{3+}, La^{3+} Cr^{3+}, Co^{3+}, Fe^{3+}, As^{3+}, Ir^{3+} Si^{4+}, Ti^{4+}, Zr^{4+}, Th^{4+}, Pu^{4+}, Vo^{2+} UO_2^{2+}, $(CH_3)_2Sn^{2+}$ $BeMe_2$, BF_3, BCl_3, $B(OR)_3$ $Al(CH_3)_3$, $Ga(CH_3)_3$, $In(CH_3)_3$ RPO_2^+, $ROPO_2^+$ RSO_2^+, $ROSO_2^+$, SO_3^+ I^{7+}, I^{5+}, Cl^{7+} R_3C^+, RCO^+, CO_2, NC^+ HX (hydrogen bonding molecules) O, Cl, Br, I,	Fe^{2+}, Co^{2+}, Ni^{2+}, Cu^{2+}, Zn^{2+}, Pb^{2+} $B(CH_3)_3$, SO_2, NO^+	Cu^+, Ag^+, Au^+, Tl^+, Hg^+, Cs^+ Pd^{2+}, Cd^{2+}, Pt^{2+}, Hg^{2+}, CH_3Hg^+ Tl^{3+}, $Tl(CH_3)_3$, BH_3 RS^+, RSe^+, RTe^+ I^+, Br^+, HO^+, RO^+ I_2, Br_2, ICN, etc. Trinitrobenzene, etc. Chloranil, quinones, etc. Tetracyanoethylene. etc.

Table 1-6 Classification of bases according to HSAB theory [77]

Hard	Border line	Soft
H_2O, OH^-, F^-, $CH_3CO_2^-$ PO_4^{3-}, SO_4^{2-}, CO_3^{2-}, ClO_4^-, NO_3^-, ROH, RO^-, R_2O, NH_3, RNH_2, N_2H_4	C_5H_5N, N_3^-, Cl^-, NO_2^-, SO_3^{2-}	R_2S, RSH, RS^-, I^-, SCN^-, $S_2O_3^{2-}$, Br^-, R_3P, R_3As, $(RO)_3P$, CN^-, RNC, CO, C_2H_4, C_6H_6, H^-, R^-

1.7 Biosorption of precious metals and alkaline metals

In recent years, biosorption has been focused for recovery of precious metals, because of abundant source, low cost, effective adsorption capacity and less pollution to environment. Large number of researches on biosorption demonstrate that bio-adsorbents have potential to gradually replace of synthetic chemical adsorbents.

The largest difference between natural and synthetic adsorbents is whether the chemical composition is complicated or not. Unlike synthetic adsorbents, bio-adsorbents contain various functional groups, such as hydroxyl, carboxyl, amino, sulfide ones *etc*.

According to mainly involved components, bio-adsorbents are classified into three classes for metal recovery: polysaccharides, polyphenols, proteins types.

1.7.1 Polysaccharides adsorbents

Polysaccharides are polymeric carbohydrate molecules composed of long chains of monosaccharide units bound together by glycosidic linkages [79]. Polysaccharide plays the important class of biological polymers which are involved in living organism at either structure or energy storage.

The typical examples of polysaccharides are cellulose and chitin. Cellulose as a content of cell walls in plants is the most abundant organic molecule on earth. Chitin has a similar chemical structure as cellulose but exists in shell of crustaceans or insects. The derivative of chitin, chitosan has number of commercial values in medicine, agriculture, industry and substance of designed chemical compound. The chemical structures of three polysaccharides are shown in Fig. 1-13.

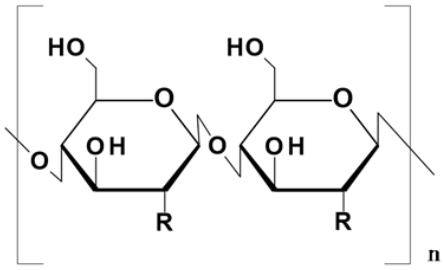

Fig. 1- 13 Structures of polysaccharides, R: NH_2 (chitosan), R: OH (cellulose), R: $NHCOCH_3$ (chitin).

Chitosan has been frequently gone through various modification by grafting functional groups to improve adsorption ability for metal adsorption. Previous workers in our lab had synthesized many kinds of modified chitosan. The structures of monocarboxymenthylated chitosan (MCM-chitosan), *N*,*N*-dicarboxymethylated or iminodiacetic acid type of chitosan (IDA-chitosan), diethylenetriaminepentaacetic acid type of chitosan (DTPA-chitosan) are shown in Fig. 1-14 [80]. The adsorptive selectivity for precious metal was improved by employing the modified materials.

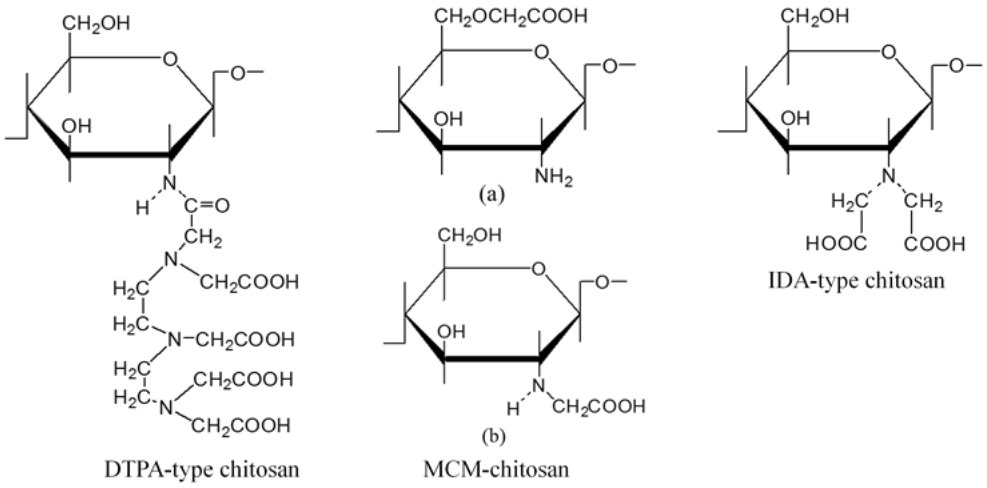

Fig. 1-14 Chemical structures of the complexane types of chemically modified chitosan [80].

In addition, crude cellulose-rich materials like waste newspaper had remarkable adsorption abilities for gold and palladium by simple modification [81].

1.7.2 Polyphenol adsorbents

Polyphenolic substances largely exist in tea leaves, fruit peels such as, grape, pomegranate and persimmon peel [82]. Phenol groups as active sites in these materials can enhance adsorption of precious metals taking place, especially through simple modification like crosslinking.

For example, persimmon peel gel was investigated on recovery of gold [83] from previous researchers, the constituents of persimmon tannin are shown in Fig. 1-15. After

phenolic compound was partly crosslinked by condensation, persimmon peel gel performed high and selective adsorption to gold adsorption.

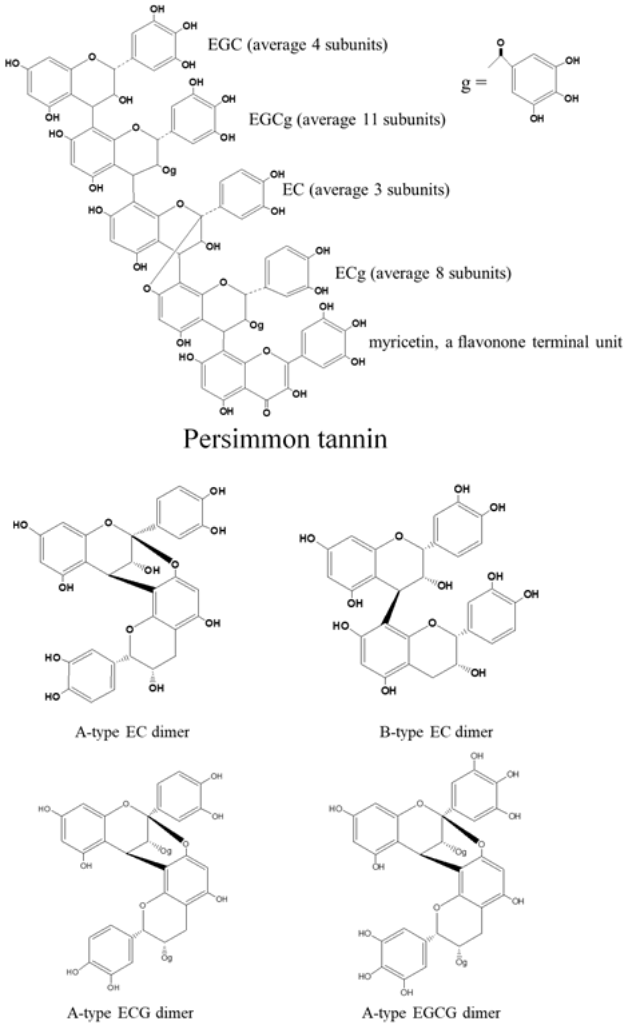

Fig. 1-15 Chemical structures of persimmon tannin and its characteristic units [84].

Even the adsorbents were already crosslinked, amounts of phenol groups are still maintained. Those phenol groups can coordinate with Au(III) ion.

Furthermore, hydroxyl-groups contained in the resin are popular used for making water softened by proton exchange with alkali ion. Hence, polyphenol biomass adsorbents with high content of hydroxyl groups can be employed as alkali metal recovery.

1.7.3 Protein rich adsorbents

Protein is built up by various amino acids, hence, protein rich adsorbents provide large scale of amido groups and together with certain amounts of coordinating atoms in residual groups like hydroxyl and sulfhydryl ones. Furthermore, in acidic media, automatical hydrolysis of protein chain can break amido bonds and produce amino acids monomers. Therefore, protein rich adsorbents have potential for precious metal adsorption by the formation of complexes between amino acids and metal ions.

The first report about interactions between ovalbumin and Au^{3+} was revealed from Craig *et* al [85]. Afterwards, complexes of Au with amino acids are gradually focused, such as cystine, alanine, glycine [86-88]. Because of the disulfide bond on cystine, it is easy to bind and reduce of gold. The selective adsorption of gold from mixture of precious metal can be improved by using biomass adsorbents with high content of cystine. Those strong interactions showed that proteins rich adsorbents as biomass adsorbents are good candidates for precious metal adsorption.

Many protein rich adsorbents for precious metal adsorption have been reported, such as egg shell membrane, soybean protein, sheep intestine, egg-yolk protein and ground fish *etc* [89-90]. These biomass adsorbents performed high efficiency for Au(III) and Pd(II) adsorption.

Because of the long molecular chain and content of various monomers, the adsorption is usually not only taken place with one kind of coordinating atom. In addition, hydrolysis of these materials is sensitive to temperature and concentration of acid solution. When it is contacted with metal ion in strongly acidic media, if the temperature is too high, material is possible dissolved into solution.

1.8 Objectives and motivation of present research works

For consciousness of saving resource and environmental protection, large scale of natural or synthesized materials have been employed for research of metal recovery. Metal recovery from electronic waste has high request for high metal selectivity of material, because the leaching solution of waste usually contains not only one kind of

precious metal. The motivation of this work relates to utilize of various kinds of secondary biomass sources and development of them as low cost but highly efficient adsorbents in the field of metal separation and recovery. To accomplish of this goal, three main classes of biomass adsorbents, polysaccharides, polyphenols and protein rich ones, were investigated for precious and alkali metals adsorption, in the present work. Based on these materials, most general method, hydrometallurgy was used for routing operation of recovery.

Therefore, above core concepts, specific viewpoints are given in the present work:

1. To select crude materials from biomass wastes according to their main content of compounds and to directly employ or modify them as high effective and selective adsorbents to specific metal adsorption
2. To study the optimal processing condition for precious and alkali metal adsorption, and to investigate the involved chemical interactions and mechanism between metal ions and adsorbents
3. To study the suitable and simple method for gold refining route after adsorption on biomass adsorbents and to realize the feasibility of commercial technological application
4. To develop commercial technology of selective cesium removal over other alkali metal ions from polluted water with low cost and under the mild condition.

1.9 References

[1] Y. J. Ding, S. G. Zhang, B. Liu, H.D. Zheng, C. C. Chang, C. Ekberg, Recovery of precious metals from electronic waste and spent catalysts: A review, Resour. Conserv. Recy., 2019, 14, 284-298.

[2] P. B. Kettler, Platinum group metals in catalysis: fabrication of catalysts and catalyst precursors, J. Org. Process Res. Dev., 2003, 7, 342-354.

[3] G.X. Chen, C. F. Xu, X. Q. Huang, J. Y. Ye, L. Gu, G. Li, Z. C. Tang, B. H. Wu, H. Y. Yang, Z. P. Zhao, Z. Y. Zhou, G. Fu and N.F. Zheng, Interfacial electronic effects control the reaction selectivity of platinum catalysts, J. Nat. Mat., 2016, 15, 564-569.

[4] T. Ishiyama and N. Miyaura, Chemistry of group 13 element-transition metal linkage -the platinum- and palladium-catalyzed reactions of (alkoxo)diborons, J. Organomet. Chem., 2000, 611, 392-402.

[5] F. A. Lewis, The palladium-hydrogen system: A survey of hydride formation and the effects of hydrogen contained within the metal lattices, Platinum Metals Rev., 1982, 26(l), 20-27.

[6] M. N. García1, K. Mori1, Y. Kuwahara and H. Yamashita, Recent strategies targeting efficient hydrogen production from chemical hydrogen storage materials over carbon-supported catalysts, NPG Asia Materials, 2018, 10, 277–292.

[7] Z. L. Wang, J. M. Yan, H. L. Wang, Y. Ping and Q. Jiang, Pd/C synthesized with citric acid: An efficient catalyst for hydrogen generation from formic acid/sodium formate, Sci. Rep. 2012, 2, 1–6.

[8] K. Jiang, K. Xu, S. Z. Zou and W. B. Cai, B-Doped Pd catalyst: Boosting room-temperature hydrogen production from formic acid−formate solutions, J. Am. Chem. Soc., 2014, 136, 4861–4864.

[9] Q. Y. Bi, J. D. Lin, Y. M. Liu, H. Y. He, F. Q. Huang and Y. Cao, Dehydrogenation of formic acid at room temperature: Boosting palladium nanoparticle efficiency by coupling with pyridinic-nitrogen-doped carbon, Angew. Chem. Int. Ed., 2016, 55, 11849–11853.

[10] J. J. Li, W. Chen, H. Zhao, X. S. Zheng, L. H. Wu, H. B. Pan, J. F. Zhu, Y.X. Chen and J. L. Lu, Size-dependent catalytic activity over carbon-supported palladium nanoparticles in dehydrogenation of formic acid, J. Catal., 2017, 352,371–381.

[11] X. Wang, G. W. Qi, C. H. Tan, Y. P. Li, J. Guo, X. J. Pang and S. Y. Zhang, Pd/C nanocatalyst with high turnover frequency for hydrogen generation from the formic acid-formate mixtures, J. Hydrog. Energy, 2014, 39, 837–843.

[12] S. Zhang, B. Jiang, K. Jiang and W. B. Cai, Surfactant-free synthesis of carbon supported palladium nanoparticles and size dependent hydrogen production from formic acid-formate solution, ACS Appl. Mater. Interfaces, 2017, 9, 24678–24687.

[13] M. Jeon, D. J. Han, K. S. Lee, S. H. Choi, J. Han, S. W. Nam, S. C. Jang, H. S. Park and C. W. Yoon, Electronically modified Pd catalysts supported on N-doped carbon for the dehydrogenation of formic acid, J. Hydrog. Energy, 2016, 41,15453–15461.

[14] Q. L. Zhu, N. Tsumori and Q. Xu, Sodium hydroxide-assisted growth of uniform Pd nanoparticles on nanoporous carbon MSC-30 for efficient and complete dehydrogenation of formic acid under ambient conditions, Chem. Sci., 2014, 5,195–199.

[15] J. P. Zhou, J. Zhang, X. H. Dai, X. Wang and S. Y. Zhang, Formic acid-ammonium formate mixture: A new system with extreme high dehydrogenation activity and capacity, J. Hydrog. Energy, 2016, 41, 22059–22066.

[16] Q. L. Zhu, N. Tsumori, and Q. Xu, Immobilizing extremely catalytically active palladium nanoparticles to carbon nanospheres: A weakly-capping growth Approach, J. Am. Chem. Soc., 2015, 137, 11743–11748.

[17] Z. P. Li, X. C. Yang, N. Tsumori, Z. Liu, Y. Himeda, T. Autrey and Q. Xu, Tandem nitrogen functionalization of porous carbon: toward immobilizing highly active palladium nanoclusters for dehydrogenation of formic acid, ACS Catal., 2017, 7, 2720–2724.

[18] C. Barnard and Johnson Matthey, Platinum group metal compounds in cancer chemotherapy, Technol. Rev., 2017, 61(1), 52–59.

[19] R. Grant, in: L. Manzeik (Ed.), International Precious Metals Institute, Allentwon, PA, 1990.

[20] Z. D. Bugarčić, J. Bogojeski and R. Eldik, Coord., Kinetics, mechanism and equilibrium studies on the substitution reactions of Pd(II) in reference to Pt(II) complexes with bio-molecules, Coord. Chem. Rev., 2015, 292, 91-106.

[21] F. L. Bernardis, R. A. Grant and D. C. Sherrington, A review of methods of separation of the platinum-group metals through their chloro-complexes, React. Funct. Polym., 2005, 65, 205-217.

[22] K. J. Naidoo, G. Klatt, K. R. Koch and D. J. Robinson, Geometric hydration shells for anionic platinum group metal chloro complexes, Inorg. Chem., 2002, 41, 1845-1849.

[23] H. A. Droll, B. P. Block and W. C. Fernelius, Studies on coordination compounds. XV. Formation constants for chloride and acetylacetonate complexes of palladium(II), J. Phys. Chem., 1957, 61, 1000-1004.

[24] H. Yoshizawa, K. Shiomi, S. Yamada, Y. Baba, Y. Kondo, K. Kondo, K. Ijichi and Y. Hatate, Solvent extraction of platinum(IV) from aqueous acidic chloride solution with tri-n-octylamine in toluene, Solvent Extr. Res. Dev., Jpn, 1997, 4, 157-166.

[25] D. Cozzi and F. Pantani, The polarographic behavior of rhodium(III) chlorocomplexes, J. Inorg. Nucl. Chem., 1958, 8, 385-398.

[26] L. G. Sillen, Stability constants, Special publication No.17, W.1, London, 1964, 283-289.

[27] M. J. Nicol, C. A. Fleming and R. L. Paul, 1987, Chapter 15, pp. 832-833 in The Extractive Metallurgy of Gold in South Africa, Edited by G. G. Stanley.

[28] N. P. Finkelstein and R. D. Hancock, A new approach to the chemistry of gold, Gold bull., 1974, 7(3), 72-77.

[29] N. N. Greenwood and A. Earnshaw, Chemistry of the Elements (2^{nd} ed.) Butterworth-heinemann.,1997, ISBN 978-0-08-037941-8.

[30] WebElements Periodic Table of the Elements / Lithium / biological information, http://www.webelements.com/lithium/biology.html), 2011.

[31] WebElements Periodic Table of the Elements / potassium / biological information, http://www.webelements.com/potassium/biology.html), 2011.

[32] WebElements Periodic Table of the Elements / sodium / biological information, http://www.webelements.com/sodium/biology.html), 2011.

[33] D. Heiserman, Exploring Chemical Elements and their compounds, 1992, pp. 201-203. ISBN 978-0-8306-3015.

[34] Alkali metal-Wikipedia, http://en.wikipedia.org/wiki/Alkali_metal#cite_note-rsc-34.

[35] E. Djamali and J. W. Cobble, J. Phys. Chem. B 2009, 113, 5200−5207.

[36] D. W. Smith, Where does resonance energy come from, A nonmathematical approach to the theory of aromaticity, J. Chem. Edu. 1977, 54, 540−542.

[37] J. Mähler and I. Presson, A study of the hydration of the alkali metal ions in aqueous solution, Inorg. Chem. 2012, 51, 425-438.

[38] EcoMaterials Center, National Institute for Materials and Science, Report No.3, worldwide supply and demand of platinum group metals and trends in the recycling of autocatalyst in Japan.

[39] J. R. Cui and L. F. Zhang, Metallurgical recovery of metals from electronic waste: A review, J. Hazard. Mater., 2008, 158, 228-256.

[40] J.R. Cui and E. Forssberg, Mechanical recycling of waste electric and electronic equipment: a review, J. Hazard. Mater., 2003, B999, 243-263.

[41] J. E. Hoffman, Recovering precious metals from electronic scrap, Jom-J. Miner. Met. Mater. Soc. 1992, 44 (7), 43-48.

[42] J. C. Lee, H. T. Song and J.-M. Yoo, Present status of the recycling of waste electrical and electronic equipment in Korea, Resour. Conserv. Recycl, 2007, 50(4), 380-397.

[43] M. Sadegh Safarzadeh, M.S. Bafghi, D. Moradkhani and M. Ojahi. Ilkhchi, A review on hydrometallurgical extraction and recovery of cadmium from various resources, Miner. Eng., 2007, 20(3), 211–220.

[44] M. Shamsuddin, Metal recovery from scrap and waste, J. Metals, 1986, 38(2), 24–31.

[45] B. Kolodziej and Z. Adamski, A ferric chloride hydrometallurgical process for recovery of silver from electronic scrap materials, Hydrometallurgy, 1984, 12(1), 117-127.

[46] P. Quinet and J. Proost, Recovery of precious metals from electronic scrap by hydrometallurgical processing routes, Miner. Metall. Process. 2005, 22(1), 17-22.

[47] A. G. Chemielewski, T. S. Urbanski and W. Migdal, Separation technologies for metals recovery from industrial wastes, Hydrometallurgy, 1997, 45(3), 333-334.

[48] S. R. La Brooy, H. G. Linge and G. S. Walker, Miner. Review of gold extraction from ores, Eng. 1994, 7(10), 1213–1241.

[49] Y. Asamoah-Bekoe, Investigation of the leaching of the platinum group metal concentrate in hydrochloric acid solution by chlorine, degree of Master of Science in Engineering thesis, 1998.

[50] R. Dorin and R. Woods, Determination of leaching rates of precious metals by electrochemical techniques, J. Appl. Electrochem., 1991, 21(5), 419.

[51] M. S. Prasad, R. Mensah-Biney and R. S. Pizarro, Modern trends in gold processing-overview, Miner. Eng., 1991, 4(12), 1257–1277.

[52] M. G. Aylmore and D. M. Muir, Miner., Thermodynamic analysis of gold leaching by ammoniacal thiosulfate using Eh/pH and speciation diagrams, Metall. Process., 2001, 18(4), 221–227.

[53] D. Zipperian, S. Raghavan and J. P. Wilson, Gold and silver extraction by ammoniacal thiosulfate leaching from a rhyolite ore, Hydrometallurgy, 1988, 19(3), 361–375.

[54] C. A. Fleming, Hydrometallurgy of precious metals recovery, Hydrometallurgy, 1992, 30(1–3), 127–162.

[55] F. T. Awadalla and G. M. Ritcey, Recovery of gold from thiourea, thiocyanate, or thiosulfate solution by reduction-precipitation with a stabilized form of sodium borohydride, Sci. Technol., 1991, 26(9), 1207–1228.

[56] F. J. Alguacil, A. Hernandez and A. Luis, Study of the $KAu(CN)_2$-Amine amberlite LA-2 extraction equilibrium system, Hydrometallurgy, 1990, 24(2), 157–166.

[57] C. Caravaca, F. J. Alguacil and A. Sastre, The use of primary amines in gold(I) extraction from cyanide solutions, Hydrometallurgy, 1996, 40(3) 263–275.

[58] M. B. Mooiman and J. D. Miller, The chemistry of gold solvent extraction from alkaline cyanide solution by solvating extractants, Hydrometallurgy, 1991, 27(1), 29–46.

[59] M. Yamada, M. R. Gandhi and A. Shibayama, Rapid and selective recovery of palladium from platinum group metals and base metals using a thioamide-modified calix[4]arene extractant in environmentally friendly hydrocarbon fluids, Sci. Rep., 2018, 8, 16909.

[60] T. Z. Yang, C. J. Shui and W. D. Bin, The synergistic mechanism of solvent extraction of gold in HCl with TOA and TOPO, J. Cent. South Univ. Technol., 1999, 6, 28-31.

[61] D. S. Xue, T. Li, Y. H. Liua, Y. H. Yang, Y. X. Zhang, J. Cui and D. B. Guo, Selective adsorption and recovery of precious metal ions from water and metallurgical slag by polymer brush graphene–polyurethane composite, React. Funct. Polym., 2019, 136, 138-152.

[62] T. Kang, Y. Park, K. Choi, J. S. Lee and J. Yi, Ordered mesoporous silica (SBA-15) derivatized with imidazole-containing functionalities as a selective adsorbent of precious metal ions, J. Mater. Chem., 2014, 14, 1043-1049.

[63] H. Tokuyama and N. Ishihara, Temperature-swing adsorption of precious metal ions onto poly(2-(dimethylamino)ethyl methacrylate) gel, React. Funct. Polym., 2010, 70, 610-615.

[64] S. M. Ding, X. Y. Zhang, X. H. Feng, Y. T. Wang, S. L. Ma, Q. Peng and W. A. Zhang, React. Funct. Polym., 2006, 66, 357-363.

[65] H. Kasaini, M. Goto, and S. Furusaki, Adsorption performance of activated carbon pellets immobilized with organophosphorus extractants and an amine: a case study for

the separation of Pt(IV), Pd(II), and Rh(III) ions in chloride media, Sep. Sci. Technol., 2001, 361(3), 2845-2861

[66] A. C. Grosse, G. W. Dicinoski, M. J. Shaw and P. R. Haddad, Leaching and recovery of gold using ammoniacal thiosulfate leach liquors (a review), Hydrometallurgy, 2003, 69, 1-21.

[67] Z. L. Dong, T. Jiang, B. Xu, Y. B. Yang and Q. Li, Recovery of gold from pregnant thiosulfate solutions by the resin adsorption technique, Metals, 2017, 7(12), 555-571.

[68] J. Mon, Y. J. Deng, M. Flury and J. B. Harsh, Cesium incorporation and diffusion in cancrinite, sodalite, zeolite, and allophane, Micropor. Mesopor. Mat, 2005, 86, 277–286

[69] L. Al-Attar, A. Dyer and R. Harjula, Uptake of radionuclides on microporous and layered ion exchange materials, J. Mater. Chem., 2003, 13, 2963–2968.

[70] S. Komarneni and R. Roy, Use of γ- zirconium phosphate for Cs removal from radioactive waste, Nature, 1982, 299, 707–708

[71] S. K. Fiskum, D. L. Blanchard, M. J. Steele, K. K. Thomas, T. Trang-Le and M. R. Thorson, Spherical resorcinol-formaldehyde resin testing for cesium removal from Hanford tank waste simulant, Sep. Sci. Technol., 2006, 41, 2461–2474.

[72] J. F. Dozol, M. Dozol and R. M. Macias, Extraction of strontium and cesium by dicarbollides, crown ethers and functionalized calixarenes, J. Incl. Phenom. Macro. Chem., 2000, 38, 1-22.

[73] B. A. Moyer and Y. Sun, in Ion Exchange and Solvent Extraction, Chap. 6, Marcel Dekker, 1998.

[74] J. C. Bryan, R. A. Sachleben, J. M. Lavis, M. C. Davis, Structural aspects of Rubidium ion selectivity by tribenzo-21-crown-71, Inorg. Chem., 1998, 37, 2749-2755.

[75] D. W. Smith, Ionic hydration enthalpies, J. Chem. Edu., 1977, 54(9), 540-542.

[76] G. M. Ritcey and A.W. Ashbrook, Solvent extraction: principles and applications to process metallurgy, part I, 1979, Chap.1, pp.6.

[77] R. G. Pearson and J. Songstad, Application of the principle of hard and soft acids and bases to organic chemistry, J. Am. Chem. Soc., 1967, 89(8), 1827-1836.

[78] R. G. Pearson, Hard and soft acids and bases, J. Am. Chem. Soc., 1963, 85, 3533-3539.

[79] http://en.wikipedia.org/wiki/Polysaccharide.

[80] K. Inoue, T. Yamaguchi, M. Iwasaki, K. Ohto and K. Yoshizuka, Adsorption of some platinum group metals on some complexes types of chemically modified chitosan, Sep. Sci. Technol., 1995, 30(12), 2477-2489.

[81] C. R. Adhikari, D. Parajuli, K. Inoue, K. Ohto, H. Kawakita and H. Harada, Recovery of precious metals by using chemically modified waste paper, New J. Chem., 2008, 32, 1634-1641.

[82] A. Bhatnagar, M. Sillanpää and A. Witek-Krowiak., Agricultural waste peels as versatile biomass for water purification – A review, Chem. Eng. J., 2015, 270, 244-271.

[83] D. Parajuli, H. Kawakita, K. Inoue, K. Ohto and K. Kajiyama, Persimmon peel gel for the selective recovery of gold, Hydrometallurgy, 2007, 87, 133-139.

[84] B. Zou, R. Z. Nie, J. Zeng, Z. Z. Ge, Z. Xu and C. M. Li, Persimmon tannin alleviates hepatic steatosis in L02 cells by targeting miR-122 and miR-33b and its effects closely associated with the A type ECG dimer and EGCG dimer structural units, J. Funct. Foods, 2014, 11, 330-341.

[85] J. P. Craig, A. G. Garrett, H. B. Williams, The ovalbumin-chloroauric acid reaction, J. Am. Chem. Soc., 1954, 76, 1570-1575.

[86] A. Abraham, A. J. Ilott, J. Miller and T. Gullion, ^{1}H MAS NMR study of cysteine-coated gold nanoparticles, J. Phys. Chem. B, 2012, 116, 7771-7775.

[87] E. A. Oraby, J. J. Eksteen, The leaching of gold, silver and their alloys in alkaline glycine–peroxide solutions and their adsorption on carbon, Hydrometallurgy, 2015, 152, 199-203.

[88] M. H. Abdalmoneam, K. Waters, N. Saikia and R. Pandey, Amino acids conjugated gold clusters: interaction of alanine and tryptophan with Au_8 and Au_{20}, J. Phys. Chem. C, 2017, 121(45), 25585-25593.

[89] T. Maruyama, H. Matsushita, Y. Shimada, I. Kamata, M. Hanaki, S. Sonokawa, N. Kamiya and M. Goto, Protein and protein-rich biomass as environmentally friendly adsorbents selective for precious metal ions, Environ. Sci. Technol., 2007, 41, 1359-1364.

[90] T. Maruyama, Y. Terashima, S. Takeda, F. Okazaki, M. Goto, Selective adsorption and recovery of precious metal ions using protein-rich biomass as efficient adsorbents, Process Biochem., 2014, 49 (5), 850-857.

Chapter 2

Precious metal ions adsorption on natural polysaccharides and modified kiwi peel adsorbents

Three typical and natural polysaccharide polymers, cellulose, chitosan, and two chitins were used to investigate for precious metals adsorptive recovery. Both of chitins exhibited the adsorption abilities for Pt(IV) and Pd(II), compared with other polysaccharide polymers. Adsorption of Pd(II) exhibited high effective, time to equilibrium of adsorption was attained within 2 h. The adsorption of Pd(II) was related to concentration of proton, due to different formation complexes of Pd(II) with chloride at various pH condition. The maximum loading capacities for Pd(II) and Pt(IV) adsorption were 0.0865 mmol g^{-1} and 0.058 mmol g^{-1}, respectively. Although the adsorption capacity is not high enough, chitin as nontoxic and resourceful material has significance of precious metal recovery, especially improve the capacity by designed modification. Hence, the crosslinked kiwi peels which mainly contain cellulose were also investigated for precious metal adsorption. Crude kiwi peel had meaningful adsorption on gold. After simple modification, adsorbents showed higher adsorption ability and selectivity to gold rather than Pd(II) or Pt(IV). Meanwhile, adsorption process was together with reduction of gold which took for long time to reach at equilibrium. Therefore, both natural and modified biomass polysaccharides adsorbents have commercial value for precious metal recovery.

2.1 Introduction

Limited resource of precious metals and with large demands for various applications urged the recovery of them to get more and more attention. Among hydrometallurgical technologies, solvent extraction and solid adsorption, which employ two different phases with a reactive interface, are frequently regarded techniques. For extraction of precious metals, some organic extractants exhibit remarkable extraction ability and selectivity [1-3]. On the contrary, because of unavoidable use of organic solvent and complicated synthesized processes of extractants, treatment of organic waste may raise the cost of recovery and block off massively industrial recovery of precious metals. On other hand, unlike organic polymer particles, synthesized resin, biomass adsorbents devote similar value to precious metal adsorption with less toxic and abundant resource [4-6]. Hence, from the viewpoint of commercial demands, biomass adsorbents are satisfied for environmental-friendly property on precious metal recovery and gradually attained popularity [7-9].

Polysaccharide are distinct class of biopolymers, universally produced in living organisms [10]. Cellulose possesses resource in the world and exists as the content of plant cell walls. Chitin is the main polymer for building up shell of crustacean. Chitosan as the derivative of chitin has high value for medicine and other application. All of them have similar structure units but with different moieties which leads to the different properties. They independently contain amount of hydroxyl, amido and amino groups, hence, it contributes to adsorption of metal ions with different mechanism such as ion-exchange and chelation [11].

Kiwi fruit is one of popular fruits in the world because of their high content of antioxidant compounds such as ascorbic acids and phenols [12-13]. The large consuming amount provides massive biomass waste-kiwi peel (KP) as well. Chen *et* al. reported synthesis of sliver nanoparticles with kiwi juice and employed it for detecting protease K [14]. Besides, crude KP has meaningful performance on heavy metals removal as well [15]. As the report mentioned, main components in KP are cellulose derivatives. In addition, Fiorentino *et*.al, reported phytochemical analysis of kiwi peel crude extracts led to isolation of vitamin E, 2, 8-dimethyl-2-(4, 8, 12-trimethyltridec-11-enyl)chroman-6-ol,

as well as α-and δ-tocopherol, 7-sterols, the triterpene ursolic acid chlorogenic acid, and 11 flavonoids. The structures of organic water insoluble compounds were shown in Fig. 2-1 and the main components in the milligrams per 100 g of fresh fruit matrix are listed in Table 2-1 [16].

Table 2-1 Amounts of compounds found in pulp and peel of kiwi fruits[a]

	Peel	**pulp**
δ-tocomonoenol (1)	1.45±0.08	0.85±0.02
α-tocopherol (2)	1.05±0.06	1.02±0.03
δ-tocopherol (3)	2.49±0.12	0.64±0.01
β-sitosterol (4)	4.84±0.20	9.28±0.45
stigmasterol (5)	3.35±0.11	2.40±0.11
campesterol (6)	1.75±0.04	2.77±0.10
stigmast-7-en-3β-ol (7)	1.81±0.07	5.32±0.29

[a]Values are reported as mg / 100 g of fw

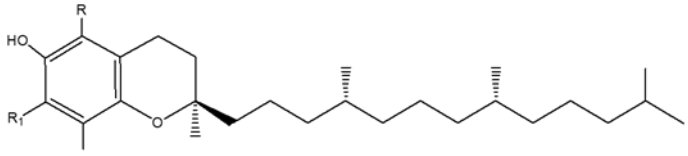

(1) R=R$_1$=H, (2) R=R$_1$=Me, (3) R=R$_1$=H

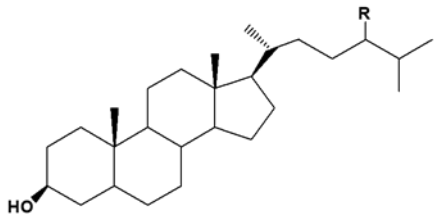

(4) R=βEt, (5) R= βEt, (6) R=αMe (7) R=βEt

Fig. 2-1 Chemical structures of compounds (1)-(7) [16].

In this work, the ability of precious metal adsorption on natural polysaccharides polymers was firstly investigated. Although some papers reported the possibility of precious metal adsorption on chitosan [17-18], chitosan itself has aqueous solubility in

acidic media which would affect the adsorption. Meanwhile, adsorption performance of all precious metals on cellulose was low. Hence, two types of chitins (Ex, s) were continuously investigated for platinum(IV) and palladium(II). The investigation was involved to pH and time cause dependencies, platinum(IV) and palladium(II) adsorption.

To further investigate the feasibility of precious metal adsorption on cellulose, KP as natural biomass containing cellulose mainly was employed. After modification with concentrated sulfuric acid, crosslinked kiwi peel (CKP) obviously exhibited high adsorption ability and selectivity for gold, over Pt(IV) and Pd(II).

Comprehensively all, either natural and modified biomass adsorbents have commercial potential values for effective precious metal adsorption in industrial application on a large scale.

2.2 Experimental

2.2.1 Materials and chemicals

Gold(III), platinum(IV) and palladium(II) chloride solutions were prepared by dissolving hydrogen tetrachloroaurate(III) tetrahydrate ($HAuCl_4 \cdot 4H_2O$), hydrogen hexachloro platinate(IV) hexahydrate ($H_2PtCl_6 \cdot 6H_2O$) and palladium(II) chloride ($PdCl_2$) respectively, purchased from Wako Pure Chemical Industries, Ltd, Japan. Cellulose was purchased from Merck KGaA, Germany. Chitin-S produced from shrimp shells was purchased from SIGMA, USA. Chitin-Ex was from Funakoshi Co., Ltd, Japan. Chitosan was from YAEGAKI Bio-industry Co. Ltd. These polysaccharides were used as they were without further purification. Crystallinity degree and deacetylation degree of both chitin materials may be different. Although, such information was not mentioned for both commercially available materials. The concentrated sulfuric acid and hydrochloric acid were also purchased from Wako Chemicals.

Kiwi fruits, zespri. imported from New Zealand, were purchased privately in Japan.

2.2.2 Preparation of adsorbents

Cellulose, chitin and chitosan powders were directly used for experiment without any treatment. While KPs were directly and cleanly removed from the fruit pulp by hand. As the pre-treatment, KPs were dried in an oven for one week at 30℃. For crosslinking, 10.0 g KPs were stirred in 50 cm^3 concentrated sulfuric acid (18.4 M) at 90℃ for 20 h. The mixtures were cooled down to room temperature and soaked into 500 cm^3 deionized water. After the filtration, the product was packed into the glass column and continuously washed with deionized until the pH of washing solution became neutral. Then, the washed product was dried at 60℃ for 48 h. Finally, the obtained cake was crushed and ground, then sieved through 150 μm mesh to keep the uniform size. Both KPs and CKPs were measured by IR spectra.

2.2.3 Preparation of test solutions

Aqueous solutions were prepared by dissolving each metal salt in 0.10 M HCl, and 0.10 M HEPES (2- (4-(2-hydroxyethyl) piperazin-1-yl) ethanesulfonic acid) buffer solution contained 0.10 M NaCl to maintain the same chloride concentration for each sample. All the solutions contained 0.10 mM metal chloride. For the adsorption isotherms tests, solution was prepared by the dissolving metal chloride in the 0.10 M HCl to be 0.10-10.0 mM. For the test solution of precious metal adsorption on CKP adsorbents, individual 1.1 mM precious metals in 0.1 M HCl were used. The pH value of the sample solution was measured by pH meter (DKK-TOA model HM-25G).

2.2.4 Adsorption tests

Except for maximum capacity of chitins test, 20 mg of polysaccharides powders were used for all tests. On the other hand, all the tests for adsorption were taken place at 30℃. For selective adsorption test, each sample powder was separately added to 2.0 cm^3 0.1 mM different kind of precious metal solution, then the mixture was shaken for 24 h. For pH dependency test, except for using various pH values of solution, other conditions

were same. After filtration, the metal concentration in the filtrated aqueous phase was measured by inductively coupled plasma atomic emission spectroscopy (ICPAES, Shimadzu ICPS-8100). After drying, metal adsorbed adsorbents were measured by Fourier transform infrared spectrophotometer (FT-IR spectra, JASCO model FTIR-410 spectrophotometer). The operational processes of precious metals adsorption are shown in Fig. 2-2

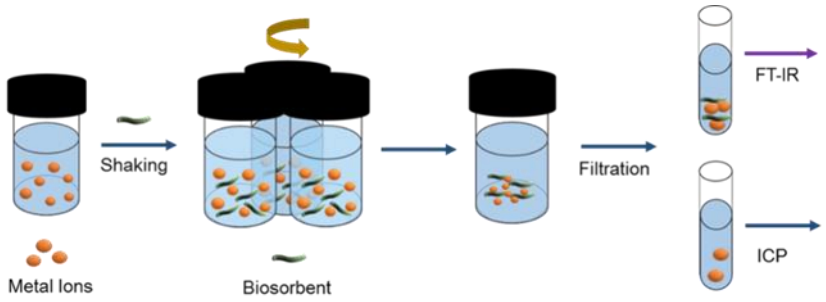

Fig. 2-2 Operational processes of precious metals adsorption.

The operations of precious metal adsorption on CKP adsorbents were similar as adsorption on polysaccharides powder. Twenty milligrams of CKP adsorbents were added into 10 cm^3 different kind of precious metals solution. The mixture was shaken for several hours at 30℃. After filtration, 40 mg of dried solid was used to measure by X-ray diffraction (XRD, Shimadzu XRD-7000). The concentration of metal solution was measured by ICP-AES as well. The morphologies of the materials were taken by Scanning Electron Microscope (SEM, Hitachi model SU-I500).

2.2.5 Evaluation of adsorption measurements

The percentage of adsorbed metal ions on the adsorbents was calculated by the equation (2.1).

$$\text{Adsorption percentage (\%)} = \frac{C_i - C_e}{C_i} \times 100 \qquad (2.1),$$

where C_i (mmol dm^{-3}) and C_e (mmol dm^{-3}) represent initial and equilibrium concentration of metal ions.

The amount of adsorbed metal on the adsorbent, (q (mmol g^{-1})) was calculated by

equation (2.2)

$$q = \frac{C_i - C_e}{W} \times V_M \quad (2.2),$$

where W represents weight of adsorbents (g) and V_M expressed volume of the test solution (dm^3).

2.3 Results and discussion

2.3.1 Precious metal adsorption on polysaccharides and kiwi peels adsorbents

2.3.1.1 Precious metal adsorption on various and polysaccharides adsorbents

The individual adsorption of Au(III), Pt(IV) and Pd(II) was separately investigated using each polysaccharide at same HCl media (0.10 M) for 24 h, as shown in Fig. 2-3. Compared with other polysaccharides, chitosan had no adsorption ability to precious metal ions, which is attributed to its high solubility in acidic solution. Both of chitins and cellulose were less soluble in acidic solution. However, both types of chitins exhibited relatively high adsorption ability to Pt (IV) and Pd (II). They were produced from the shells of crustacea such as prawn and crabs with highly natural crystalline. The formation of complexes between carbonyl groups of chitins and Pd (II) may attribute to the superior adsorption percentage than those of Pt(IV) and Au(III). In addition, the hydrogen bond between chlorine from anionic chloro-complex of Pt (IV) and nitrogen-hydrogen of chitin may be related to high adsorption.

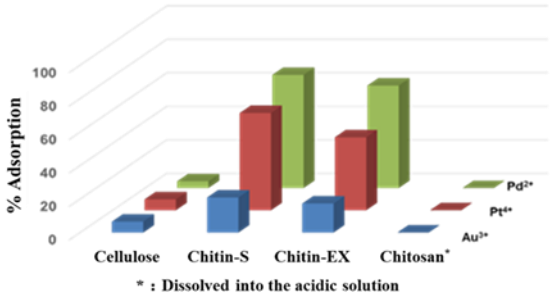

Fig. 2-3 % adsorption of Au(III), Pd(II) and Pt(IV) on polysaccharides tested in 0.10 M HCl at 30.0℃.

2.3.1.2 Selective adsorption of precious metals on crosslinked kiwi peels adsorbents

The individual of Au(III), Pd(II) and Pt(IV) adsorptions on kiwi peels (KPs) and crosslinked kiwi peels (CKPs) in 0.1 M HCl solution were investigated. Although the result of Fig. 2-3 showed less gold adsorption on pure cellulose powder, KP performed remarkable property of gold adsorption which is attributed to the high content of hydroxy organic insoluble compound as shown in Fig. 2-4.

While, CKP exhibited high adsorption ability and selectivity to gold rather than those to other precious metals. When unreacted impurities on KPs were dissolved into aqueous phase and washed out, consequently, the main components for metal adsorption were exposed to reactional phase. Meanwhile, the production of ether groups by crosslinking improved the coordination with gold ions on the adsorbents in the extent.

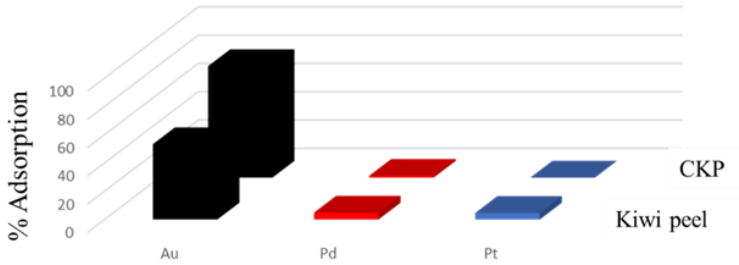

Fig. 2-4 Individual adsorption of 1.0 mM Au(III), Pd(II) and Pt(IV) on crude and crosslinked kiwi peels in 0.1 M HCl for 24 h at 30℃.

2.3.2 Effect of shaking time of precious metals adsorption on polysaccharides and crosslinked kiwi peels adsorbents

2.3.2.1 Effect of shaking time of Pt(IV) and Pd(II) adsorption on chitins adsorbents

The effects of shaking time on Pt(IV) and Pd(II) adsorption on chitin adsorbents in 0.10 M HCl media are shown in Figs. 2-5(a) and (b). The equilibrium for Pd(II) adsorption was attained within 2 h, whereas the adsorption of Pt(IV) reached to equilibrium after 36 h. The difference in time to equilibrium is caused by the different hydration shells between Pd(II) and Pt(IV). The chitin-EX exhibited slightly higher adsorption for Pd(II) than chitin-S, which may be attributed to particle size (number of adsorption sites) and crystallinity.

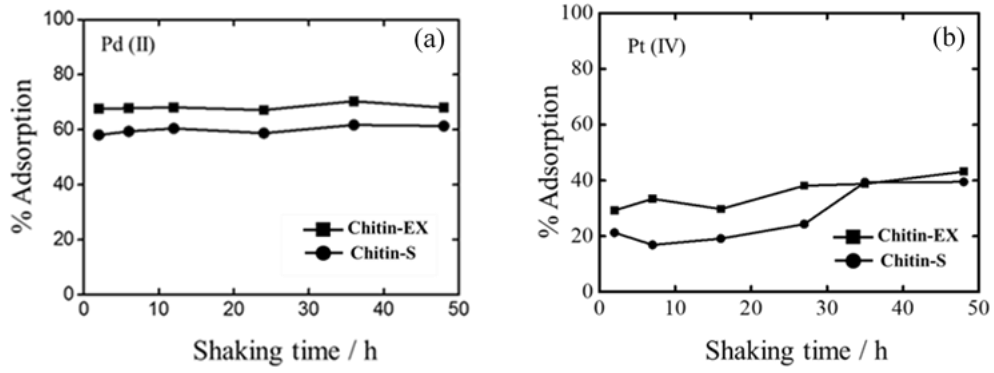

Fig. 2-5 Effect of shaking time on adsorption of (a) Pd(II) and (b) Pt(IV) on chitin adsorbents in 0.10 M HCl at 30.0℃.

2.3.2.2 Effect of shaking time of precious metals adsorption on crosslinked kiwi peel adsorbents

Because of excellent adsorption ability on CKP, individual effect of shaking time of Au(III), Pd(II) and Pt(IV) was investigated, as shown in Fig. 2-6. The adsorptions of Pd(II) and Pt(IV) barely took place at all time period, while, gold adsorption percentage increased with increase of contacting time, finally reached at 36 h. Although the time to reach equilibrium become longer than adsorption of Pd(II) or Pt(IV) on chitins, but CKP exhibited good performance for gold adsorption.

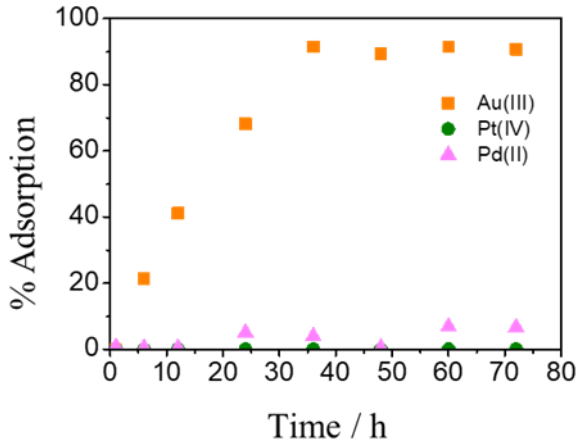

Fig. 2-6 Effect of shaking time on adsorption of 1.1 mM Au(III), Pd(II) and Pt(IV) on CKP adsorbents in 0.10 M HCl at 30.0℃.

2.3.2.3 Factor to shaking time of Au (III) adsorption on CKP adsorbents

For further study on long time for gold adsorption to reach equilibrium, the samples at different shaking time were washed by deionized water and dried, measure XRD. As shown in Fig. 2-7, the original CKP showed one broad peak which means it existed as amorphous structure. On the contrary, after uptake of Au(III) ions, extra four peaks

gradually appeared. The four peaks increased with the increase of contacting time with Au(III) ions while the original peak at 22.42° gradually disappeared. According to references reported by the previous worker in our lab and other researcher, four peaks at 37.85°, 43.87°, 64.19°, 77.29°, correspond to metallic gold [19-24]. In the other words, the reduction of Au(III) ions also happened through of the gold adsorption process. As increase of Au(III) reduction, the rate of adsorption process was consequently suppressed. Therefore, time to reach saturated adsorption became 36 h.

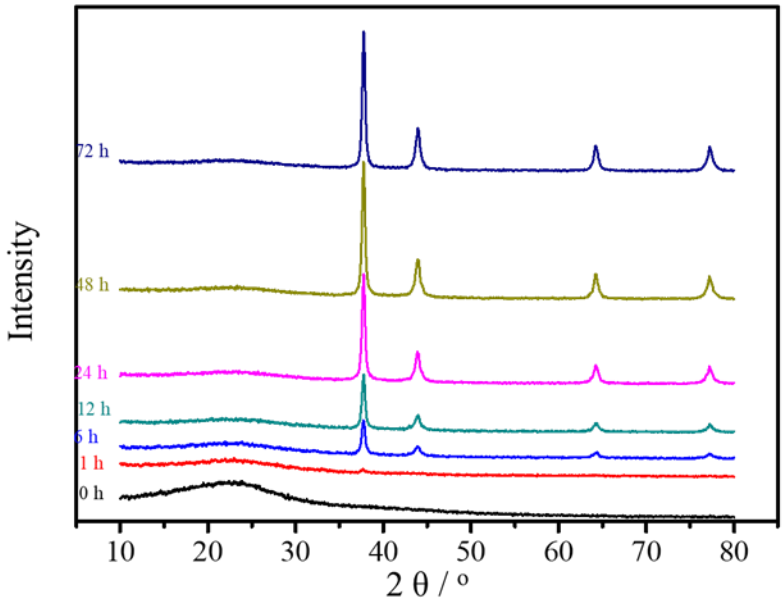

Fig. 2-7 XRD spectra of CKP adsorbents in different contacting period with Au(III) ions.

2.3.3 Effect of pH on Pt(IV) and Pd(II) adsorption

The effect of pH on Pd(II) adsorption is shown in Figs. 2-8 (a) and (b). The change between initial and equilibrium pH values were small. At the constant of chloride ion concentration, adsorption percentage increased with increase of pH value. The change of adsorption between Pd(II) and Pt(IV) at various pH regions is different. Pd(II) mainly existed as the $PdCl_4^{2-}$ anion under high chloride concentration condition. As the chloride concentration decreased, Pd(II) species was changed gradually to such as $[PdCl(H_2O_3)]^+$,

$Pd(OH)^+$ and Pd^{2+} [19]. The carboxyl groups on chitin can form complexes with Pd^{2+}.

The effect of pH on Pt(IV) adsorption is shown in Fig. 2.8 (b). Pt(IV) adsorption percentage is lower than Pd (II) one. Most of Pt (IV) exist as an anionic chloro-complexes ($PtCl_6^{2-}$) in 0.10 M HCl solution [20].

Chlorine atom from choroanion complex of Pt(IV) may form hydrogen bond with amido proton from chitin during Pt (IV) adsorption. Therefore, chloride concentration by changing HCl concentration showed weak effect on adsorption percentage of Pt(IV).

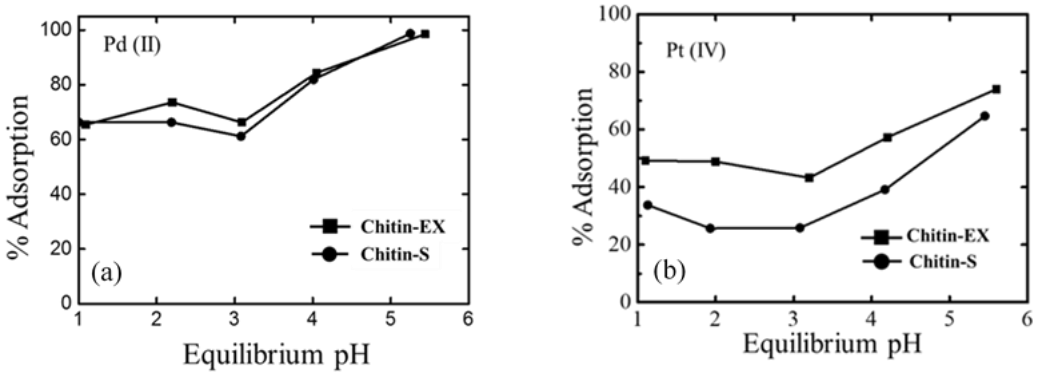

Fig. 2-8 Effect of pH on adsorption of (a) Pd(II) and (b) Pt(IV) at 30.0°C for 24 h.

2.3.4 Adsorption isotherms of Pt(IV) and Pd(II)

The adsorption isotherms of Pd (II) and Pt(IV) on chitin-EX and chitin-S is shown in Figs. 2-9 (a) and (b), respectively. The results were applied to the Langmuir isotherm, which equations are represented in the equations (2.2) and (2.3):

$$\frac{C_e}{q_e} = \frac{1}{q_m b} + \frac{C_e}{q_m} \quad (2.3),$$

where q_e is the amount of metal ion adsorbed (mmol g^{-1}), C_e is equilibrium concentration of (mmol dm^{-3}), q_m is maximum adsorption capacity on each chitin (mmol g^{-1}) and b (dm^{-3} g^{-1}) is the adsorption equilibrium constant that relates to the adsorption energy. The values of q_m and b were calculated by the slope and intercept of plot C_e/q_e vs. C_e, so the reciprocal number of slope represents for q_m.

In 0.10 M HCl solution, chitin-EX showed better adsorption percentage on Pt(IV)

than chitin-S (shown in Fig. 2-9 (b)). Hence loading capacity of Pt(IV) was investigated using chitin-EX. After calculation, the q_m value as the maximum loading capacity for Pt(IV) was estimated to be 0.0865 mmol g^{-1}.

Between two chitins, they showed similar adsorption percentages for Pd(II) at 0.10 M HCl media (shown in Fig. 2-9 (a)). The maximum loading capacity of Pd(II) was estimated to 0.058 mmol g^{-1}. Although the loading capacities of chitins for precious metals are not remarkably high, chitins is the natural and green material, and still have potential for the industrial use.

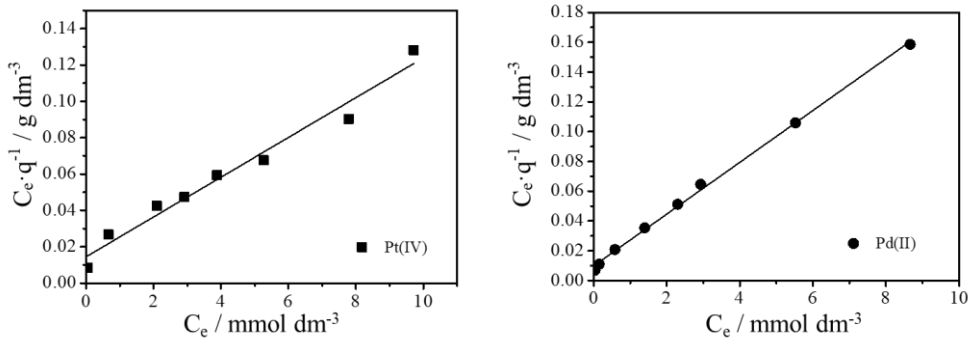

Fig. 2-9 Langmuir analysis of adsorption isotherms of (a) Pt(IV) on chitin-EX and (b) Pd(II) on chitin-S in 0.1M HCl media at 30.0℃ for 24 h.

2.3.5 IR spectra of polysaccharides and crosslinked kiwi peel adsorbents

To further study on the adsorption sites in adsorbents for precious metals adsorption on chitins, the difference before and after crosslinking of KP was observed by FT-IR spectra as shown in Figs. 2-10 and 2.11.

Because of the difference in crystallinity between chin-EX and chitin-S with same functional groups, only the Pd(II) and Pt(IV) adsorption on chitin-Ex was investigated. Figure 2-10 (a) shows the different amount of adsorbed Pd(II) (mmol / g) on chitin-EX from 0 to 0.027 mol kg^{-1}. The peaks at 3200 cm^{-1} of all samples are assigned as phenolic O-H stretching. Peaks at 3500 cm^{-1} and 1558 cm^{-1} belong to -NH stretching. Stretching

vibration of -CN peak appeared at 1076 cm^{-1}. The peaks around 1650 cm^{-1} are identified as the stretching vibrations of C=O groups. The amount of adsorbed Pd(II) was too less to observe so much details after adsorption. However, slight shift of C=O peak as the increased amount of Pd(II) demonstrated the adsorption may have relation to coordination of oxygen atom with Pd^{2+} ion.

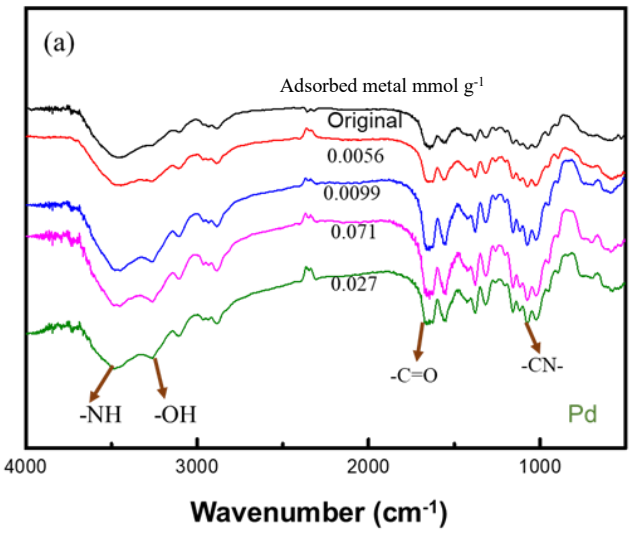

Fig. 2-10 (a) FT-IR spectra of adsorbed amount of Pd(II) on chitin-EX.

Figure 2-10 (b) shows the different amount of adsorbed Pt(IV) (mmol / g) on chitin-EX. The identified functional groups were same as Pd(II) adsorption on chitin-EX. While the shifted peaks are different, peak of -NH slightly shifted to lower frequency with the increase of adsorbed Pt(IV). That illustrated the mechanism between Pd(II) and Pt(IV) is different. Pt(IV) has strong coordination with chloride anion. The adsorption of Pt(IV) is probably caused by hydrogen bond between chlorine atom from complex choroanions of Pt(IV) and amido proton from chitin.

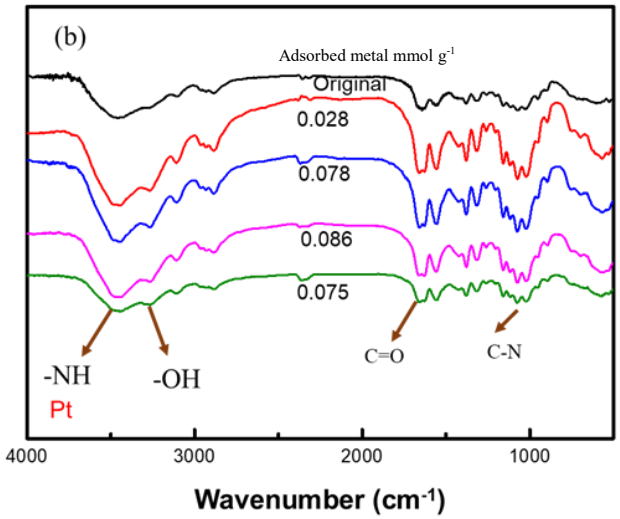

Fig. 2-10b FT-IR spectra of adsorbed amount of Pt(IV) on chitin-EX.

The possible reaction schemes of Pd(II) and Pt(IV) adsorption on chitins are shown in scheme 2-1. Adsorption of Pd(II) was taken place by coordination with carbonyl oxygen atom and by hydrogen bond of amide proton and chloride at same time. The Pt(IV) has strong interaction and the structure of complexes of $[PtCl_6]^{2-}$ is octahedron with chloride because of the high charge center. Hence, the adsorption of Pt(IV) took place by formation of hydrogen bond.

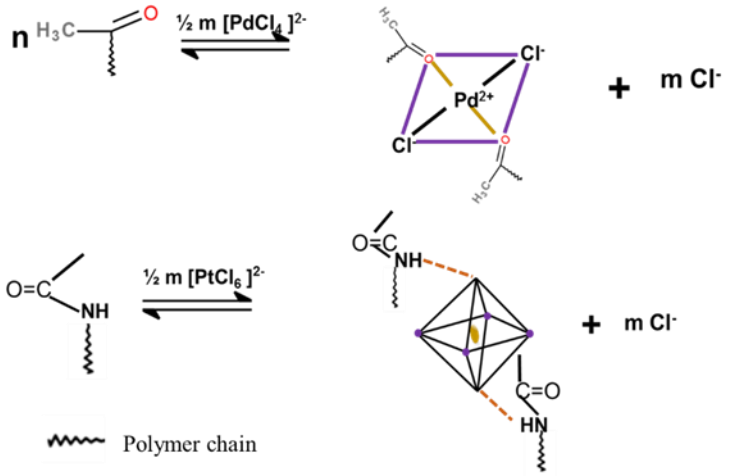

Scheme 2-1 Possible reactional adsorptions of Pd(II) and Pt(IV) on chitins.

The FT-IR spectra of KP and CKP are also measured as shown in Figs. 2-11 (a) and (b). The KP was too soft to grind powder and to mix into KBr powder. The intensity of

peak consequently much weaker than that of CKP. Hence, each spectrum was separately shown compare. At Fig. 2-11(a), the broad peak from KP around 3590-3243 cm^{-1} belongs to stretching of -OH group. After crosslinking, the interaction of hydrogen bond between hydroxyl in molecule was broken. Therefore, interaction of hydrogen bond among polymer chain made the -OH peak on CKP shifted to lower frequency as shown in Fig. 2-11(b). It means that crosslinking was partly taken place and hydroxyl sites still remain on the polymer chain. That could provide the functional group for coordination with gold. In addition, the new peak at 1179 cm^{-1} assigned as C-O-C stretching, the production of this group sufficiently proved that the crosslinking happened. More interesting point is that peak of C=O (1604 cm^{-1}) on CKP was weaker than that of on KP (1623cm^{-1}). From the spectra, it means some of the water soluble compounds were washed out and some of organic insoluble compounds still existed.

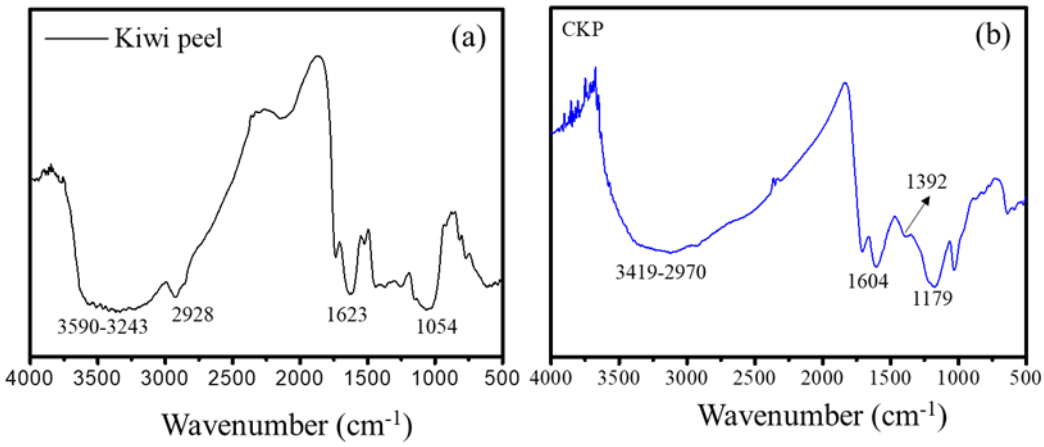

Fig. 2-11 FT-IR spectra of (a) KP and (b) CKP.

2.4 Conclusions

In this study, natural polysaccharide polymers were investigated on precious metal adsorption. In 0.10 M HCl solution, two chitins exhibited the superior ability of precious metal adsorption. The time to reach equilibrium for Pd(II) is shorter than that of Pt(IV),

caused by the configuration of different hydration shell surrounding Pd(II) and Pt(IV) chloride complexes. Furthermore, the adsorption percentage increased as the increase of pH value on Pd (II) adsorption, while, Pt(IV) adsorption was not changed clearly by the change of pH value. The adsorption mechanisms of Pd(II) and Pt(IV) on chitins were depended on different complexes formation. Although the adsorption capacity is not sufficiently enough, chitin as nontoxic and resourceful material has significance of precious metal recovery.

In addition, considered poor performance of Au(III) adsorption on pure cellulose powder and feasibility of precious metals adsorption on modified polysaccharides, the precious metals adsorption on natural biomass waste-kiwi fruit peels with high content of cellulose was investigated. Because of high content of hydroxyl groups, KP exhibited remarkable adsorption performance for Au(III). Furthermore, the adsorption ability of gold was drastically improved after the crosslinked with concentrated sulfuric acid. The preferable selectivity for gold over Pd(II) and Pt(IV) was also observed. The adsorption process totally involved not only to adsorption but also reduction Au(III), therefore, adsorption time to reach equilibrium was suppressed by reduction. On the other hand, FT-IR spectra of CKP demonstrated the hydroxyl groups still existed on the polymer chains after the crosslinking which provides the chance to coordinate with Au(III).

In summary, natural polysaccharides adsorbents not only have superiority of resource but also perform valuable application for precious metal adsorption by simple modification method. Generally, the leaching solution from electronic waste becomes the mixture of precious metal. From viewpoint of that, biomass waste with high content of polysaccharides has potential prospect for large scale application for industry because of the adsorption with high ability and selectivity. It may realize the recycling of resource by employing low cost and high effectiveness materials.

2.5 References

[1] H. Narita, T. Suzuki and M. Tanaka, Recent reseach in solvent extraction of platinum group metals J. Japan Inst. Met. Mater., 2017, 81(4),157-167.

[2] P. Malik and A. P. Paiva, A novel solvent extraction route for the mutual separation of platinum, palladium, and rhodium in hydrochloric acid media, Solvent Extr. Ion Exch., 2010, 28, 49-72.

[3] M. Iwakuma and T. Oshima, Y. Baba, Chemical structure-binding/extractability relationship using new extractants containing sulfur and nitrogen atoms as donor atoms for precious metals, Solvent Extr. Res. Dev., Jpn., 2008, 15, 21-35.

[4] T. Ito, R. Nagaishi, T. Kimura and S. Y. Kim, Study on radiation effects on (MOTDGATOA) / SiO_2-P adsorbent for separation of platinum groups metals from high-level radioactive waste, Radioanal. Nucl. Chem., 2015, 305(2), 419-427.

[5] A. Warshawsky, M. M. B. Fieberg, P. Mihalik, T. G. Murphy and Yvonne B, The separation of platinum group metal (PGM) in chloride media by isothiouronium resins, Separation & Purification Reviews, 1980, 9(2), 209-265.

[6] A. Uheida, M. Iglesias, C. Fontas, M. Hidalgo, V. Salvado, Y. Zhang and M. Muhammed, Sorption of palladium(II), rhodium(III) and platinum(IV) on Fe_3O_4 nanoparticles, J. Colloid and Interface Sci., 2006, 301(2), 402-408.

[7] T. Maruyama, Y. Terashima, S. Takedo, F. Okazaki and M. Goto, The separation selective adsorption and recovery of precious metal ions chloride using protein-rich biomass as efficient adsorbents, Process Biochem., 2014, 49, 850-857.

[8] Y. Xiong, C. R. Adhikari, H. Kawakita, K. Ohto, K. Inoue and H. Harada, Selective recovery of precious metals by persimmon waste chemically with modified with dimethylamine, Bioresour. Technol., 2009, 100(18), 4083-4089.

[9] P. Ramakul, Y. Yanachawakul, N. Leepipatpiboon and N. Sunsandee, Biosorption of palladium(II) and paltinum(IV) from aqueous solution using tannin from Indian almond (Terminalia Catappa L.) leaf biomass: kinetic and equilibrium studies, J. Chem. Eng.,

2012, 193-194(15), 102-111.

[10] E. Vandamme, S. D. Baets and A. Steinbuchel, Polysaccharides I: Polysaccharides, Polymers, Wiely -VCH, 2002, p.5-5.

[11] J. L. Cortina, E Meinharadt, O.Roijals, V. Marti, Modification and preparation of polymeric adsorbents for precious-metal extraction in hydrometallurgical processes, React. Funct. Polym., 1998, 36, 149-165.

[12] G. Du, M. Li, F. Ma and D. Liang, Antioxidant capacity and the relationship with polyphenol and vitamin C in actinida fruits, Food Chem., 2009, 113, 557-562.

[13] G. I. Kvesitadze, A. G. Kalandiya, S. G. Papunidze and M. R. Vanidze, Identification and quantification of ascorbic acid in kiwi fruit by high-performance liquid chromatography, Appl. Biochem. Microbiol., 2001, 37, 215-218.

[14] B. B. Chen, H. Liu, C. Z. Huang, J. Ling and J. Wang, Rapid and convenient synthesis of stable silver nanoparticles with kiwi juice and its novel application for detecting protease K, New J. Chem., 2015, 39, 1295-1300.

[15] K. M. Al-Qahtani, Water purification using different waste fruit cortexes for the removal of heavy metals, J. Taibah Uni. Sci., 2016, 10(5), 700-708.

[16] A. Fiorenitino, B. D'Abrosca, S. Pacifico, C. Mastellone, M. Scognamiglio and P. Monaco, Identification and assessment of antioxidant capacity of phytochemicals from kiwi fruits, J. Agric. Food Chem., 2009, 57, 4148-4155.

[17] W. S. W. Ngah and K. H. Liang, Adsorption of gold(III) ions onto and N-carboxy-methyl chitosan: equilibrium studies, Ind. Eng. Chem. Res., 1999, 38, 1411-1414.

[18] K. Inoue, Y. Baba, K. Yoshizuka, H. Noguchi and M. Yoshizaki, Selectivity series in the adsorption of metal ions on a resin, Chem. Lett., 1988, 1281-1284.

[19] D. Parajuli, C. R. Adhikari, M. Kuriyama, H. Kawakita, K. Ohto, K. Inoue and M. Funaoka, Selective recovery of gold by novel lignin-based adsorption gel, Ind. Eng. Chem. Res., 2006, 45, 8-14.

[20] D. Parajuli, H. Kawakita, K. Inoue, K. Ohto and K. Kajiyama, Persimmon peel gel for the selective recovery of gold, Hydrometallurgy, 2007, 87, 133-139.

[21] D. Parajuli, C. R. Adhikari, H. Kawakita, S. Yamada, K. Ohto and K. Inoue, Chestnut pellicle for the recovery of gold, Bioresour. Technol., 2009, 100, 1000-1002.

[22] B. Pangeni, H. Paudyal, M. Abe, K. Inoue, H. Kawakita, K. Ohto, B. B. Adhikari and S. Alam, Selective recovery of gold using some cross-linked polysaccharide gels, Green Chem., 2012, 14, 1917-1927.

[23] K. Inoue, M. Gurung, H. Kawakita, K. Ohto, D. Parajuli, B. Pangeni and S. Alam, Chapter 5 Development of novel biosorbents for gold and their application for the recovery of gold from spent mobile phones, The recovery of gold from secondary sources ed. By S. Sabir, World Scientific Publishing Co. Ltd., 2016, 143-171.

[24] S. Krishnamurthy, A. Esterle, N. C. Sharma and S. V. Sahi, Yucca-derived synthesis of gold nanomaterial and their catalytic potential, Nanoscale Res. Lett., 2014, 9, 627-636.

[25] Z. Hubickl and A. Wolowicz, Adsorption of palladium(II) from chloride solutions on amberlyst A29 and amberlyst A 21 resin, Hydrometallurgy, 2009, 96, 159-165.

[26] H. A. Droll, B.P. block and W. C. Fernrlius, Studies on coorination compounds. XV. formation constants for chloride and acetylacetonate complexes of palladium (II), J. Phys. Chem., 1957, 61, 1000-1004.

Chapter 3

Selective cesium adsorptive removal using crosslinked tea leaves

To removal radioactive cesium from polluted environment, tea leaves as cheap, environment-friendly and abundant bio-adsorbents have been investigated on alkali metals adsorption. Fresh and used tea leaves (FT and UT) were found to have high efficiency and selectivity for cesium adsorption, after the crosslinking with concentrated sulfuric acid. Calculation of proton exchanged amount suggested that adsorption mechanism of three alkali metals on crosslinked tea leaves involves a cationic exchange with a proton from the hydroxyl groups of the crosslinked tea leaves, as well as coordination with ethereal oxygen atoms to form the chelation. Based consideration of the practical view on treatment of polluted water, the competitive adsorption of Cs^+ and Na^+ ions was investigated by the batch-wise method and column chromatographical separation. Unlike conventional ion exchange and chelate resins with less selectivity for Cs^+ over coexisting cations, both crosslinked fresh (CFT) and crosslinked used tea leaves (CUT) exhibited Cs selectivity over Na. In addition, batch adsorption studies revealed that the cesium adsorptions were driven by Langmuir isotherm model, the capacities of both crosslinked tea leaves for cesium adsorption were determined to be around 2.5 mmol g^{-1}. The adsorption capacities are sufficiently higher in comparison with those of synthetic polymers, inorganic ion-exchangers, and other bio-adsorbents.

3.1 Introduction

Cesium, most active alkaline metal, is generally used in the photoelectric cells and various optical instruments [1]. Natural cesium mainly exists as ^{133}Cs, also slightly inclusive of other 11 radioactive isotopes. Three among them were concerned about the radioactive hazardous isotope because of their long-term of half-life, ^{134}Cs (2.1 years), ^{135}Cs (2.3 million years), ^{137}Cs (30.17 years) [2]. Radioactive ^{137}Cs, as a representative fission product of ^{235}U, has specifically increased the utilization in a nuclear power plant. The Fukushima Daiichi nuclear power plant accident at Okuma, Fukushima, Japan, produced massive hazardous nuclear waste in the form of dust into the atmosphere. Thus, released nuclear waste contains hazardous radioactive cesium, which were eventually adsorbed onto soil and were contaminated into the groundwater and nearby seawaters *etc*. When water was contaminated by the cesium and other radioactive elements and reached into human body through the food chain, they cause several health problems including cancers for longer terms. Therefore, the method and technique to reduce cesium pollution have been utmost required.

For cesium recovery, solid adsorption and solvent extraction as general methods, have been applied. Some extractants exhibit remarkable efficiency on cesium(I) extraction because of specific macrocyclic structures [3,5], while they also exhibited some disadvantages such as much amount consumption of organic solvents. Metal ion adsorption either on the surface or inner adsorbents from aqueous solution can, therefore, be an alternative method without employing complicated synthetic extractants and diluents. In addition, compared to the synthetic adsorbents such as organic compounds and polymers [6,7], the adsorbents obtained from the natural resources-minerals and bio-adsorbents [8,9], have a simple modified method, less pollution and most importantly low-cost way for a valuable cesium recovery. While conventional ion-exchange resins preferably adsorb not monovalent metal ions such as Cs^+, but coexisting multivalent ions.

Recently, because of the characteristics of environmental friendliness, and large

wealthy resource of adsorbents, the studies on metal adsorption using bio-mass adsorbents has been focused for serval years [10-12]. The presence of various active functional groups, like amino, hydroxyl, carboxylic acid, and carbonyl groups, *etc*. in adsorbents makes them available for chelation or complexation with metal ions. As the effective and cheaper materials of bio-adsorbents, tea leaves owe to high yield and consumption in the world. In addition, the chemical composition of tea leaves constitutes alkaloids, proteins, amino acids, carbohydrates, polyphenols, chlorophyll, volatile compounds, fluoride, minerals, trace elements and other undefined compounds [13,14]. Remarkably, the phenolic components in tea leaves have more than 10 kinds of structures. In the green tea, flavan-3-ol and flavonols are the main substances. Black tea produced by fermentation of green tea leaves mainly contains gallic acid derivatives, flavonols, and thearubigins [15,16]. Therefore, the presence of these groups provides the potential benefit to metal recovery by the ion-exchange or complexation with the active groups. It was reported that Cr(VI) adsorption on tea waste / Fe_3O_4 composite and the mechanism involved electrostatic attraction, reduction process, ion exchange and surface complexation *etc* [17]. In addition, Wan *et* al. reported the adsorption of heavy metals, Pb(II), Cd(II) and Cu(II), was based on ion-exchange with the phenolic hydroxyl groups [18]. The successful removal of heavy metals on tea leaves implies the potential adsorption of even monovalent alkali metals. While, based on this purpose, factor of dehydration of Cs^+ by increasing coordinating atoms should be considered as well.

Hence, the crosslinking of the phenol groups in the fresh and used tea leaves with concentrated sulfuric acid was carried out to estimate the content of various phenolic groups. Both the crosslinked tea leaves were continuously applied to other alkali metals (Na and K) adsorption to elucidate the adsorption mechanism. Furthermore, the potential recovery of Cs on two types of crosslinked tea leaves by batch method and chromatographical column was investigated.

3.2 Materials and methods

3.2.1 Reagents

Analytical grade alkali metal chlorides (CsCl, KCl, and NaCl) and alkali metal hydroxide (CsOH, KOH, and NaOH), purchased from Wako Reagent Co., Ltd., Japan, were used to prepare sample solutions. The concentrated sulfuric acid and hydrochloric acid were also purchased from Wako Chemicals. The fresh and used tea leaves were kindly supplied by Ochachamura Mine Tea MFG., Co., Ureshino city, Saga, Japan.

3.2.2 Preparation method for adsorbents

The used tea leaves were stored in a freezer to prevent from getting moldy. As the pre-treatment, the leaves were dried in an oven for 72 h at 60℃. For crosslinking, 15.0 g fresh and used tea leaves were stirred in 50 cm^3 concentrated sulfuric acid (18.4 M) at 90℃ for 20 h. The mixtures were cooled down to room temperature and soaked into 500 cm^3 deionized water. After the filtration, the product was packed into the glass column and continuously washed with deionized water until the pH of washing solution became neutral. Then, the washed product was dried at 60℃ for 48 h. Finally, the obtained cake was crushed and ground and sieved through 150 μm mesh to keep the uniform size. The images and the micrographs of tea leaf surfaces before and after the crosslinking were measured by SEM and XRD.

3.2.3 Batch adsorption experiments

The pH of alkali metal solution was adjusted by mixing of 1.0 mM MOH (alkali metal hydroxide) solution and 1.0 mM MCl (alkali metal chloride) which contained 0.10 M HCl solution. The pH value of time dependency test solution was 2.6 by the adjustment

of alkali metal hydroxide and HCl solution. Fifty milligrams adsorbents were added to 10 cm^3 of all the metal samples. Then the mixture was shaken at 150 rpm at 30℃ for 24 h. After filtration, metal concentration of an aqueous solution was measured by atomic absorption spectrophotometer (AAS Shimadzu model AA-6650) and IR spectra of the adsorbents were measured by FTIR spectrophotometer (JASCO model FTIR-410 spectrophotometer) after drying. For maximum adsorption capacity test, the different concentrations of alkali metal solution were prepared by the direct addition of different amounts of MCl powder into 10.0 mM MOH solution. The solution of concentration lower than 10.0 mM was diluted by deionized water.

The batch methods of adsorption processes for alkali metal are same as precious metals adsorption on polysaccharides, graphically shown in Fig. 2-2 in Chapter 2.

3.2.4 Column adsorption experiment

The column chromatographic setup was provided by the peristaltic pump (IWAKI PST-100N, Japan), connected to 8 mm diameter glass column in which glass beads, cotton, and 0.15 g (volume is 0.515 cm^3) adsorbents were successively packed. Deionized water was first passed into the column, then water was exchanged with the co-existing metal ions: Cs^+ and Na^+, at the constant flow rate, 5.52 $cm^3\ h^{-1}$ for crosslinked fresh tea leaves (CFT) and 5.85 $cm^3\ h^{-1}$ for crosslinked used tea leaves (CUT), respectively. The concentration of Cs^+ and Na^+ coexisting in solution were adjusted to be 1.84 and 2.68 mM for the experiment using CFT, while the concentrations were to 1.80 mM and 2.39 mM for using CUT. The pH values of both feed solutions were adjusted to 8.9 by the measurement of pH meter. At the equilibrium, pH values were changed to around 7.7 (CFT) and 7.4 (CUT), and they were close to the neutral solution and similar to the batch experimental pH values. Finally, the solution passed through the column was collected at constant interval by the fraction collector (BIORAD Model 2110 Fraction Collector). At fixed flow rate, the solution volume of each sample collection was calculated and the

metal concentrations of every sample were measured by atomic absorption spectrophotometer (AAS, Shimadzu model AAS-6650) to obtain the amount of the adsorbed metal. At the saturated state of the adsorption, the sum of the molar mass of the adsorbed metal divided by the mass of the adsorbent corresponded to adsorption capacity. After the adsorption reached a breakthrough, the adsorbed metal ions were eluted with dilute HCl solution (pH 1.9) by using the peristaltic pump at the constant flow rate. The eluted flow rates for the experiments using CFT and CUT were adjusted to 4.68 and 4.62 $cm^3\ h^{-1}$. The eluted solutions were collected by the same procedure as a breakthrough test.

3.2.5 Evaluation of adsorption measurements

The alkali metal concentrations of all solutions were measured by AAS. The pH value of the sample solution was measured by pH meter. The FT-IR spectra of all the samples were measured in the range of 4000-400 cm^{-1} wave number with FTIR spectrophotometer by using the KBr pellet method. The micrographs of the metal loading materials were taken by SEM. The images of XRD of the tea leaves and crosslinked tea leaves were also measured.

The calculation of adsorption percentage (Ad%) and amount of adsorbed alkali metal ions on adsorbents (q) are same as mentioned in section 2.23.

3.3 Results and discussion

3.3.1 Adsorption of cesium ions on crude and crosslinked tea leaves

The SEM images of tea leaves before and after the crosslinking are shown in Figs. 3-1 (a), (b), (c) and (d). The surfaces of UT already have been soaked into water before modification, then dried were more folded and layered than those of FT. After crosslinking, smooth surfaces of both materials meant the unreacted substance was not

left.

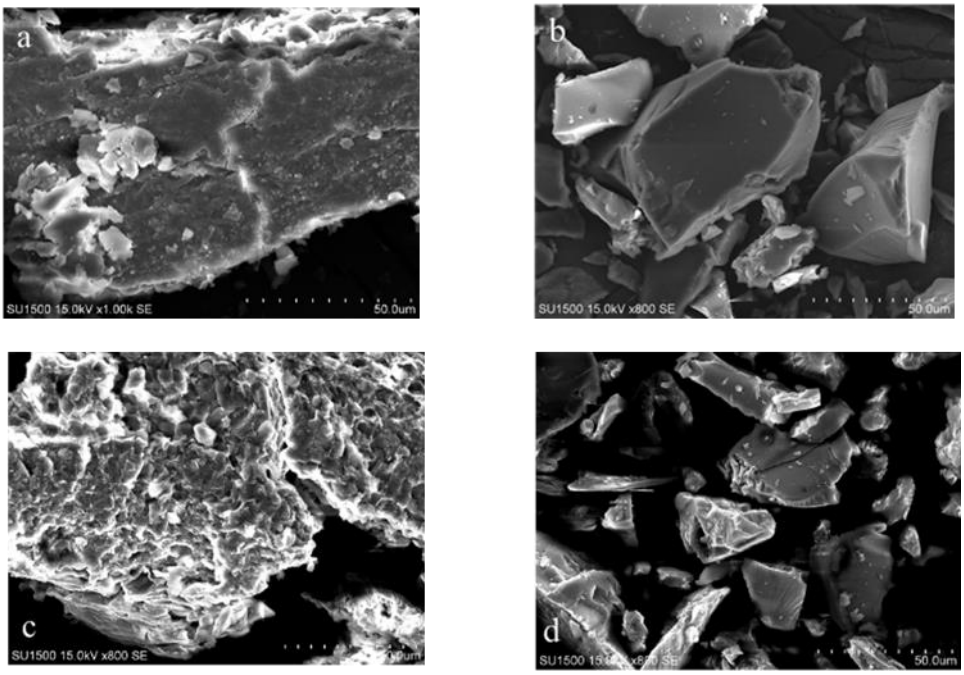

Fig. 3-1 SEM images of tea leaves before and after the crosslinking, (a) FT, (b) CFT, (c) UT and (d) CUT.

The XRD analysis of materials metal loading samples are shown in Figs. 3-2 (a) and (b). The result showed subtle but important information for the crosslinking. Four tea leaves have amorphous structure without any sharp peaks but with broad folding peaks except UT. The UT had a peak, while CUT had no peaks. It can be a good evidence that UT was successfully crosslinked. By careful observation, the folding points of the crosslinked materials were slightly shifted to the higher angles than those of the original ones. It means that lattice spaces of the crosslinking materials became narrower than those of the original ones. The crosslinking formed ethereal bonds by condensation of phenolic groups, consequently distance between molecules became closer. Therefore, it is also good evidence that materials were successfully crosslinked.

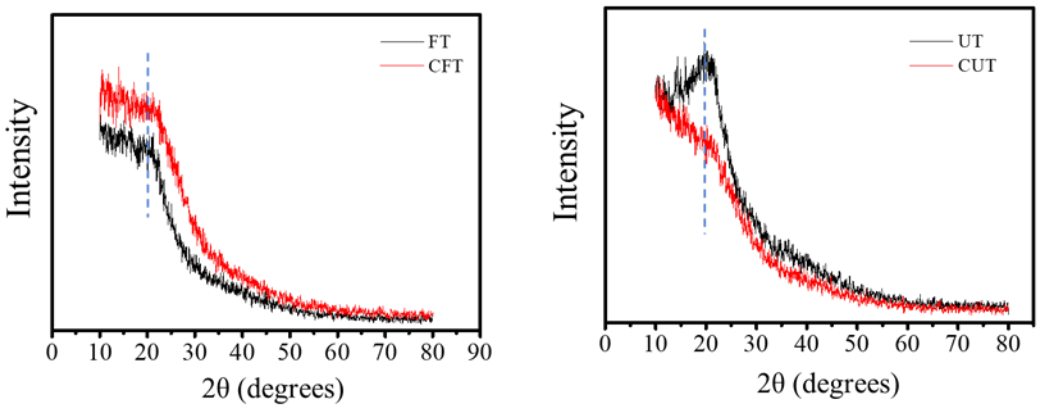

Fig. 3-2 X-ray diffraction patterns of (a) fresh and (b) used tea leaves before and after the crosslinking.

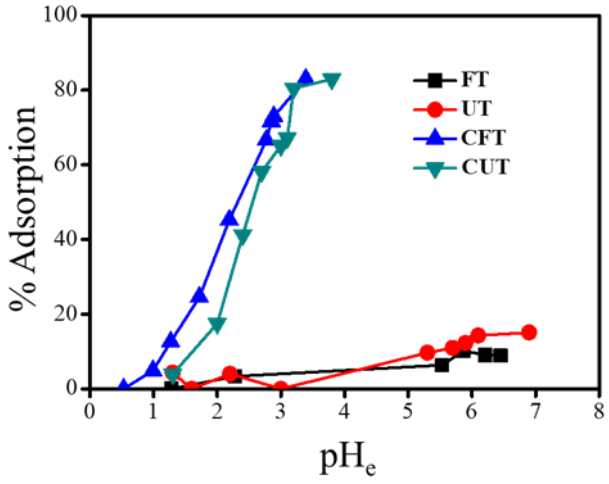

Fig. 3-3 Adsorption of Cs^+ ions on crude and crosslinked tea leaves as a function of equilibrium pH, adsorbent weight=0.05 g, solution volume=10.0 cm^3, $[Cs^+]_i$ =1.0 mM, shaking time=24 h.

Adsorption of Cs^+ ions on crude and crosslinked tea leaves at different pH values are shown in Fig. 3-3. Both of the crosslinked adsorbents, CFT and CUT showed the better performance of Cs^+ adsorption than FT and UT at various pH values. Since the heating of crude tea leaves with concentrated sulfuric acid, some polymers, such as cellulose and hemicellulose [19,20] were partly hydrolyzed to soluble product. With the washing treatment, removal of large number of unreacted substance on adsorbents and the expose of reactional core obviously improved the activity of materials for adsorption.

The alkali metal cations are coordinated with water molecules in aqueous phase [21,22]. In the figure, the Cs^+ adsorption on both CFT and CUT is sensitively dependent on pH values of aqueous solutions, hence the adsorption mechanism is related to the ion-exchange.

Furthermore, the production of ether groups through crosslinking could coordinate with Cs^+ ion to replace its coordination with oxygen atoms of water molecules. Hence, by the function of coordination, Cs^+ was promoted to contact with hydroxyl groups and the ion exchange reaction takes place as shown in the schematic images.

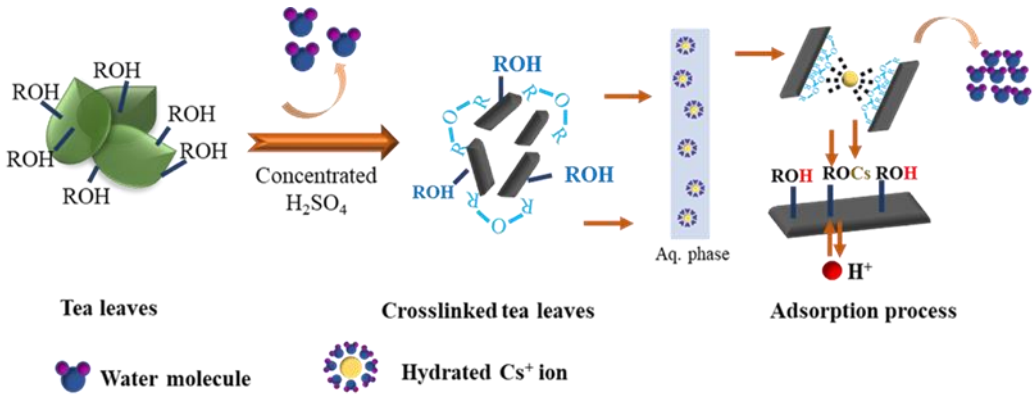

Scheme 3-1 Modification of tea leaves and Cs adsorption process in aqueous phase.

3.3.2 Effect of shaking time on adsorption of alkali metal ions

Because of the low adsorption potential of crude FT and UT, the alkali metal ion adsorption on two crosslinked adsorbents was only focused in the subsequent experiments. The effect of shaking time on adsorption of alkali metal ions on the crosslinked adsorbents is shown in Figs. 3-4 (a) and (b). Cesium has the largest ionic radius among ions examined, consequently has the lowest charge density among of alkali metals. Adsorption of alkali metal ions on crosslinked adsorbents was sufficiently fast to reach equilibrium within 6 h. Thus, it was found that crosslinked adsorbents exhibited a high effect on adsorption of alkali metal ions.

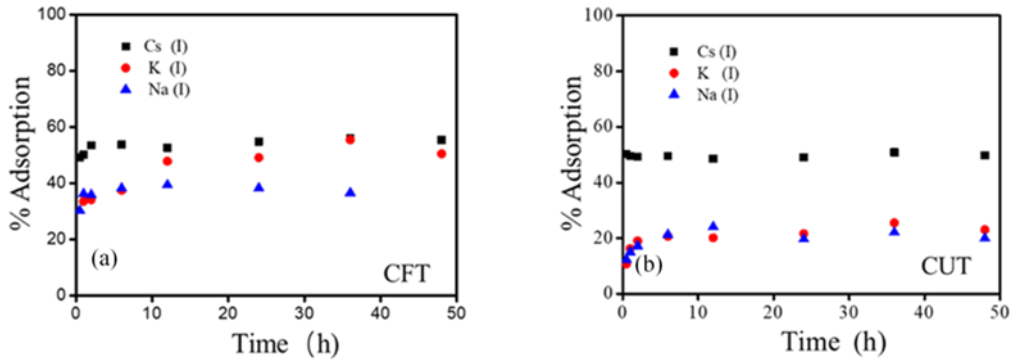

Fig. 3-4 Effect of time for alkali metal ion adsorption on (a) CFT adsorbents and (b) CUT adsorbents, adsorbent weight=0.05 g, solution volume=10.0 cm^3, $[M^+]_i$ =1.0 mM, pH_e=2.5, shaking time= several hours.

3.3.3 Effect of pH on adsorption of alkali metal ions

For the further study on the Cs^+ ion adsorption mechanism on crosslinked tea leaves and other alkali metal (Na, and K) ions, adsorption was investigated at different pH range (1-11) as well.

The effect of equilibrium pH (pH_e) on adsorption percentage is shown in Figs. 3-5 (a) and (b). The fitting curves theoretically drawn in the figures will be discussed later. Metal ion with smaller ionic radius has higher electron density, consequently higher hydration energy than that with larger radius. Larger Cs^+ is easily dehydrated than smaller K^+ and Na^+. It is the reason why Cs^+ was slightly selectively adsorbed on tea leaves type adsorbents over smaller two ions. The Cs^+ selectivity over smaller ions was caused by such different hydration energy based on different ionic radii.

The adsorption percentage was increased with increasing pH value, and the pH value was dramatically dropped after the adsorption, because protons were released from crosslinked adsorbents and ion-exchanged with metal ion. It is reasonable that the adsorption reaction of alkali metal ion is driven by cationic exchange. The adsorption reaction is written by equation (3.1):

$$M^+ + ROH \overset{K_{ad}}{\rightleftharpoons} ROM + H^+ \quad (3.1),$$

where M and ROH represent alkali metal and active polyphenolic sites of adsorbents in crosslinked tea leaves, and K_{ad} represents the equilibrium adsorption constant of alkali metal ion.

Equation (3.1) indicates that one alkali metal cation was adsorbed on one phenolic group. One proton was released from a phenolic hydroxyl group at the same time.

The equilibrium adsorption constant of alkali metal ion is represented by equation (3.2), where η represents the amount of substance (mol).

$$K_{ad} = \frac{\eta_{ROM}\ \eta_{H^+}}{\eta_{ROH}\ \eta_{M^+}} \quad (3.2)$$

Here ratio of metal concentration between solid and aqueous phases is simply defined as distribution ratio as described in equation (3.3). The M_{ROH} and m_{ROH} represent the molecular weight of adsorbents (g mol^{-1}) and the weight (g) of adsorbents. The q is amount of adsorbed metal on the adsorbents (mmol g^{-1}).

$$D = \frac{q}{C_e} = \frac{(C_i - C_e)\,V_m}{C_e\ m_{ROH}} \quad (3.3)$$

$$\frac{\eta_{ROM}}{\eta_{ROH}} = \frac{(C_i - C_e)\,V_M}{m_{ROH}/M_{ROH}} \quad (3.4)$$

Equation (3.3) represents the mole ratio between the raw adsorbents and absorbed metal adsorbents.

After derivation of equations (3.2-4), taking logarithm, equation (3.5) is obtained.

$$\log D = \log K_{ad} - \log M_{ROH} + pH_e \quad (3.5)$$

The relationship between log *D* and equilibrium pH value (pH_e) is linear. The effect of equilibrium pH on distribution ratio is shown in Figs. 3-6(a) and (b). All plots lie on the straight lines with certain slopes listed in Table 3-1. All of the slopes are close to 1, which it adequately indicates that all adsorption reactions of alkali metal ions are driven by the cationic exchange, namely, one proton was released by loading one cation.

Although used tea leaves were supplied after use for beverage and it was expected that water-soluble molecules were dissolved and lost before the crosslinking. The slope of crosslinked tea leaves was closed to 1, which means that the slightly different amount of ether groups in tea leaves hardly affected on Cs^+ adsorption.

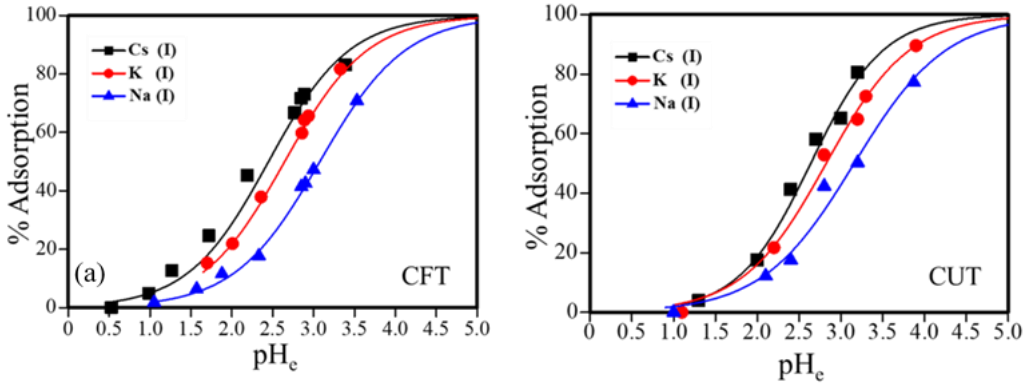

Fig. 3-5 Effect of pH dependency on adsorption of alkali metal ions on (a) CFT adsorbents and (b) CUT adsorbents at 303K, adsorbent weight=0.05 g, solution volume=10.0 cm^3, $[M^+]_i$ =1.0 mM each, shaking time=24 h.

Table 3-1 Calculated slope value of alkali metal ions based on the Equation (3.5)

Adsorbent	**Cs^+**		**K^+**		**Na^+**	
	Slope	R^2	Slope	R^2	Slope	R^2
CFT	0.822	0.9863	0.858	0.9953	0.831	0.9919
CUT	0.997	0.9795	0.861	0.9860	0.780	0.9510

The intercepts of the fitting equation in Figs. 3-6 (a) and (b) represent for the logarithm value of the ratio of K_{ad} and M_{ROH}, used "a" to represent as follows. Base on this, unified the equations (2.1), (3.1), (3.6-7) to obtain equation (3.8).

$$Ad = \frac{C_i - C_e}{C_i} = 1 - \frac{C_e}{C_i} \tag{3.6}$$

$$\frac{Ad}{1-Ad} = \frac{K_{ad}\, m_{ROH}}{V_M\, M_{ROH}\, [H^+]} = \frac{a\, m_{ROH}}{V_M\, [H^+]} \tag{3.7}$$

$$Ad\ \% = \frac{100\, a\, m_{ROH}}{V_M\, 10^{-pH_e} + a\, m_{ROH}} \tag{3.8}$$

The eq. (3.8) was reflected to plot the fitting curve in Figs. 3-5, each curve of alkali metal ions was calculated with the respective slopes value in Table 3.1. The logarithm value of the ratio of K_{ad} and M_{ROH} (replaced as a) by the calculation of fitting equation results. All the R square values of linear lines drawn in Figs. 3-6 (a) and (b) are higher than 0.99. All experimental data of adsorption percentage in Figs.3-5 (a) and (b) are very reliably closed to the calculated curve.

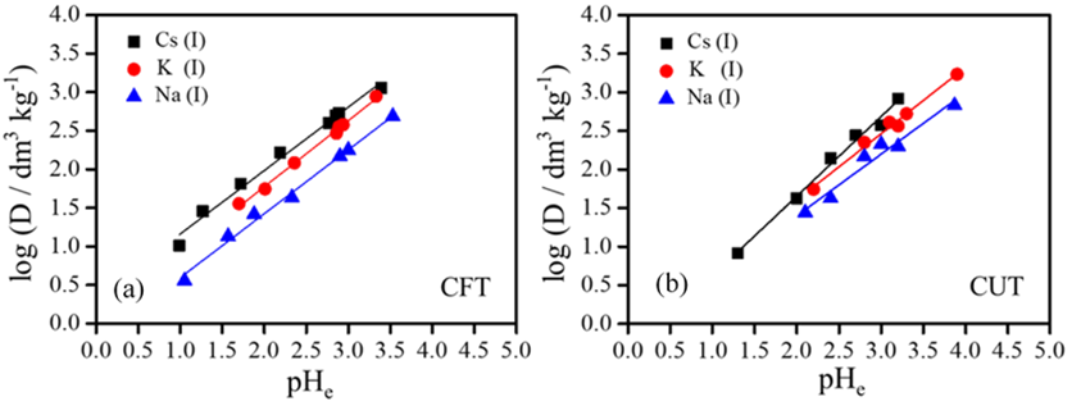

Fig. 3-6 Effect of pH_e value on distribution ratio of alkali metal ion at 303K, (a) CFT adsorbents and (b) CUT adsorbents, adsorbent weight=0.05 g, solution volume=10.0 cm^3, $[M^+]_i$ =1.0 mM each, shaking time=24 h.

3.3.4 Adsorption isotherms of Na^+ and Cs^+ ions on crosslinked fresh and used tea leaves adsorbents

Large existence of sodium ions leads to the unavoidable containing in the polluted water in nature. Hence, the adsorption isotherms for Na^+ and Cs^+ ion on CFT and CUT adsorbents under similar pH_i (around 11) condition were investigated as shown in Figs. 3-7 (a) and (b), respectively. The adsorption amounts of adsorbents for Na^+ and Cs^+ ions increased with the increase of initial metal concentration and reached at the maximum loading capacity. The results show that metal adsorption is classified into the Langmuir

models [23] which was described at Chapter 2.

By the fitting on the experimental data, the maximal adsorption capacities of Cs^+ and Na^+ on CUF adsorbents are 2.3 and 2.4 mmol g^{-1}, while those on CFT adsorbent are 2.5 and 2.2 mmol g^{-1}.

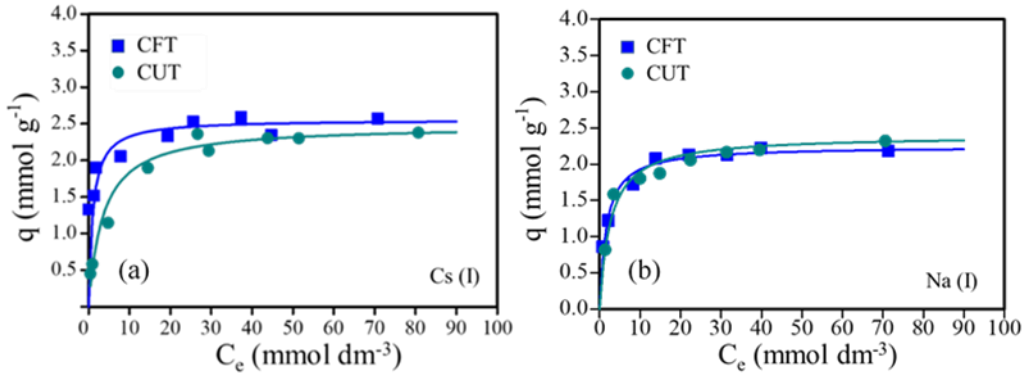

Fig. 3-7 Adsorption isotherms: (a) Cs^+ ion on CFT and CUT adsorbents, (b) Na^+ ion on CFT and CUT adsorbents, adsorbent weight=0.05 g, solution volume=10.0 cm^3, pHe=7.0 ± 1.0 (Cs^+) and 7.5 ± 0.5 (Na^+), shaking time=24 h.

To confirm the validity of the obtained maximum adsorption capacities, linearly transformed equation was obtained. Base on equation, the Langmuir parameters, and maximal adsorption capacities can be calculated from the intercept and the slope of the straight line by linear regression analysis and the obtained values are listed in Table 3-2. The R^2 values of both adsorbents are higher than 0.99, also verified that adsorption is governed by the Langmuir model. On the other hand, the maximal capacities of Cs^+ and Na^+ on CUF adsorbents are 2.48 and 2.40 mmol g^{-1}, while those on CFT adsorbents are 2.56 and 2.25 mmol g^{-1}. Due to the pretreatment before experiment, UT was soaked into water before, the water soluble substances were partially removed, hence, it had slightly higher capacity than that Cs^+ adsorption of CFT. Since those values correspond to the values obtained from Figs. 3-8 (a) and (b), particularly confirm the reliability of values. In addition, the Cs^+ adsorption capacities on CUF and CFT adsorbents were compared with those obtained by using other adsorbents with batch method as listed in Table 3-3. As the comparison, the Cs^+ capacities on both types of crosslinked adsorbents are

sufficiently high. Especially for used tea leaves, they are much economical than the fresh tea leaves but have the similar capacity on Cs^+ ion adsorption as CFT.

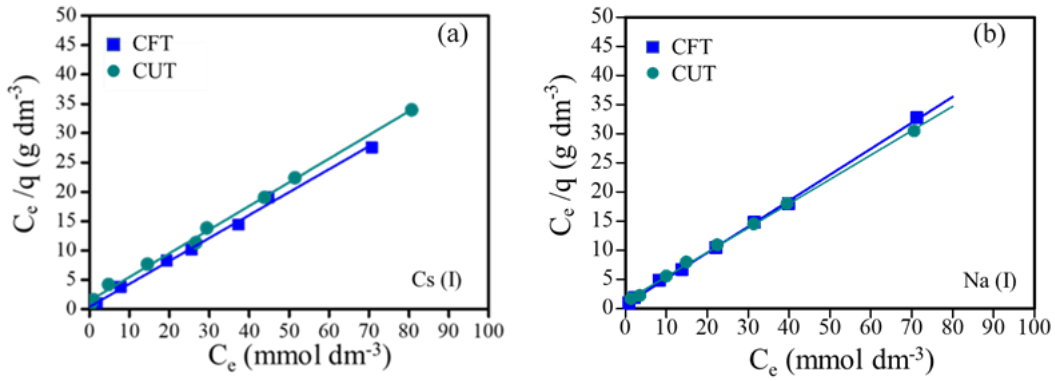

Fig. 3-8 The Langmuir isotherm kinetic models: (a) Cs^+ ion adsorption on CFT and CUT adsorbents, (b) Na^+ ion on CFT and CUT adsorbents, adsorbent weight=0.05 g, solution volume=10.0 cm^3, pHe=7.0 ± 1.0 (Cs^+) and 7.5 ± 0.5 (Na^+), shaking time=24 h.

Table 3-2 Langmuir isotherm constants for adsorption of Na^+ and Cs^+ on adsorbents

	CUT adsorbent			**CFT adsorbent**		
	q_m (mmol g^{-1})	b (dm^3 $mmol^{-1}$)	R^2	q_m (mmol g^{-1})	b (dm^3 $mmol^{-1}$)	R^2
Na^+	2.40	0.6431	0.999	2.25	0.3182	0.999
Cs^+	2.48	0.2802	0.997	2.56	0.9950	0.996

Table 3-3 Comparisons of adsorption capacities of present adsorbents with various kinds of other adsorbents for Cs^+ ion reported in the literature

Adsorbent	Adsorption capacity (mmol g^{-1})	pH	Temperature (K)	Reference
Layered metal sulfide (KMS-1)	1.70	≈ 7.0 (pH_e)	298	24
Sericite	0.050	5.0 (pH_i)	298	25
RIP of clay minerals	0.250	7.0 (pH_i)	_	26
Prussian blue	1.254	Water	298	27
Biomass of marine algae	0.248	5.5 (pH_i)	303	28
Arca shell biomass	0.036	5.5 (pH_i)	298	29
CUT	2.48	7.0 ±1.0 (pH_e)	303	Present work
CFT	2.56	7.0 ±1.0 (pH_e)	303	Present work

Note, "-": temperature was not mentioned in the article. "pH_i and pH_e": initial and equilibrium pH value.

3.3.5 Chromatographical separation of Cs^+ over Na^+ ions using crosslinked tea leaves

Based on the investigation of adsorption isotherm of Na^+ on crosslinked tea leaves by batch experimental result, high adsorption capacity of Na^+ may cause competition of Cs^+ adsorption in the solution with co-existing metal ions. Hence the essential investigation on adsorption of Cs^+ in excessive Na^+ solution by column chromatographical technique was studied.

Figures 3-9 (a) and (b) show the breakthrough profiles of Cs^+ and Na^+ adsorption on CFT and CUT, respectively. The metal selectivity given here was followed by the result shown in Fig. 3-5 (a) and (b).

Furthermore, adsorption capacities of the adsorbents towards to Cs^+, as listed in Table 3-4, the capacity is much higher than that of Na^+. For CFT adsorbents, the

adsorption capacities of Cs^+ and Na^+ were evaluated as 0.992 and 0.528 mmol g^{-1}. For CUT adsorbents, the capacities of Cs^+ and Na^+ were 0.804 and 0.491 mmol g^{-1}. The selectivity of CUT and CFT towards to Cs^+ is jointly decided by the lower hydration energy and stable coordination. The CFT and CUT adsorbents still sufficiently exhibited high ability to remove Cs^+ from co-existing solution.

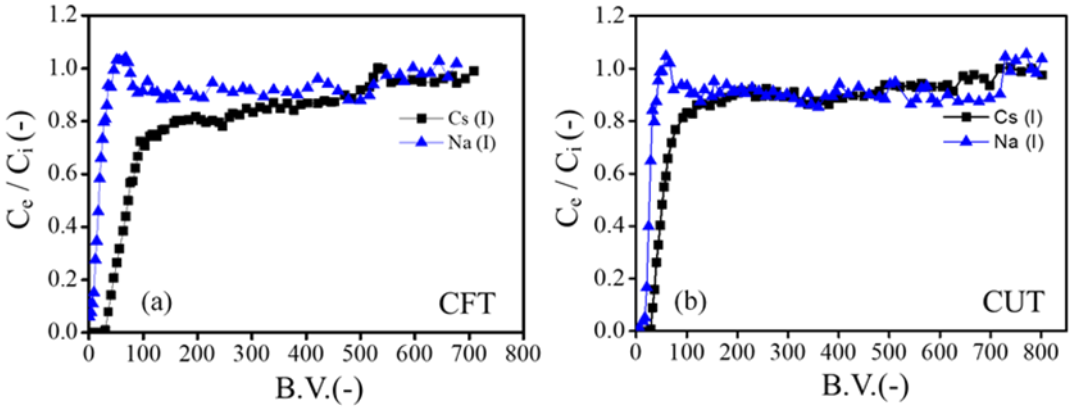

Fig. 3-9 Breakthrough profiles of Cs^+ and Na^+ ions upon passing the column packed with (a) CFT adsorbents and (b) CUT adsorbents, pH_e= 7.7 (CFT) and 7.4 (CUT), weight of adsorbents= 0.15 g (0.515 cm^3), $[Cs^+]_i$ = 1.84 mM (CFT), 1.80 mM (CUT), $[Na^+]_i$ = 2.68 mM (CFT), 2.39 mM (CUT), flow rate= 5.52 cm^3 h^{-1} (CFT) and 5.85 cm^3 h^{-1} (CUT) .

After the saturation of the adsorbent bed, it was eluted by HCl solution with pH value adjusted to 1.9 to recover the adsorbed metal ions, the elution profiles are shown in Figs. 3-10 (a) and (b). It was found that massive metal ions were immediately released in a short period. Finally, all metal ions were eluted, as listed in Table 3-4. The high efficiency of recoveries implies that tea leaves have the potential to be practical contaminated water treatment, especially for used tea leaves.

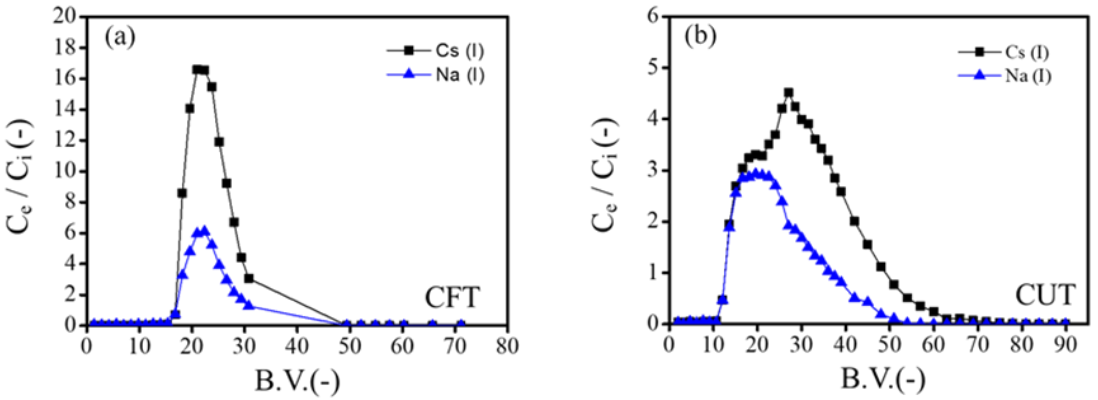

Fig. 3-10 Elution profiles of the adsorption Cs^+ and Na^+ ion on (a) CFT adsorbents and (b) CUT adsorbents with HCl solution, pH= 1.9, flow rate= 4.68 $cm^3\ h^{-1}$ (CFT), 4.62 $cm^3\ h^{-1}$ (CUT).

Table 3-4 Separation and removal Cs^+ from the mixture of Na^+ ions

	CUT adsorbent			CFT adsorbent		
	Adsorbed (mmol g^{-1})	Eluted (mmol g^{-1})	% Recovery	Adsorbed (mmol g^{-1})	Eluted (mmol g^{-1})	% Recovery
Na^+	0.491	0.484	98.57	0.528	0.497	94.13
Cs^+	0.804	0.716	89.05	0.992	0.951	95.78

3.3.6 Fourier-transfer infrared analysis

For the further study on the adsorption sites in adsorbents for alkali metal adsorption, FT-IR spectra of a series of the adsorbents before and after the metal adsorption were studied as shown in Figs. 3-11 (a) and (b). The broad bands at 3310- 3430 cm^{-1} of all materials are assigned as phenolic O-H stretching. After the crosslinking, the peaks became smaller. The peaks around 1600 cm^{-1} are identified as the stretching vibrations of C=C groups derived from benzene rings. These peaks can be relative standard to O-H stretching peaks, because they were not changed after the crosslinking. The O-H stretching peaks also became broader and shifted lower frequency. After the crosslinking, hydroxyl groups were partially converted into ethereal groups, and the remaining hydroxyl groups easily formed hydrogen bonds with the ethereal oxygen atoms. The other reason why the strong hydrogen bonds were observed in FTIR spectra was that the

distance between molecules became closer by the crosslinking. This was coincident with the result of XRD and also supported the successful crosslinking.

In addition, after the Cs^+ loading, the peaks became sharper and shifted to a higher frequency. That result proved that phenolic protons were exchanged with Cs^+. The result proves that the adsorption took place by cationic exchange. The medium bands around 2930 and 2850 cm^{-1} of two types of crude tea leaves are attributable to C-H stretching frequencies. The sharp band around 1600 cm^{-1} of two types of tea leaves is identified as the stretching vibrations of C=O groups. After the crosslinking, the degradation of some polymers led to the weaker intensity of C-H and lower frequency shift of C=O on CFT and CUT. The moderate peaks appeared at 1160 cm^{-1} belong to C-O-C stretching vibrations, caused by the formation of new C-O-C linkages produced from the condensation reaction of hydroxyl groups. Furthermore, the ethereal peaks of CFT and CUT were slightly shifted to 1180 cm^{-1} after the adsorption. That was caused by the coordination of ethereal oxygen atoms to Cs^+. In other words, during the adsorption, the oxygen atoms of ether groups coordinated with Cs^+ instead of oxygen atoms from water molecules coordinating to Cs^+. These results strongly supported that the crosslinking of the adsorbents converted hydroxyl groups into ethereal oxygen atoms easily coordinating to Cs^+ for dehydration, and consequently the adsorption reaction was enhanced not only by proton exchange mechanism but also coordination with ether groups.

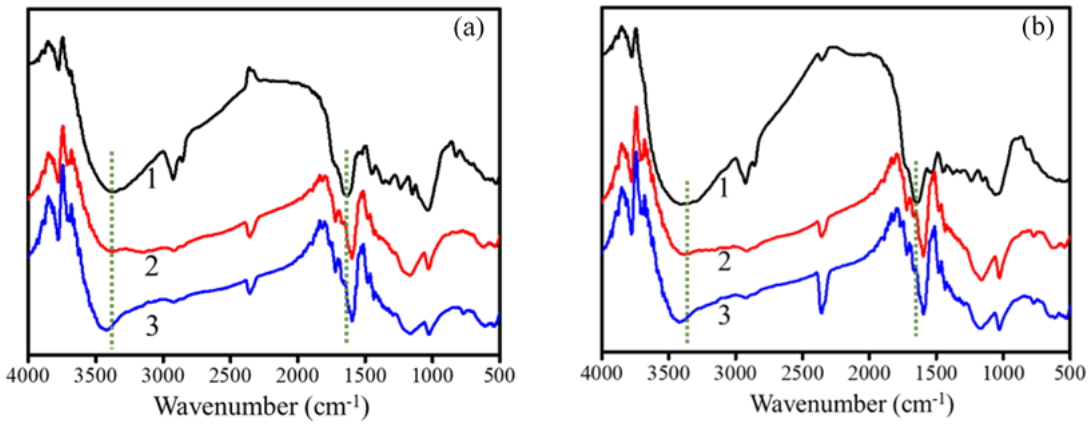

Fig. 3-11 FT-IR spectra of adsorbents, (a) 1 FT, 2 CFT, 3 CFT- adsorbed Cs^+ and (b) 1 UT, 2 CUT, 3 CUT-adsorbed Cs^+.

3.4 Conclusions

Both the fresh and used tea leaves as environmentally friendly bio-sorbents, exhibited the excellent adsorption performance of alkali metal ions by crosslinking with concentrated sulfuric acid. Adsorption reaction of alkali metal cations involved coordination and ion exchange. The coordination of oxygen atoms of ether groups to metal ion enhanced the efficiency of adsorption. Following by Langmuir model, compared with the maximal capacities of Cs^+ ions with batch method on synthesized chemicals, minerals, and other bio-adsorbents, those on the crosslinked tea leaves exhibited the superior uptake because of the rich phenolic functional groups. Water-soluble molecules were partially eluted and such small lost had no suppression to adsorption capacity of CUT, it was similar to that of CFT. The selective separation of Cs^+ in excessive Na^+ solution was investigated by using column chromatography. The crosslinked tea leaves exhibited Cs^+ selectivity over Na^+. The elution of the loaded Cs^+ ion was successfully achieved with a low concentration of the acidic solution in a short period. Even used tea leaves exhibited comparable adsorption behavior to the fresh ones after the crosslinking. Due to the sensitivity to solution of pH, crosslinked tea leaves have the potential to be constantly reused material for cesium removal after acidic elution to come true the reused resources.

Low cost and environmentally friendly adsorbents were easily prepared and can be candidates for cesium removal from polluted water.

3.5 References

[1] J. Peterson, M. MacDonell, L. Haroun and F. Monette, Argonne National Laboratory, Radiological and chemical fact sheets to support health risk analyses for contaminated areas, Argonne National Laboratory, EVS, Human Health Fact Sheet, 2005.

[2] M. P. Unterweger and R. Fitzgerald, Update of NIST half-life results corrected for

ionization chamber source-holder instability, Appl. Radiat. Isot., 2014, 87, 92-94.

[3] C. Xu, J. C. Wang and J. Chen, Solvent extraction of strontium and cesium: a review of recent progress, Solvent Extr. Ion Exch., 2012, 30, 623-650.

[4] R. G. Shuler, C. B. Bowers Jr., J. E. Smith Jr., V. van Brunt and M. W. Davis Jr., The extraction of cesium and strontium from acidic high activity nuclear waste using a purex process compatible organic Extractant, Solvent. Extr. Ion Exch., 1985, 3, 567-604.

[5] I. V. Smirnov, E. S. Stepanova, M. Y. Tyupina, N. M. Ivenskaya, S. R. Zaripov, S. R. Kleshnina, S. E. Solov'eva and I. S. Antipin., Extraction of cesium and americium with p-alkylcalix[8]arenes from alkaline solutions, Radiochem., 2016, 58, 329-335.

[6] A. Y. Zhang and Z. F. Chai, Adsorption property of cesium onto modified macroporous silica-calix[4]arene-crown based supramolecular recognition materials, Ind. Eng. Chem. Res., 2012, 51, 6196-6204.

[7] M. A. Olatunji, M. U. Khandaker and H. N. M. E. Mahmud, Adsorption kinetics, equilibrium and radiation effect studies of radioactive cesium by polymer-based adsorbent, J. Vinyl Addit. Technol., 2018, 24, 347-357.

[8] B. C. Bostick, M. A. Vairavamurthy, K. G. Karthikeyan and J. Chorover, Cesium adsorption on clay minerals: an EXAFS spectroscopic investigation, Environ. Sci. Technol., 2002, 36, 2670-2676.

[9] C. Chen and J. L. Wang, Removal of Pb^{2+}, Ag^{+}, Cs^{+} and Sr^{2+} from aqueous solution by brewery's waste biomass, J. Hazard. Mater., 2008, 151, 65-70.

[10] M. Thirumavalavan, Y. L. Lai and J. F. Lee, Fourier transform infrared spectroscopic analysis of fruit peels before and after the adsorption of heavy metal ions from aqueous solution, J. Chem. Eng. Data, 2011, 56, 2249-2255.

[11] X. J. Hu, J. S. Wang, Y. G. Liu, X. Li, G. M. Zeng, Z. L. Bao, X. X. Zeng, A. W. Chen and F. Long, Adsorption of chromium (VI) by ethylenediamine-modified cross-linked magnetic chitosan resin: Isotherms, kinetics and thermodynamics, J. Hazard. Meter., 2011, 185, 306-314.

[12] X. K. QuYang, R. N. Jin, L. P. Yang, Z. S. Wen, L. Y. Yang, Y. G. Wang and C. Y.

Wang, Partially hydrolyzed bamboo (phyllostachys heterocycla) as a porous bioadsorbent for the removal of Pb (II) from aqueous mixtures, J. Agric. Food Chem., 2014, 62, 6007-6015.

[13] C. Cabrera, R. Giménez and M. C. López, Determination of tea components with antioxidant activity, J. Agric. Food Chem., 2003, 51, 4427-4435.

[14] M. Reto, M. E. Figueira, H. M. Filipe and C. M. M. Almeida, Chemical composition of green tea (camellia sinensis) infusions commercialized in Portugal, Plant Foods Hum Nutr., 2007, 62, 139-144.

[15] G. P.-Caro, J. M. M.-Rojas, J.M.; N. Brindani, D. D. Rio, M. E. J. Lean, Y. Hara and A. Crozier, Bioavailability of black tea theaflavins: absorption, metabolism, and colonic catabolism, J. Agric. Food Chem., 2017, 65, 5365-5374.

[16] D. D. Rio, A. J. Stewart, W. Mullen, J. Burns, M. E. J. Lean, F. Brighenti and A. Crozier, HPLC-MSn analysis of phenolic compounds and purine alkaloids in green and black tea, J. Agric. Food Chem., 2004, 52, 2807-2815.

[17] S. S. Fan, Y. Wang, Y. Li, J. Tang, Z. Wang, J. Tang, X. D. Li and K. Hu., Facile synthesis of tea waste/Fe_3O_4 nanoparticle composite for hexavalent chromium removal from aqueous solution, RSC Adv., 2017, 7, 7576-7590.

[18] S. L. Wan, N. Qu, F. He, M. K. Wang, G. B. Liu and H. He, Tea waste-supported hydrated manganese dioxide (HMO) for enhanced removal of typical toxic metal ions from water, RSC Adv., 2015, 5, 88900-88907.

[19] M. J. Taherzadeh and K. Karimi, Acid-based hydrolysis processes for ethanol from lignocellulosic materials: a review, Bioresources, 2007, 2, 472-499.

[20] W. A. Farone and J. E. Guzens, Method of producing sugars using strong acid hydrolysis of cellulosic and hemicellulosic materials, U.S Patent, 1996, 5,562,777.

[21] J. Mähler and I. Persson, A study of the hydration of the alkali metal ions in aqueous solution, Inorg. Chem., 2012, 51, 425-438.

[22] D. W. Smith, Ionic hydration enthalpies, J. Chem. Edu., 1977, 54, 540-542.

[23]I. Langmiur, The constitution and fundamental properties of solids and liquids. II

Liquids, J. Am. Chem. Soc., 1917, 39, 1848-1906.

[24] M. J. Manos, M. G. Kanatzidis, Highly efficient and rapid Cs+ uptake by the layered metal sulfide $K_2xMnxSn_3$-xS_6 (KMS-1), J. Am. Chem. Soc., 2009, 131, 6599-6607.

[25]J. O. Kim, S. M. Lee and C. Jeon, Adsorption characteristics of sericite for cesium ions from an aqueous solution, Chem. Eng. Res. Des., 2014, 92, 368-374.

[26] J. Lee, S. M. Park, E. K. Jeon and K. Baek, Selective and irreversible adsorption mechanism of cesium on illite, Appl. Geochem., 2017, 85, 188-193.

[27] B. Hu, B. Fugetsu, H. Yu and Y. Abe, Prussian blue caged in spongiform adsorbents using diatomite and carbon nanotubes for elimination of cesium, J. Hazard. Mater., 2012, 217-218, 85-91.

[28] R. J. Rad, H. Ghafourian, Y. Asef, S. T. Dalir, M. H. Sahafipour and B. M. Gharanjik, Biosorption of cesium by native and chemically modified biomass of marine algae: introduce the new biosorbents for biotechnology applications, J. Hazard. Mater., 2004, B116, 125-134.

[29] S. Dahiya, R. M. Tripathi and A. G. Hegde, Biosorption of heavy metals and radionuclide from aqueous solutions by pre-treated arca shell biomass, J. Hazard. Mater., 2008, 150, 376-386.

Chapter 4

Effective and selective adsorption of gold from precious metals on unmodified biomass adsorbents-human hair

The recovery of gold was supported by the natural and low-cost biomass waste, human hair (HH). The favorable selectivity of HH for Au(III) over Pd(II) and Pt(IV) provided the visible method for separation of precious metals. After the adsorption on HH and followed elution with deionized water and thiourea, loaded Pt(IV) and Pd(II) were completely removed and the gold could be refined from the HH by incineration in muffle furnace. The comparison of Au(III) adsorption among several amino acids contained in HH verified that the main component is cystine. Comprehensively, the adsorption processes involved not only adsorption, but also oxidation of S-S bond and the reduction of Au(III). Moreover, the batch adsorption data was fitted to the Langmuir isotherm model and the maximum Au(III) adsorption capacity or HH and white human hair (WHH) were calculated as 3.00 mmol g^{-1} and 3.24 mmol g^{-1}. Without any chemical modification, the HH and WHH performed the excellent capacity to Au(III) adsorption than other biomass materials.

4.1 Introduction

The limited resources, excessive demand and huge production of electronic waste have forced the recovery of precious metals to become the essential technical concern[1]. Electronic wastes contain various metals, also includes three or more precious metals. While the amount ratio of each metal is differently employed in materials, it leads to different content of precious metals and other heavy metals in leaching solution. That situation requests materials with the high selectivity for precious metals. Biomass adsorbents are gradually focused on the characteristics of environmentally-friendly and rich resource, low cost, as well as high adsorption capacity, selectivity and effectivity for

target metal ions. Hence, the bio-adsorption with advantageously integrated characteristics leads to attracted attention.

As mentioned before, there are three classical mainly chemical content of materials in bio-adsorbents [2-8]. And last two chapters already separately introduced the investigation of precious metals and alkali metals adsorption on polysaccharides polymer and phenolic biomass adsorbents. Hence, the present chapter would introduce the precious metal adsorption on protein rich biomass adsorbents. Typical protein rich substances of them for precious metal adsorption are including egg shells and soybean *etc*. Meanwhile, as a protein-rich substance in nature, new material, HH is focused on this research. HH is naturally derived and annual amount production approximately reach to 5.9 tons (based on the exported amount of HH at India and the calculation of population in the world at 2011) [9,10].

HH consists 65-95 % protein along with water, lipids, polysaccharides, pigments, nucleic acids, and trace elements [11], therefore, it has the valuable potential for precious metals recovery. HH is built up by parts: shaft, root and bulb. The hair shaft is composed of three different kinds of epithelial cells, cuticle, cortical and medullary [12]. Cuticle is the outmost layer, which includes the epicuticle, the A-layer, the exocuticle, the endocuticle, inner layer and cell membrane complex (CMC). The endocuticle has high content of acidic and basic proteins [13]. CMC can bind the cuticle and corticle cells together and contain low sulfuric amino acids, lipids and fatty acids [14]. In addition, cortex as the major part of human hair contains low Sulphur keratin. Several dozen microfibrils build up the cortical cell and the macrofibrils are made up by protein units. The hair proteins can be classified as disulfide proteins crosslinking proteins, the intermediate filament proteins, keratin associated proteins and disulfide and isodipeptide crosslinked mercaptolyse resistant protein [18]. They are existed in the cuticle layers, CMC and in nuclear remnants.

There are various kinds of amino acids in HH as shown in Table 4-1. Based on this advantage, HH is used for scientific studies [15,16]. Moreover, sulfur atom as the important

element in HH is focused on the cosmetic treatment [19].

More worthy is that cystine is main component in HH (13 % to 18 %) and can provide stability to HH when it is exposed to reducing, oxidizing and hydrolysis agents or weathering [17]. It specifically contributes to high wet strength, moderate swelling and insolubility by crosslinking protein to stabilize the hair fiber [18]. Besides, due to the containing disulfide bonds, cystine is popularly applied to immobilization of protein molecules by adsorption on the self-assembled monolayers of cystine or similar molecules on gold or other metal substrates based on the HSAB theory [20-22].

Table 4-1 Amount amino acids present in normal human hair in order their quantity [18].

Amino acid	**Amount**
Cysteine	17.5
Serine	11.7
Glutamic acid	11.1
Threoni	6.9
Glycine	6.5
Leucine	6.9
Valine	5.9
Arginine	5.6
Aspartic acid	5.0
Alanine	4.8
Proline	3.6
Isoleucine	2.7
Tyrosine	1.9
Phenylalanine	1.4
Histidine	0.8

Hence, considering of the active content in HH, the adsorption of precious metals on

HH was studied in the present work. The main mechanism of Au (III) adsorption on HH was studied, cystine was verified as the main functional factor for the adsorption. The precious metals were successfully separated by adsorption, elution and incineration methods. Finally, the refining gold was achieved. Furthermore, HH still kept the integral shape after gold adsorption. Herein, HH as the natural bio-adsorbents from the life waste has the high efficiency for gold recovery with the low cost.

4.2 Materials and Methods

4.2.1 Reagents

Gold(III), platinum(IV), palladium(II), sliver(I) solutions were prepared from the hydrogen tetrachloroaurate(III) tetrahydrate ($HAuCl_4 \cdot 4H_2O$), hydrogen hexachloroplatinate(IV) hexahydrate ($H_2Pt_6 \cdot 6H_2O$), palladium(II) chloride and sliver nitrate respectively. All of them were purchased from Wako Pure Chemical Industries, Ltd, Japan. The hydrochloric acid, nitric acid, ethanol and amino acids (*L*-cystine, *L*-alanine, glycine, *L*-glutamic acid and *L*-serine) were purchased from Wako Chemicals as well. The *L*-arginine was purchased from SIGMA, USA. The crude human hairs were provided from barber shop in Saga city (Japan). The deuterium oxide (D_2O) was purchased from SIGMA-Aldrich, USA. The deuterium chloride (DCl, 35% solution in D_2O. 99.5%) was purchased from Wako Pure Chemical Industries, Ltd, Japan. All the human hair for the experiment was supplied from the barber shop in Saga, Japan.

4.2.2 Preparation method for adsorbents

For unified length, HH was cut as possible as 1-2 mm. To remove the impurities (oil, dust, scurf *etc*.), 3.0 g of cut hair were stirred in the ethanol for an hour and stayed overnight. After the removal of impurities, the clean hairs were dried at room temperature

and stored in the shade.

4.2.3 Experiments of precious metal adsorption in acidic media

All the samples for batch adsorption and elution experiments were shaken at 150 rpm and 30°C. The precious metal solutions were prepared in two kinds of acidic medias, HCl (except silver) and HNO_3. Metal salts were separately dissolved into the different concentration of acidic media. Each sample had 20.0 mg adsorbents and was independently added into 10.0 cm^3, 1.0 mM metal solution and shaken for 24 h. After filtration, metal concentration of an aqueous solution was measured. Samples of time dependency test were the mixture of 20.0 mg adsorbents with 10.0 cm^3 of 0.1 M HNO_3 solution including 1.0 mM each precious metal solution and shaken for different time intervals. For maximum adsorption capacity test, each sample containing 20.0 mg adsorbents was separately mixed with 10.0 cm^3 different concentration of precious metal solution in 0.10 M HNO_3 solution media and shaken for 24 h. After drying, the adsorbents were measured by SEM, digital microscope, XRD and IR spectra. For metal separation, 20.0 mg human hair were mixed along with 10.0 cm^3 mixture of 1.0 mM Pt (IV), Pd(II), and Au(III) in different concentration of HNO_3 and shaken for 24 h. After adsorption of mixed precious metals in the 0.1 M HNO_3, each HH sample was washed with 10.0 cm^3 deionized water 3 times. Then it was mixed with 5.0 cm^3, 0.05 M thiourea in 0.01 HCl media and shaken for different time intervals. The metal concentration of eluted solution was measured by ICP-AES.

4.2.4 Au (III) loading experiment with amino acidic solution

Different amino acid powder (0.021 mmol) was independently dissolved into 10.0 cm^3 of 1.0 mM Au(III) in 0.10 M HNO_3 solution. The mixture was shaken at 150 rpm, 30°C for 24 h. After filtration by 45 μm membrane filter, the metal concentration of the solution was measured by ICP-AES.

4.2.5 Au (III) loading with cystine

The 1 mg (0.00416mmol) *L*-cystine powder was dissolved into 1 cm^3 D_2O containing trace of DCl. After ^1H NMR measurement, the solution was mixed with 45 mg (0.109 mmol) $HAuCl_4 \cdot 4H_2O$ powder and remeasured ^1H NMR for the different time interval (0h, 1h, 14.5h).

4.2.6 Gold refining from human hair

To refine the gold from the HH after metal adsorption, 0.5 g HH adsorbing gold was incinerated in the muffle furnace at 800℃ for 2 h.

4.2.7 Evaluation of adsorption measurements

The precious metal concentrations of all solutions were measured by Inductively Coupled Plasma Atomic Emission Spectrometer (ICP-AES, Shimadzu model ICPS-8100). The spectra of all the samples were measured by FTIR in the range of 4000-400 cm^{-1} wave number. The crystalline structures of the samples were measured by XRD. The images of microscope were collected on the digital microscope (KEYENCE VHX-1000). The micrographs were taken by SEM. The ^1H NMR spectra were recorded on a Mercury 400 MHz spectrometer (Agilent technology NMR 400 MHz system). The HH after adsorption of Au (III) was burned in muffle furnace (Yamato model FO100) The elements in samples were measured by Energy Dispersive Spectrometer (EDS) from the support of Liaoning University.

The batch method of adsorption processes are similarly described in Chapter 2.

The calculation of adsorption percentage (Ad%) and amount of adsorbed precious metal ions on adsorbents (q) are same as mentioned in Chapter 2.23.

The elution amount from the HH was calculated by equation (4.1):

$$\% \text{ Elution} = \frac{\eta_E}{\eta_{Ad}} \times 100 \quad (4.1),$$

where the η_E and η_{Ad} individually stands for the eluted and adsorbed molar quantities (mmol).

4.3 Results and discussion

4.3.1 Time course dependency of precious metals adsorption on human hair

The effect of shaking time on Au(III), Pd(II), and Pt(IV) adsorption in 0.1 M HNO_3 is shown in Fig. 4-1. Compared with longer time to reaching adsorption equilibrium for Pt(IV) and Pd(II) on HH, it only took 24 h to reach equilibrium for Au(III) adsorption. Because of the low adsorption performance of Pd(II) and Pt(IV), shaking time for equilibrium of all precious metals adsorption was determined to be 24 h. Long term of adsorption caused by the reduction of Au(III), similar to adsorption on kiwi peel.

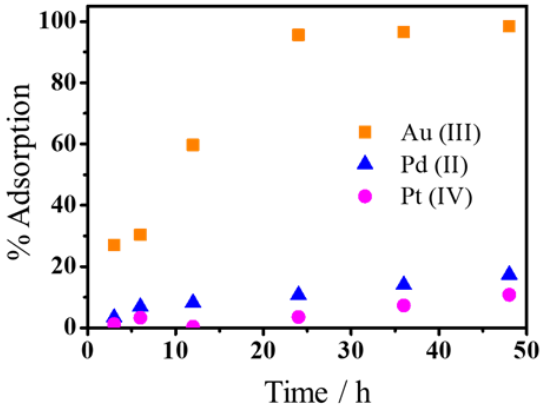

Fig. 4-1 Effect of shaking time on Au(III), Pd(II) and Pt(IV) adsorption on HH in competitive system of 0.10 M HNO_3 media at 303K, $[\text{Precious metal}]_i$ = 0.1 mM.

4.3.2 Adsorption of precious metals in individual and competitive systems

To discuss about the selective adsorption of precious metals on HH, the precious metals adsorption in individual and competitive systems was investigated.

Effect of nitric acid concentration on percentage adsorption of precious metals on HH and WHH in individual system is shown in Figs. 4-2 and 4-4. At 0.1 M nitric acid concentration, the adsorption percentages of Pd(II) and Pt(IV) were 15.4 and 4.4%, which of time to reaching equilibrium as the value of 48 h in Fig. 4-1, illustrating that the shaking time for 24 h seems to be sufficient. Both of HH and WHH exhibited high selectivity for Au(III) over other precious metals, although Au(III) adsorption was suppressed at low concentration of nitric acid.

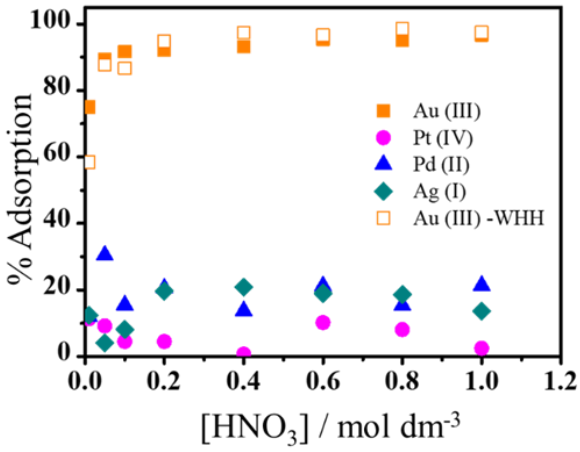

Fig. 4-2 Effect of nitric acid concentration on percentage adsorption of precious metals on HH in individual system at 303K, $[\text{Precious metal}]_i$ = 0.1 mM.

To consider the factor of acid affecting to selectivity, the adsorption in HCl media was also as shown in Fig. 4-3. The Au(III) adsorption on HH was remarkably suppressed, particularly at high concentration of hydrochloric acid. Obviously, compared the conditions of 0.1 M HNO_3 and HCl, the percentage of adsorption was decreased from 90%

to 25%. That illustrates the adsorption of Au(III) had relation with concentration of chloride anion. On the contrary, Pd(II) adsorption was not drastically suppressed with increase of HCl concentration.

According to HSAB theory [23], "soft" metals such as Au(III) and Pd(II) have high affinity with "soft" donor atoms. The suppressed Au(III) adsorption was probably caused by charge of the chemical species of Au(III), which was from Au^{3+} to $AuCl_4^-$ [24,25]. The chemical species of Pd(II) also changed from Pd^{2+} to $PdCl_4^{2-}$. This difference in adsorption behavior between two soft metal ions means that adsorption mechanism of Au(III) and Pd(II) on HH is different.

Interestingly, the Au(III) adsorption on WHH had similar performance as that adsorption on HH. The obvious difference between the black HH and WHH is the amount content of melanin, the similar percentage revealed melanin has no relation to the reaction in the adsorption process.

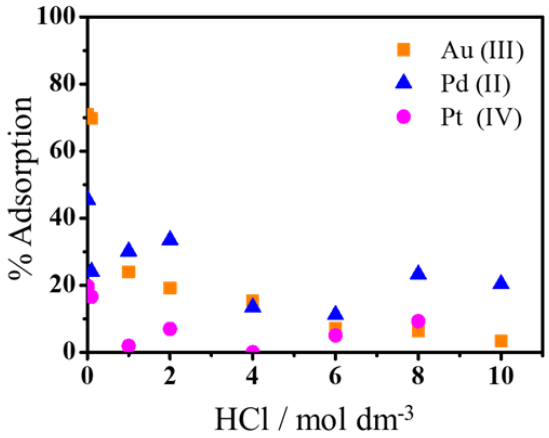

Fig. 4-3 Effect of hydrochloric acid concentration on percentage adsorption of precious metals on HH at 303K, $[\text{Precious metal}]_i$ = 0.1 mM.

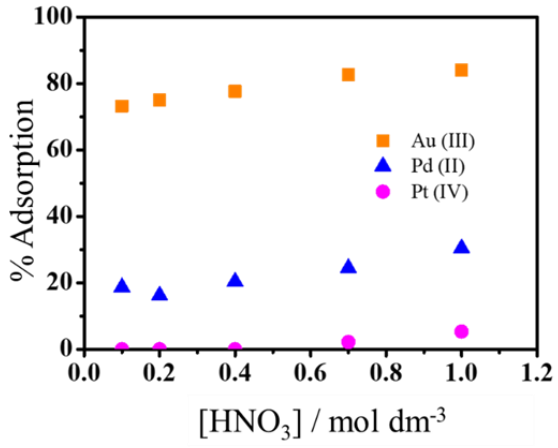

Fig. 4-4 Effect of nitric acid concentration on percentage adsorption of precious metals on HH in competitive system at 303K, $[\text{Precious metal}]_i$ = 0.1 mM.

Precious metal adsorption on HH in competitive systemin in nitric acid media was investigated as well, as shown in Fig. 4-4.

Apparently, HH exhibited high selectivity for Au(III) over Pd(II) and Pt(IV). Compared with the individual adsorption, the adsorption of Au(III) was slightly suppressed by the Pd(II) adsorption but there was no adsorption of Pt(IV). Refer to the result of HCl media, this result of suppressed adsorption of Au(III) in competitive system was probably attributed to the mixture of other precious metals salts ($PdCl_4^{2-}$ and $PtCl_6^{2-}$) increased the chloride concentration. While, Pd(II) adsorption was slightly enhanced, it may also be caused by difference in chemicals species related to Au(III) and Pd(II) adsorption. In other words, Pd(II) adsorption was not only related to the species which are different from Au(III) adsorption but also slightly had interaction with other chemicals in HH.

4.3.3 Adsorption Langmuir isotherms of precious metals on human hair and white human hair

The adsorption isotherms for precious metal ions on HH in 0.10 M HNO_3 was investigated as shown in Fig. 4-5 (a). The adsorption amounts of Au(III) on HH increased

with the increase of initial Au(III) concentration and finally reached the maximum loading capacity. Unlike the Au(III) result, the much lower adsorption capacities of HH were exhibited for Pd(II) and Pt(IV) sufficiently with the perfect selectivity for Au (III). The results of metal adsorption were classified into the Langmuir models [26].

To confirm the validity of the maximum adsorption capacities of Au (III) on HH and WHH, the transformed Langmuir adsorption isotherms of Au (III) ion were observed shown in Fig. 4-5 (b). The regression coefficients (R^2) values were over 0.99, so the Langmuir isotherm model was fitted to the experimental data. Langmuir parameters and maximal adsorption capacities were calculated from the intercept and the slope of the straight lines by linear regression analysis and listed in Table 4-2. The WHH possessed the comparable to or even higher adsorption capacity (3.24 mmol g^{-1}) than that of HH (3.04 mmol g^{-1}).

In addition, the Au (III) adsorption capacity on HH was compared with those obtained by using other biomass materials as listed in Table 4-3. As the comparison, the HH as the unmodified biomass waste has the adequately high capacity for Au(III) adsorption.

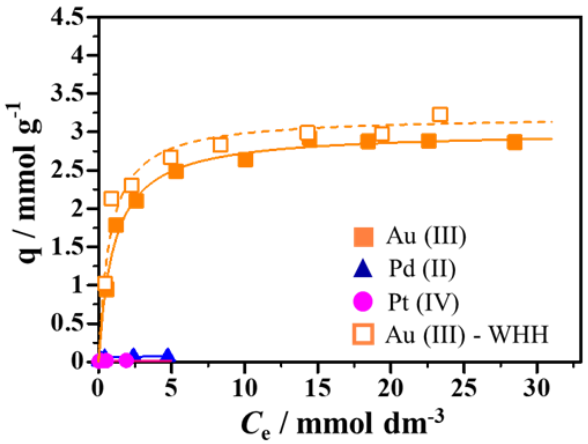

Fig. 4-5 (a) Adsorption isotherms of precious metals on HH and Au (III) on WHH in 0.1 M nitric acid media at 303K.

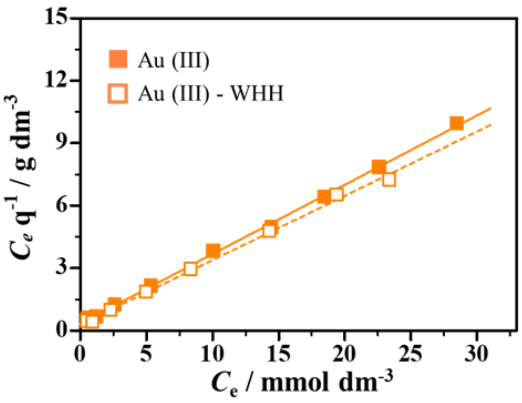

Fig. 4-5 (b) The Langmuir isotherm kinetic model of Au (III) adsorption on HH and WHHH in 0.1 M nitric acid media at 303K.

Table 4-2 Langmuir isotherm constants for adsorption of Au (III) on HH and WHH.

Adsorbents	**q_m (mmol g^{-1})**	**b (dm^3 mmol^{-1})**	**R^2**
HH	3.00	0.9598	0.9995
WHH	3.24	0.9939	0.9984

Table 4-3 Comparison of adsorption capacities of Au (III) on the present adsorbent with various bio-adsorbents.

Adsorbents	**Adsorption capacity (q_m) (mmol g^{-1})**	**Reference**
Silk sericin	1.0	[27]
Eggshell membrane	3.13	[28]
Modified Lagerstroemia speciose leaves (PEI-LS)	1.52	[29]
Modified cellulose (TDAC)	0.175	[30]
Raw date pits	0.396	[31]
Modified wood powder	4.31	[32]
Calcium alginate	1.47	[33]
Human hair (HH)	3.04	Present work
White human hair (WHH)	3.24	Present work

4.3.4 The oxidation states of Au on human hair after adsorption

It has been reported in our previous works that the adsorbents derived from biomass wastes, containing polyphenols, pectic acid, cellulose, not only adsorbed Au(III) but also reduced it. HH also has a possible behavior to reduce Au(III) similar as kiwi peel. To confirm the valence state of Au on HH after the adsorption, the XRD analysis of Au(III)-loaded HH was carried out, the spectra is shown in Fig. 4-6. None of crystalline morphology was observed on the original HH. While the sharp peaks were observed on Au(III)- loaded HH at around 2θ values of 38.29°, 44.39°, 64.74° and 77.62°, which correspond to spectra of gold crystalline nanoparticles reported by the previous workers in lab [34-38] and other researchers [39]. This phenomenon is accordance with result in Au(III) adsorption and reduction on crosslinked kiwi peel. They both needed the long time to reach adsorption equilibrium. Hence, it demonstrated that the reduction of Au (III) took place during the adsorption process on HH.

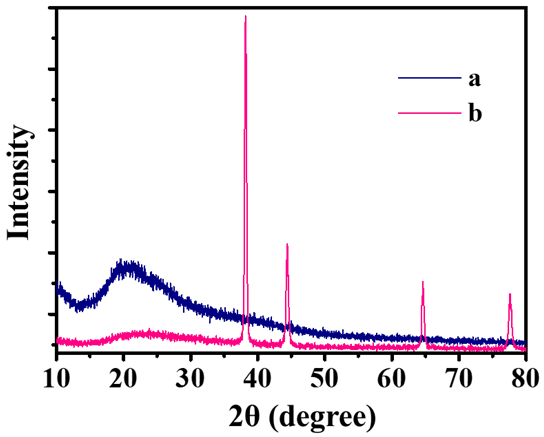

Fig. 4-6 XRD spectra of (a) Original HH and (b) Au(III)-loading (1.07 mmol g^{-1}) HH.

4.3.5 Characterization of human hair and loading Au (III) human hair

For the further study on the reduction of Au (III), the surface morphologies of HH

before and after the Au(III) adsorption were measured by SEM as shown in Figs. 4.7a-c and digital micrograph analysis as shown in Figs. 4.7 (d) and (e).

Since supplied HH was used without any specific collection, the diameters are not uniform as shown in Fig. 4-7 (a). As corresponding to XRD data, the outmost layer of HH was covered with visible aggregates of metallic gold particles after the adsorption, as shown in Fig. 4-7 (b). And the surface was not broken by soaking into acidic media long time or reaction with Au(III). To find out whether the inner layer had gold particle or not, HH after the gold loading was cut into smaller size. And the surface of cut section was taken as in Figure 4-7(c). There was no gold particle on the cut section. While gold particles were only observed on the outmost layer, which means the adsorption and reduction processes were taken placed on the surface of HH. It also illustrates that the adsorption may be taken place by two possible situations. First, Au(III) ions may just had interaction with the compound from the outmost layer of HH. Secondly, the compound from inner layer may be carried to the outmost layer and adsorbed and reduced Au(III) ions.

The coverage of gold particles was increased with the increased amount of gold adsorption. Gold particles were observed as digital micrograph not only on the black HH shown in Fig 4-7 (d) but also on the white one as shown in Fig. 4-7 (f). Therefore, the WHH still has the potential for valuable adsorption capacity, which strongly supports the results shown in Figs. 4-2, 4-5 (a) and (b).

To refine the loaded gold from HH, 0.5 g HH loading gold nanoparticles was incinerated in the muffle furnace at 800°C for 2 h, then 0.050 g gold was obtained. The metallic gold aggregated as the threadlike formation after the refine as shown in Fig. 4-7 (e) The obvious observation demonstrated the commercial value of HH and feasibility for gold recovery by this simple method.

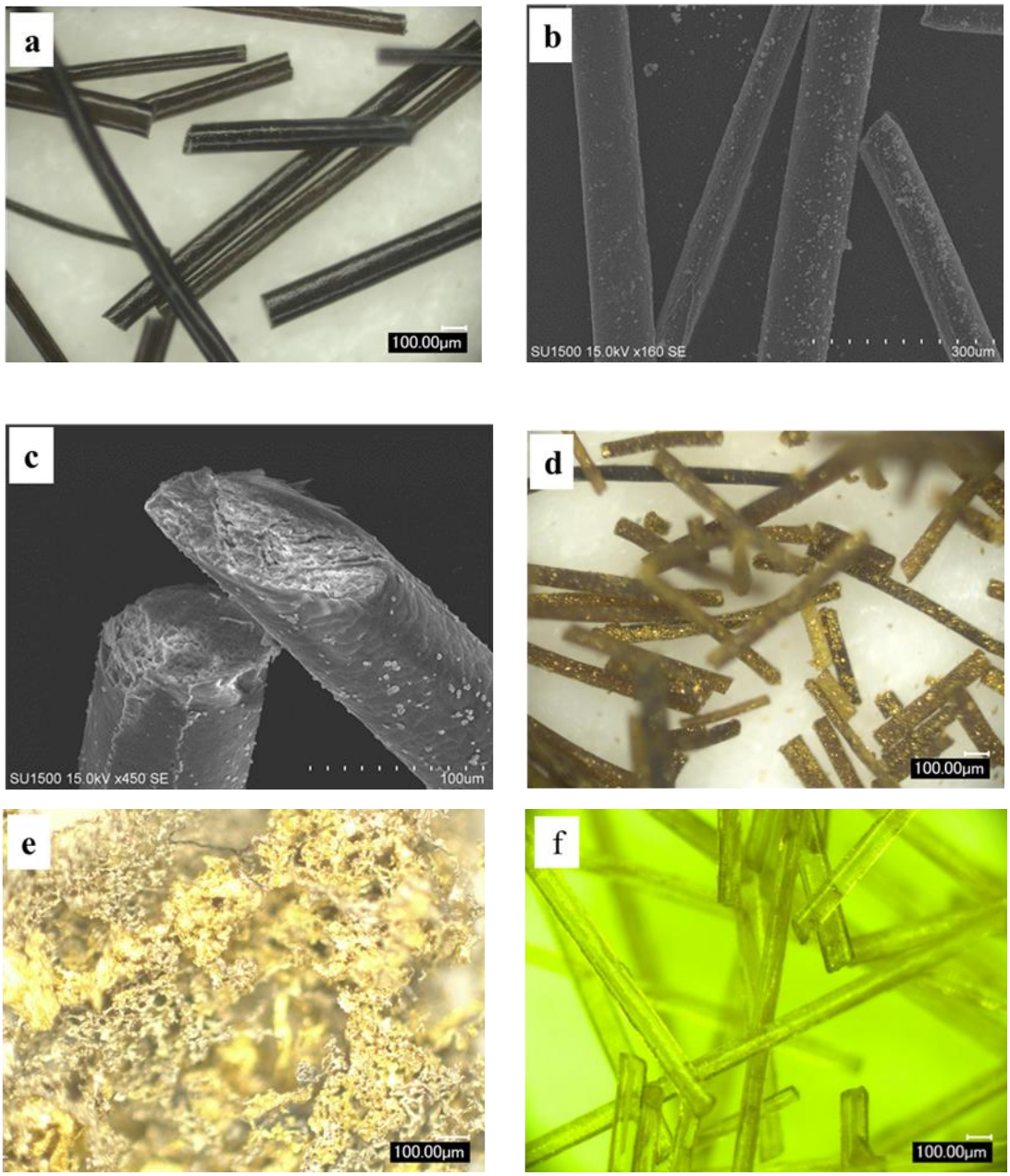

Fig. 4-7 SEM and microscope images of HH before and after Au (III) adsorption: (a) original HH; (b) Au(III)-loading HH(0.493 mmol g^{-1}); (c) the cut section of Au(III)-loading-HH; (d) Au(III)-loading HH (2.881 mmol g^{-1}); (e) the burned Au(III)-loading HH (f) Au(III) loading WHH (0.532 mmol g^{-1}).

4.3.6 Mechanism of gold adsorption on human hair

Because of advantage of high content of proteins, HH probably works for the gold adsorption. On the other side, protein can be partly hydrolyzed to amino acids in acidic media. Therefore, from those viewpoints, main active components on Au(III) adsorption may relate to amino acids. From Table 4-1 listing the information for the amount ratio of amino acids included in HH, dominant component is *L*-cystine. Hence, several high percentage content of amino acid monomers were investigated for interaction with Au(III).

Assuming the percentage amount of protein in human is 90, 20 mg HH (same amount as the previous test sample) contains around 3.15 mg (0.013 mmol) cystine. Hence, based on that calculation, around 0.022 mmol of each monomer amino acid: *L*-cystine, *L*-serine, *L*-glutamic, glycine, *L*-arginine and alanine was separately investigated. These amino acids were independently employed for adsorption of 1.0 mM Au (III) in 0.10 M HNO_3. As shown in Fig. 4-8, cystine was the most effective for Au(III) adsorption among same molar amount of amino acids employed and it comparably works as adsorption percentage for HH.

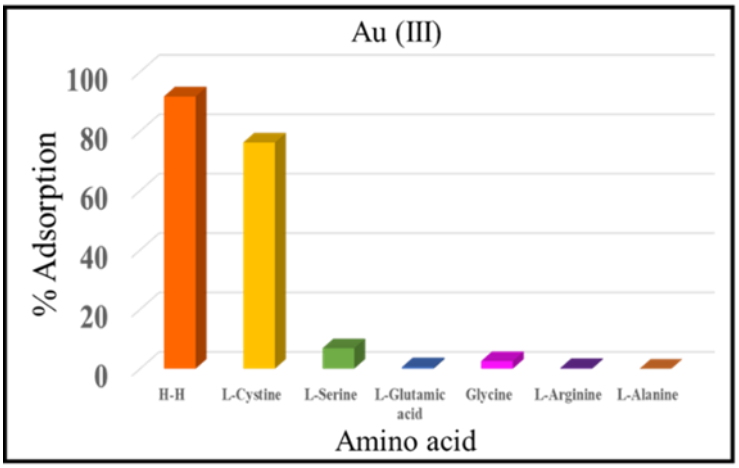

Fig. 4-8 Individual adsorption of 1.0 mM Au (III) on various amino acid in 0.10 M nitric acid media.

The adsorption percentage of gold from each amino acid and its content percentage in HH are listed in Table 4-4. Cystine is the highest content amino acid in HH and its

monomer had the highest adsorption of Au(III).

The chemical structures of amino acids are shown in Fig. 4-9. It is clearly found that all of them contain the same functional groups: carboxyl and amino groups. While the only difference related to the reaction with Au(III) is the sulfhydryl group rather than amido one. Because included disulfide bond belongs to soft base can form complexes with soft acid Au(III). Meanwhile, the neglectable point is that *L*-serine had meaningful adsorption percentage, because of the additional functional hydroxyl group. Consequently, amino acids together with hydroxyl group may interact with Au(III) ion as well. The two factors led to the higher adsorption percentage of Au(III) on HH than that on monomer cystine.

Table 4-4 Adsorption percentage of Au with different amount percentage amino acids in HH.

Amino acid	**Amount in %**	**Molar quantities (mmol)**	**Adsorbed amount (mmol)**	**Adsorption %**
L-Cystine	17.5	0.0221	0.00747	76.2
L-Serine	11.7	0.0236	0.000617	6.89
L-Glutamic	11.1	0.0210	4.81E-05	0.49
Glycine	6.5	0.0246	0.000252	2.6
L-Arginine	5.6	0.0222	2.4 E-05	0.245
Alanine	4.8	0.0214	0	0

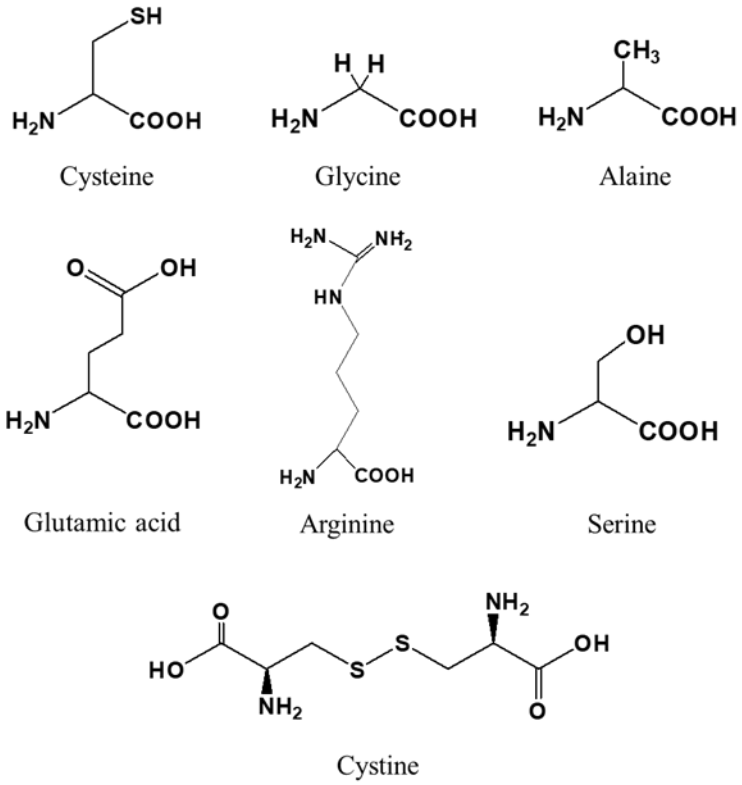

Fig. 4-9 Chemical structures of amino acids contained in HH.

The cortex of hair shaft between medulla and cuticle is built up by hundreds of macrofibrils which are fiber-shaped forming structural units consisting protein. Based on the images shown in Figs. 4-7 (a)-(d), the gold particles were found only on the surface of HH, it illustrated that the cystine was produced by hydrolysis of protein on side chain and complexed with Au(III) ions as S-Au-S bond at outmost layer on HH. And the Au(III) ion was reduced by the oxidation cystine.

The mixture solution of cystine monomer and Au(III) ions was filtrated by membrane filter. After filtration, the membrane was observed by digital micrograph. As shown in Fig. 4-10, a lot of gold particles were accumulated on the membrane after the interaction. It means that cystine has ability to reduce Au(III) ions. That was why gold particles existed on the surface of HH

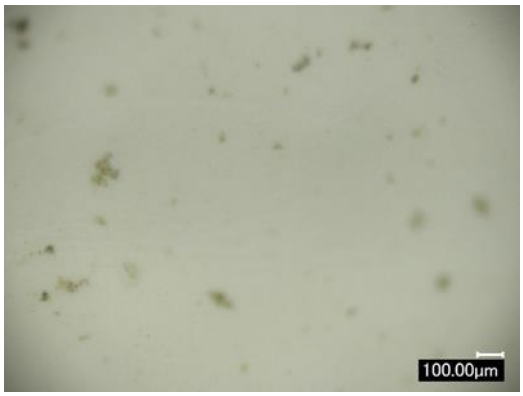

Fig. 4-10 Digital image of surface of filter membrane after filtration of cystine with Au(III) mixed solution.

Cystine as the most effective compound for Au(III) adsorption among amino acids, gathered and reduced Au(III) on the surface of HH. Besides, serine with hydroxyl groups also showed perceivable contribution to adsorption.

4.3.7 Changed content of element on human hair before and after Au(III) adsorption

To further validate that the production cystine to adsorption is from which layer of HH. Original HH and Au loading HH were measured by EDS. As shown in the Figs. 4-11, surface of hair contains a number of sulfur atom, that means outmost layer of contains sulfur content protein. The meaningful content indicated that the protein on the outmost layer had potential for Au(III) adsorption. For EDS measurement, apparatus focused on the surface to detect the element component of material. Hence, all of the surfaces can not be reflected, especially for Au(III) loading HH, surface was not completely covered by gold particles. The limited detected region led the report to indicate some area of surface contained gold and some of area had no gold on same measured samples. Such as shown in Fig. 4-11(b), Au(III) adsorption on HH in 0.1 HCl media, the adsorption percentage was 70%, but detected area was not covered by gold particle. Therefore, element content of Au percentage was almost 0. But the point is that content of sulfur was improved compared with HH. It illustrated the amino acid from partial hydrolysis of

protein was produced at acidic media.

In 0.1 M HNO_3, the loading gold on HH was measured twice at different detected point as shown in Figs. 4-11 (c) and (d). The corresponding detected points are shown in Fig. 4-12 (a) and (b). Au content on two detected points are different as shown in Figs. 4-11 (c) and (d), but they had similar sulfur contents. It demonstrated that sulfur is the active atom to Au(III) complexes and reduction.

As the result in Fig. 4-8, S-S bond in cystine is the predominant component for Au(III) adsorption on HH.

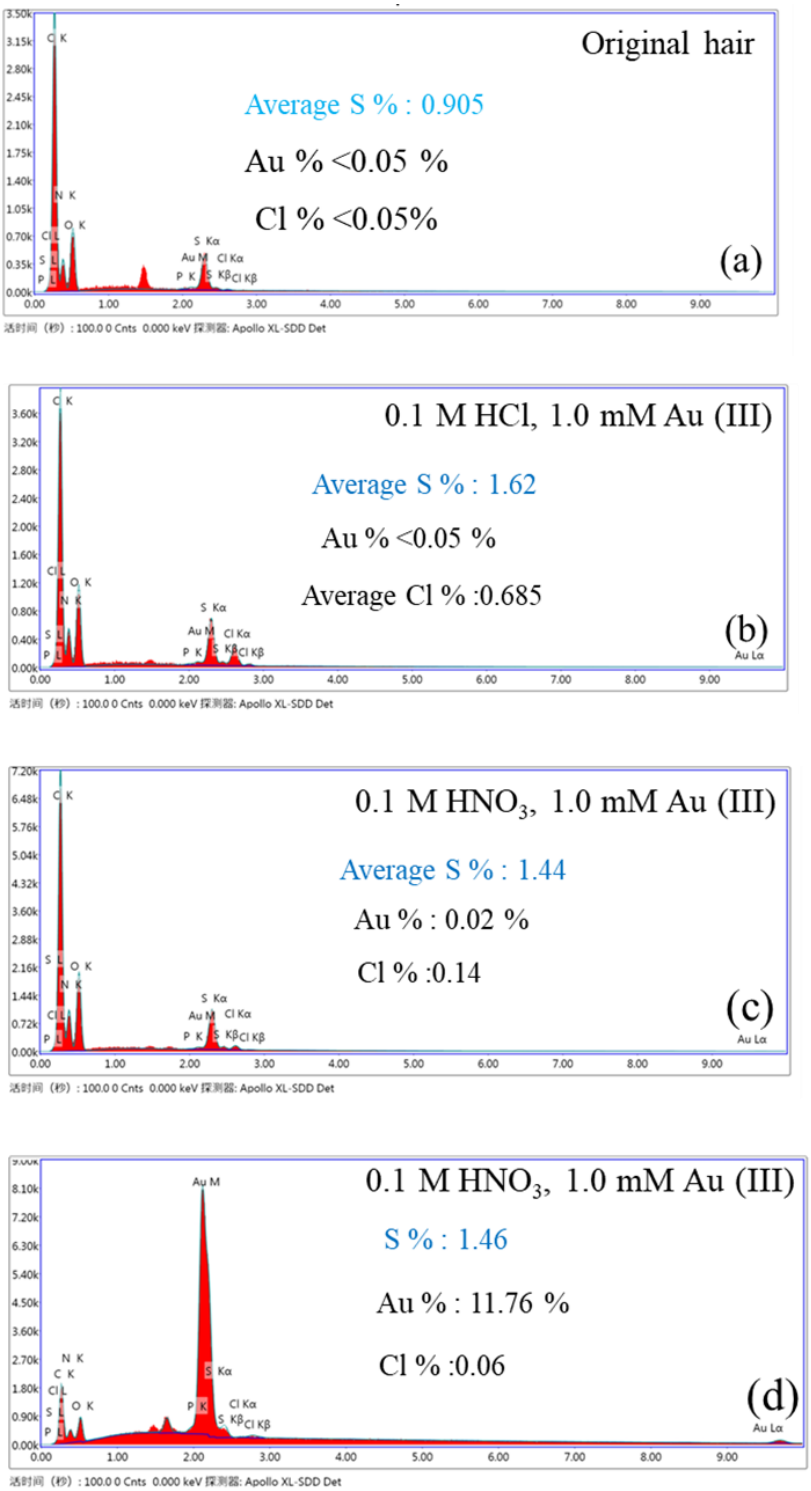

Fig. 4-11 Analysis of EDS before and after gold loading on the surface of HH (a) original HH, (b) Au loaded HH in HCl, (c) and (d) same sample with different detected area of Au loaded HH in HNO_3.

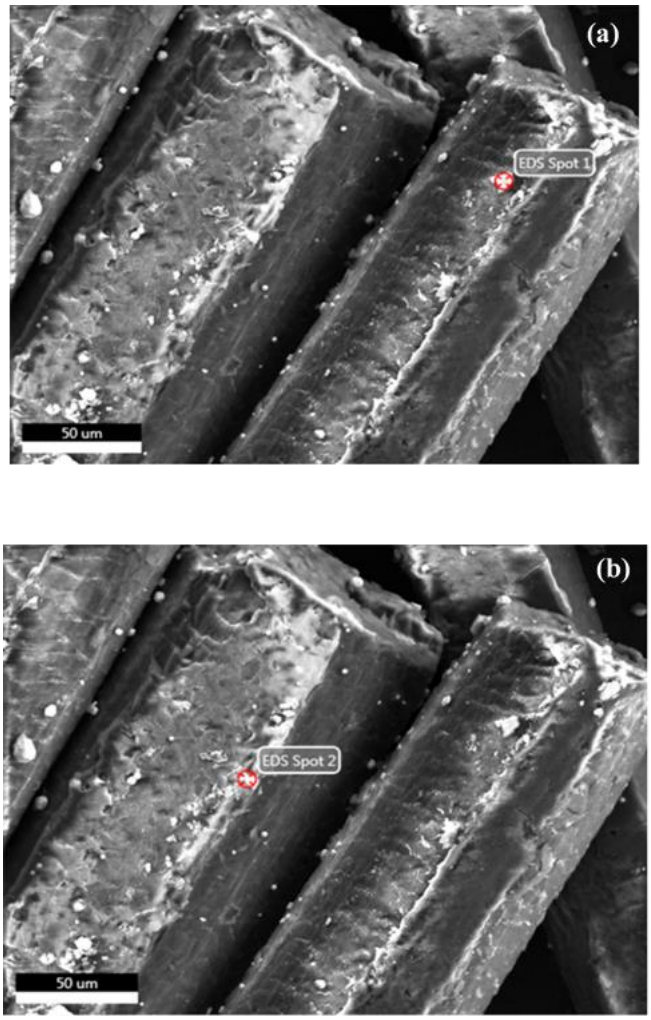

Fig. 4-12 Images of reported source of detected point on the surface of HH (a) corresponded to report in 4.11 (c) and (b) corresponded to reported in 4.11(d).

4.3.8 FT-IR analysis of original and gold loading human hair

For the further investigation on the mechanism of Au(III) adsorption on HH, FT-IR spectroscopy was employed. The spectra of original and gold loading HH are shown in Fig. 4-13. The peaks shown at 3612 cm^{-1} and 1521 cm^{-1} correspond to N-H stretching and bending vibrations. In addition, asymmetric stretching of COO^{-1} was observed at 1693 cm^{-1} on HH and shifted to 1659cm^{-1} after the gold loading [40,41], illustrated the amino acid from product of part hydrolysis of protein. Moreover, the weak band observed around the

2200 cm^{-1} attributed to -SH group. It was disappeared after gold loading which meant the formation of S-Au-S. Hence, corresponded the result from gold adsorption on amino acids, the predominant group involved to adsorption was SH.

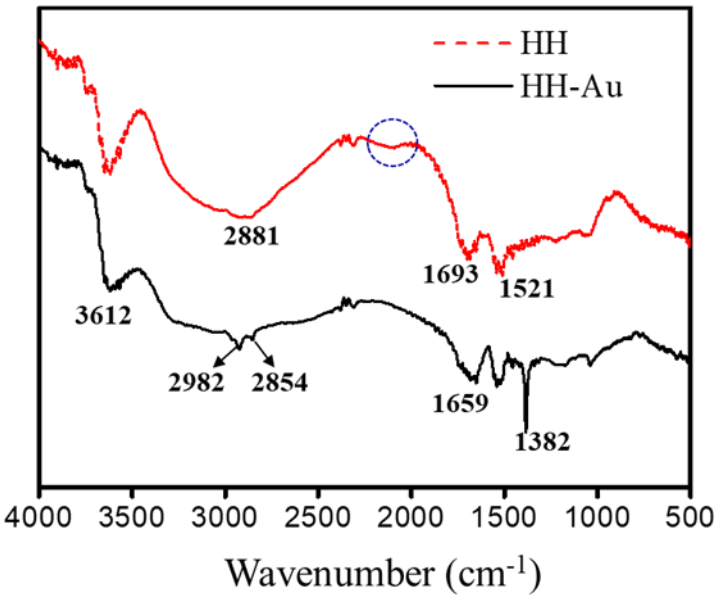

Fig. 4-13 FTIR spectra of original HH and Au(III)-loading HH (0.42 mmol g^{-1}).

4.3.9 ^{1}H NMR spectra of the cystine and cystine-coated gold nanoparticles

It has been found that cystine plays important role for Au(III) adsorption on HH. To deeply study the reaction between Au(III) and cystine, the cystine monomer and cystine contacted with Au(III) at different contacting time in D_2O-DCl solution were observed by ^{1}H-NMR spectroscopy. The ^{1}H NMR spectra are shown in Figs. 4-14 (a)-(d). The peaks for the -CH and -CH_2 of cystine protons appeared at 4.1-4.18 ppm and 3.0-3.3 ppm. Probably due to the molecular chirality, the methylene protons of CH_2S group appeared as double doublets. After the reactant, the formation of S-Au-S led to the peaks of methine and methylene shifting up. Meanwhile, peaks of -SH (1.2 ppm) and -CH_2SH (3.0-3.1 ppm) were observed to demonstrate the fragment of cystine to cysteine during forming the

complex.

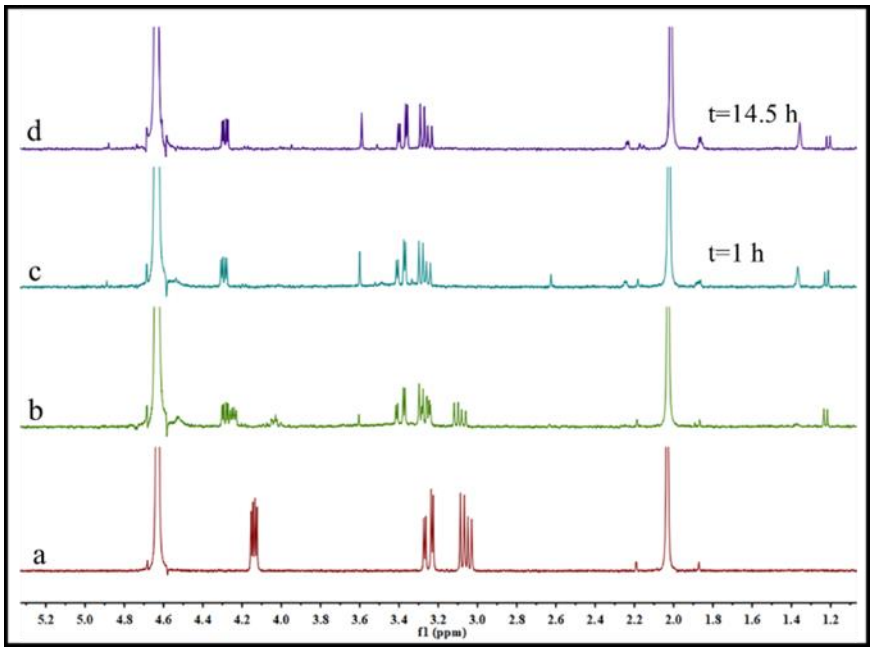

Fig. 4-14 ^{1}H NMR spectrum of (a) cystine in D_2O-DCl, (b) Au(III) mixture (0 h), (c) Au(III) mixture (1h later), (d) Au (III) mixture (14.5 h later).

4.3.10 The proposed adsorption model

Comprehensively, the adsorption processes of gold on HH involved adsorption and the reduction of auric ion on the surface of HH. The schematic representation is shown in Scheme 4-1. During the sulfur atom bound to auric ion, the reduction of gold took place, as mention by the followed equations 4.2-4.4:

$$R\text{-}S\text{-}S\text{-}R + AuCl_4^- + 3e^- \rightarrow R\text{-}S\text{-}Au\text{-}S\text{-}R + 4Cl^- \quad (4.2)$$

$$2H_2O \rightarrow O_2 + 4H^+ + 4e^- \quad (4.3)$$

Combined the eq. (4.2)-(4.3), the eq. (4.4) was observed:

$$4R\text{-}S\text{-}S\text{-}R + 4AuCl_4^- + 6H_2O \rightarrow 4R\text{-}S\text{-}Au\text{-}S\text{-}R + 16Cl^- + 3O_2 + 12H^+ \quad (4.4)$$

In nitric acid, complexes of $AuCl_4^-$ were not stable in extremely low concentration of chloride anion. Stronger electronegativity of chloride anion led to the stable complexes formation with Au(III), the reduction of Au(III) was suppressed at much amount of

chloride surround. Sulfur atom has less negativity than chloride atom. Hence, the complexes were suddenly transferred by binding of Au as S-Au-S bond then Au was reduced.

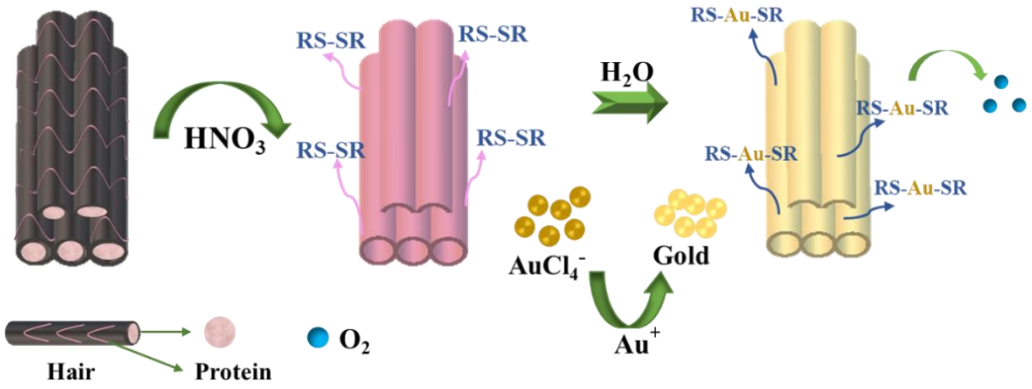

Scheme 4-1 Proposed adsorption of Au(III) on HH model.

4.3.11 Elution of Pd (II) from human hair after competitive adsorption

Based on the high selectivity for Au(III) on HH in competitive system, the practical application of HH for mutual separation of precious metals was considered. The HH was eluted by 0.05 M thiourea in 0.01 M HCl after the adsorption of mixed precious metals solution in 0.1 M HNO_3 media, as shown in Fig. 4-15. Because none of the Pt (IV) adsorption hardly took place, the elution percentage was treated as zero. While Pd (II) ions were completely eluted within 5 min. Au (III) ions were only slightly eluted. Remaining gold was refined from the HH by incineration in muffle furnace. Thus, combined the two result, the separation and recovery of gold from leaching solution of precious metals are feasible by using HH. The processes involved three simple steps to observe pure gold: adsorption Au(III) from leaching solution, complete elution of loaded Pd(II) ion and incineration of the loading gold. HH as the unmodified material successfully may realize the cheaper and effective precious metal recovery.

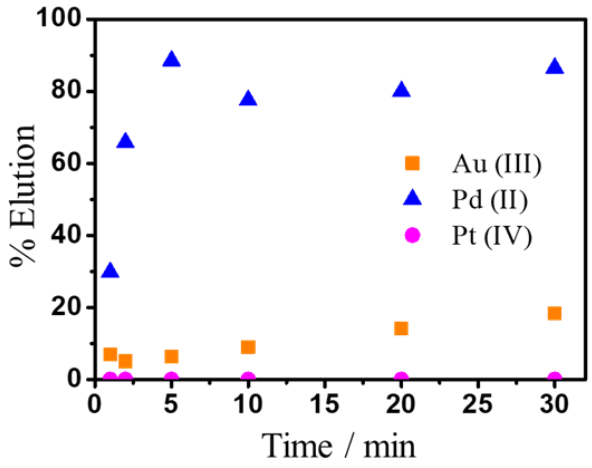

Fig. 4-15 Elution of loaded precious metals from HH with 0.05 M thiourea containing 0.01 M hydrochloric acid at 303K.

4.4 Conclusion

Protein rich biomass waste, without any modification, was successfully applied to the separation of precious metals and recovery of gold. Either in hydrochloric acid or nitric acid media, HH exhibited preferable selectivity for Au(III) adsorption over Pd (II) and Pt (IV) at individual system. While the HH was widely adaptable to various concentrations of nitric acid and exhibited efficient adsorption ability in high concentrations of nitric acid compared with that in HCl solution. Although in the competitive system, Au(III) adsorption was slightly suppressed by Pd(II) adsorption. WHH also exhibited excellent performance and selectivity for Au(III) adsorption.

The maximum loading capacities of gold on HH and WHH were 3.00 and 3.24 mmol g^{-1} and sufficiently higher than those of other bio-adsorbents. The gold particles were observed on the surface of HH and WHH. The amount of gold particles on the surface increased with those increase of adsorbed amount. The four peaks of XRD spectra proved the reduction of Au(III) during the adsorption processes. The reduction caused long time to reach adsorption equilibrium.

Protein contained in HH is also a candidate for gold adsorption. The relation between monomer amino acids and Au(III) ion was investigated. The result demonstrated that cystine with highest content in HH is the predominate component to Au(III) adsorption. The hydroxyl group with less content in HH showed perceivable adsorption. The results from EDS, FT-IR and ^{1}H NMR demonstrated that cystine component can form the complex with Au(III) and reduce Au(III) by oxidation of S-S bond. Comprehensive, the proposed adsorption model was drawn.

To study the perfect method for gold recovery, the elution of Pd(II) from HH after soaking into leaching solution of precious solution was investigated. The high effective elution of Pd (II) and less elution of Au(III) showed the potential to remove Pd(II) from Au(III) loading hair. On the other hand, the refinement of gold from HH after individual Au(III) adsorption was successful by incineration. Thoroughly, those results indicated the practicability of gold recovery from leached precious metal solution by using HH. In summary, the method of gold recovery included three steps, adsorption of Au(III) from mixed precious metal solution, complete elution of Pd(II) from the loading Au(III) HH and refine of gold from the eluted hair by incineration.

Human hair as the waste bio-adsorbents, has the effective ability and selectivity for gold recovery. It has tremendous potential for practical application to gold recovery in commercial situation.

4.5 References

[1] H. Öfner and F. Zaera, Ethylene adsorption on platinum: kinetics, bonding, and relevance to catalysis, J. Am. Chem. Soc., 2002, 124, 10982-10983.

[2] H. J. Zheng and L. M. Wang, Banana peel carbon containing functional groups applied the selective adsorption of Au (III) from waste printed circuit boards, J. Soft Nanosci. Lett. 2013, 3, 29-36.

[3] D. Parajuli, K. Hirota and K. Inoue, Trimethylamine-modified lignophenol for the

recovery of precious metals, Ind. Eng. Chem. Res., 2009, 48, 10163-10168.

[4] Y. Xiong, C. R. Adhikari, H. Kawakita, K. Ohto, K. Inoue and H. Harada, Selective recovery of precious metals by persimmon waste chemically modified with dimethylamine, Bioresour. Technol., 2009, 100, 4083-4089.

[5] T. Maruyama, H. Matsushita, Y. Shimada, I. Kamata, M. Hanaki, S. Sonokawa, N. Kamiya and M. Goto, Protein and protein-rich biomass as environmentally friendly adsorbents selective for precious metal ions, Environ. Sci. Technol., 2007, 41, 1359-1364.

[6] B. C. Choudhary, D. Paul, A. U. Borse and D. J. Garole, Surface functionalizes biomass for adsorption and recovery of gold from electronic scrap and refinery wastewater, J. Sep. Purif. Technol., 2018, 195, 260-270.

[7] A. Ramesh, H. Hasegawa, W. Sugimoto, T. Maki and K. Ueda, Adsorption of gold (III), platinum (IV) and palladium (II) onto glycine modified crosslinked chitosan resin, J. Bioresour. Technol., 2008, 99, 3801-3809.

[8] J. S. Lim, S. M. Kim, S. Y. Lee, E. A. Stach, J. N. Culver and M. T. Haris, Quantitative study of Au (III) and Pd (II) ion biosorption on genetically engineered tobacco mosaic virus, J. Colloid. Interface Sci., 2010, 342, 455-461.

[9] A. Gupta, Human hair “waste” and its utilization: gaps and possibilities, Waste Management, 2014, 2014, 1-17.

[10] United nations, https://population.un.org/wpp/Download/Standard/Population.

[11] C.R. Robbins, Chemical and physical behavior of human hair, 3rd ed. New York: Springer-Verlag, 1994. pp. 10-391.

[12] M. A. Van Steensel, R. Happle and P. M. Steijlen, Molecular genetics of the hair follicle: The state of the art, Proc. Soc. Exp. Biol. Med., 2000, 223,1-7.

[13] L. J. Wolfram, Human hair: A unique physicochemical composite, J. Am. Acad. Dermatol., 2003, 48, S106-14.

[14] P. Jolle, H. Zahn and H. Hocker, Formation and Structure of Human Hair, 1997, 67(1),853-853.

[15] A. Nakamura, M. Arimoto, K. Takeuchi, and T. FUJII, A rapid extraction procedure

of human hair proteins and identification of phosphorylated species, J. Biol. Pharm. Bull. 2002, 25, 569—572.

[16] S. Shin, A. Lee, S. Lee, K. Lee, J. Kwon, M. Y. Yoon, J. Hong, D. Lee, G. H. Lee and J. Kim, Microwave-assisted extraction of human hair proteins, Anal. Biochem., 2010, 407, 281–283.

[17] S. Hilterhaus-Bong and H. Zahn, Contributions to the chemistry of human hair. I. analyses of cystine, cysteine and cystine oxides in untreated human hair, Int. J. Cosmetic Sci., 1987, 9, 101-110.

[18] C.R. Robbins and C.H. Kelly, Amino acid composition of human hair, Text Res. J., 1970, 40, 891-6.

[19] H. Zahn, F. J. Wortman, H. Hocker, Chemie and Aufbau der Wolle., Chemie in Unserer Zeit., 1997, 31, 280-90.

[20] Z. F. Ma and H. L. Han, One-step synthesis of cystine-coated gold nanoparticles in aqueous solution, Colloids Surf., A: Physicochem. Eng., 2008, 317, 229–233

[21] J. D. Zhang, Q. J. Chi, J. U. Nielsen, E. P. Friis, J. E. T. Andersen, and J. Ulstrup, Two-Dimensional Cysteine and Cystine Cluster Networkson Au (III) Disclosed by Voltammetry and in Situ Scanning Tunneling Microscopy, Langmuir, 2000, 16, 7229-7237.

[22] R. G. Pearson and J. Songstad, Application of the Principle of hard and soft acids and bases to organic chemistry, Org. Biol. Chem., 89, 1967, 1827-1836.

[23] R. G. Pearson, Hard and soft acids and bases, J. Am. Chem. Soc., 1963, 85, 3533-3539.

[24] L. G. Sillén, A. E. Martell and J. Bjerrum, Stability constants of metal-ion complexes, Special publication (Royal Soc. Chem.) No. 17, 1964, 288-289.

[25] M. J. Nicol, C. A. Fleming and R. L. Paul, The chemistry of the extraction of gold, 1987, Chap. 15, pp.831-905.

[26] I. Langmiur, The constitution and fundamental properties of solids and liquids. II

Liquid., J. Am. Chem. Soc., 1917, 39, 1848-1906.

[27] X. Q. Chen, K. F. Lam, S. F. Mak and K. L. Yeung, Precious metal recovery by selective adsorption using biosorbents, J. Hazard. Meter., 2011, 186, 902-910.

[28] S. Ishikawa, K. Suyama, K. Arihara and M. Itoh, Uptake and recovery of gold ions from electroplating wastes using eggshell membrane, Bioresour. Technol., 2002, 81, 201-206.

[29] B. C. Choudharya, D. Paul, A. U. Borse and D. J. Garole, Surface functionalized biomass for adsorption and recovery of gold from electronic scrap and refinery wastewater, Sep. Purif. Technol., 2018, 195, 260-270.

[30] A. D. Dwivedi, S. P. Dubey, S. Hokkanen, R. N. Fallah and Mika Sillanpää, Recovery of gold from aqueous solutions by taurine modified cellulose: An adsorptive–reduction pathway, Chem. Eng. Jpn., 2014, 255, 97-106.

[31] H. M. Al-Saidi, The fast recovery of gold (III) ions from aqueous solutions using raw date pits: Kinetic, thermodynamic and equilibrium studies, J. Saudi. Chem. Soc., 2016, 20, 615-624.

[32] D. Parajuli, K. Hirota, and K. Inoue, Trimethylamine-modified lignophenol for the recovery of precious metals, Ind. Eng. Chem. Res., 2009, 48, 10163-10168.

[33] E. Torres, Y. N. Mata, M. L. Blázquez, J. A. Muñoz, F. González and A. Ballester, Gold and silver uptake and nanoprecipitation on calcium alginate beads, Langmuir, 2005, 21, 7951-7958.

[34] D. Parajuli, C. R. Adhikari, M. Kuriyama, H. Kawakita, K. Ohto, K. Inoue and M. Funaoka, Selective recovery of gold by novel lignin-based adsorption gel, Ind. Eng. Chem. Res., 2006, 45, 8-14.

[35] D. Parajuli, H. Kawakita, K. Inoue, K. Ohto and K. Kajiyama, Persimmon peel gel for the selective recovery of gold, Hydrometallurgy, 2007, 87, 133-139.

[36] D. Parajuli, C. R. Adhikari, H. Kawakita, S. Yamada, K. Ohto and K. Inoue, Chestnut pellicle for the recovery of gold, Bioresour. Technol., 2009, 100, 1000-1002.

[37] B. Pangeni, H. Paudyal, M. Abe, K. Inoue, H. Kawakita, K. Ohto, B. B. Adhikari

and S. Alam, Selective recovery of gold using some cross-linked polysaccharide gels, Green Chem., 2012, 14, 1917-1927.

[38] K. Inoue, M. Gurung, H. Kawakita, K. Ohto, D. Parajuli, B. Pangeni and S. Alam, Chapter 5 Development of novel biosorbents for gold and their application for the recovery of gold from spent mobile phones, The recovery of gold from secondary sources ed. By S. Sabir, World Scientific Publishing Co. Ltd., 2016, pp. 143-171.

[39] S. Krishnamurthy, A. Esterle, N. C. Sharma and S. V. Sahi, Yucca-derived synthesis of gold nanomaterial and their catalytic potential, Nanoscale Res. Lett., 2014, 9, 627-636.

[40] R. A. Soomro, A. Nafady, Sirajuddin, N. Memon, T. H. Sherazi and N. H. Kalwar, *L*-cysteine protected copper nanoparticles as colorimetric sensor for mercuric ions, Talanta, 2014, 130 415–422.

[41] L. Li, Q. L. Zhang, Y. P. Ding, X. Y. Cai, S. Q. Gu and Z. Y. Cao, Application of L-Cysteine capped core-shell CdTe/ZnS nanoparticles as a fluorescence probe for cephalexin, Anal. Methods, 2014, 6, 2715-2721.

Chapter 5
Overall conclusions and future direction

5.1 Overall conclusions

Demand and supply of precious metals urgently request the recycling utilization of metal to develop the improvement of sustainable technology and society, to satisfy human life. Because of the fast industry substitution and innovation of production, increasing generation of electronic waste is hard to be neglected. Meanwhile, the complicated metal composition in electronic waste brings the issue for metal recovery. Especially for precious metals, electronic waste contains less amount of precious metal than those of others such as heavy metals. Therefore, the recovery technology of precious metal from such electronic waste requests specific selectivity.

Hydrometallurgy is the most frequent technology for metal recovery in industry. Separation of each metal from leaching solution plays the important role in hydrometallurgy. Generally employed methods in separation include precipitation, solvent extraction, liquid-solid adsorption and ion exchange. Precipitation is normally used for primary separation of metals. Solvent extraction and liquid-solid adsorption are the core methods for stepwise separation of metal. Ion-exchange is used for alkali or alkaline earth metals, for example, water purification, change the amount of calcium or magnesium to make the water soft *via* the ion exchange resin.

Solvent extraction and liquid-solid adsorption have high abilities and adequate selectivity to metal separation. However, the processes of extraction involve several steps for synthesis of extractant, use of large amount of organic solvent. Although employing of synthesized solid adsorbent can decrease the use of organic solvent, the complicated synthesis steps are inevitable.

Facing those problems led to many researchers focusing on green and low cost

materials. Biomass adsorbents for metal adsorption have attracted attention in the past decades, due to the abundant resource and bare pollution to environment. The complicated content and composition of biomass waste make them potential for various metal adsorption by simple methods.

Dominant component in biomass wastes, they are simply divided into three classes, polysaccharides, polyphenols, protein rich materials. Hence, four representative substances, chitins, kiwi peels, tea leaves and human hair were respectively selected for investigation of precious metals and alkali metals adsorption.

Typical and natural polysaccharides adsorbents: chitin, cellulose and chitosan powder, were firstly employed for gold, platinum and palladium adsorption. Two types of chitin from different resources had better performance on palladium and platinum adsorption than cellulose. Because of the solubility of chitosan into acidic solution, chitosan was hardly employed. The adsorption capacity of natural chitins was remarkable, it has potential to improve by simple modification. The adsorption mechanisms of Pd(II) and Pt(IV) on chitins were also different.

To further study whether the modification of natural polysaccharides can improve the ability of precious metal adsorption, natural large cellulose contained biomass adsorbents-kiwi peels was investigated for precious metal adsorption. The high adsorption ability and selectivity for Au(III) over Pd(II) or Pt(IV) on simple modified KP by crosslinking had effect on adsorption. In addition, the result of XRD illustrated the reduction of Au(III) took place during all adsorption processes. It also led to long time to reach adsorption equilibrium time.

Fresh and used tea leaves as the polyphenol adsorbents were studied for cesium removal. After the crosslinking with concentrated sulfuric acid, the crosslinked fresh and used tea leaves performed high adsorption ability than the crude tea leaves to cesium. The maximum capacities of cesium on crosslinked tea leaves were sufficient high compared with other reported materials. Considered the real situation of cesium polluted water containing large amount of sodium and some of potassium, adsorption of three alkali metals was independently investigated. The proton exchange mechanism of alkali adsorption on crosslinked tea leaves was verified and the reaction was helped by coordination between oxygen atoms from ether groups and metal ion to remove the water

molecules around the metal. Therefore, both crosslinked tea leaves had preferable selectivity of cesium due to its low hydration energy. Moreover, the mixed solution with cesium and over concentration of sodium was separated by chromatographic column. The completely separation revealed the practical value of tea leaves for cesium removal in industrial application.

At last, the successful adsorption of gold from precious metal on protein rich biomass adsorbents human hair was studied. Without any modification, either the white or black hair had performed high ability of gold adsorption than those of platinum or palladium adsorption. Gold adsorption capacity of human hair is much higher than some of the reported biomass adsorbents. After the adsorption, human hair was not damaged and aggregated gold particle on its surface rather than inner layer was observed. By contacting gold with various amino acids monomer, cystine component was confirmed as the predominate component for to gold adsorption. The total processes of Au(III) adsorption on human hair related to formation of complexes between cystine component and Au(III), reduction of Au(III) and aggregation of gold particles on human hair.

The slightly adsorbed Pd(II) on human hair was completely eluted from human hair within 5 min after competitive adsorption. Furthermore, the successful refinement of pure gold from gold loading human hair by incineration revealed the practical recovery of pure gold from mixed precious metals leaching solution. The processes include three steps: adsorption of gold on human hair from mixed solution, elution of palladium from gold loading human hair, refine the gold from the eluted human hair.

All the results indicate that biomass waste has the ability comparable to extractant or synthesized adsorbents for precious metal adsorption. With more resource advantage and friendly to environment. Therefore, biomass waste has more superior potential for commercial application of metal recovery in industrial scale.

5.2 Future direction

Firstly, crosslinked kiwi peel had good ability and selectivity to Au(III) adsorption. However, the exact maximum gold adsorption capacity of crosslinked peel is still necessary to be investigated. Meanwhile, the mechanism of gold adsorption with

chemical component on crosslinked peel needs to be studied. In addition, because Au(III) exists as [$AuCl_4^-$] complex anion in the solution, the concentration of HCl may have effect on the adsorption. The adjust concentrations of [Cl^-] and [H^+] should be independently investigated.

Secondly, considered the excellent performance of gold adsorption on human hair, improvement of amino acids release onto HH by controlling the adsorption temperature may achieve the most utilization of human hair.

Thirdly, separation of gold from precious metals is important processes in hydrometallurgy, but all the processes of gold recovery from real electronic waste are worth to be deeply studied. For example, disassemble the mobile phone and leach the precious metal into aqueous phase. Then gradually separate each precious metal from leaching solution by different kinds of biomass waste such as chitin or human hair. Finally, refine the pure metal from the metal loading adsorbents.

At last, highly efficient recovery with low cost is the ultimate goal for economy. While, utilization of second resource is complicated work. The coexistence of several metals makes of the equipment on electronic waste. And the percentage of each metal component has big gap. Therefore, recovery of gold from large amount of heavy metals challenges biomass adsorbents to recovery work. A series of studies still need to be investigated.